Maria Katharina Höller, BSc

A game-based multiclass Brain-Computer Interface for natural upper limb control

MASTER'S THESIS

to achieve the university degree of

Diplom-Ingenieurin

Master's degree programme: Biomedical Engineering

submitted to

Graz University of Technology

Supervisor

Univ.-Prof. Dipl.-Ing. Dr.techn. Gernot Müller-Putz

Institute of Neural Engineering

Co-Supervisor
Dipl.-Ing. Andreas Schwarz

Graz, October 2018

AFFIDAVIT

I declare that I have authored this thesis independently, that I have not used other than the declared sources/resources, and that I have explicitly indicated all material which has been quoted either literally or by content from the sources used. The text document uploaded to TUGRAZonline is identical to the present master's thesis.

_____
Date

_____
Signature

Acknowlegements

While there is only one name on the cover of this thesis, credit is due to many more. First, I would like to thank Andreas Schwarz, as he guided me through the perils of science. Without his expertise and friendship this work would have never been possible. Furthermore, I would like to express my gratitude to Prof. Dr. Gernot Müller-Putz, for not only giving me the opportunity to gain a wealth of knowledge and experience in this field, but also for his counsel in the supervision in this work. I also want to thank my colleagues at the Institute for Neural Engineering, as their camaraderie and advice made my time there enlightening as well as enjoyable. Finally, I want to thank my family and friends for the constant encouragement, support and motivation.

Abstract

In most sensorimotor rhythm (SMR) based brain-computer interfaces (BCI) the tasks performed for control are often far removed from the actual goal. The idea of a BCI based on movement-related cortical potentials (MRCPs) is to use the actual task for control in order to develop a more intuitive BCI. Also the monotony of calibration and training of a BCI can be tiring and demotivating as tasks have to repeated many times. A game based training structure might be an option to motivate subjects and improve their experience.

In this thesis, a BCI based on the discrimination between MRCPs using a computer game as the paradigm was built and evaluated. Evaluation was done incorporating an online experiment with 10 subjects. For this a recording paradigm based on the BCI Trainer game of the More-Grasp project was built. Data for three upper limb movement execution classes, palmar close grasp, lateral close grasp, and supination, were recorded. This data was then used to find an ideal classification time point by cross validation and using it to train a classifier. Each subject then played the game using the BCI, where they received feedback in form of an avatars hand performing the correct movement and the score increasing, when the movement class was detected correctly.

The scores and results showed that every subject had significant control over the three classes. On average each subject scored 67 correct out of 135 trials which represents an accuracy of about 50%. The comparison of the offline and online results suggest the performance might be increased by further training to perfect the timing of the performed movement. These results confirm the suitability of using MRCPs in combination with the BCI Trainer game for an online BCI. Though the system in its current form is not an solution for dependable three class control, it represents a promising starting point towards building a independent more versatile system in the future.

Keywords: BCI, MRCPs, Classification, LDA, Game based

Kurzfassung

In den meisten klassischen Brain-Computer Interfaces (BCIs) hat die durchgeführte Bewegungsaufgabe, die zur Steuerung dient, meist nicht viel mit dem tatsächlichen Ziel zu tun. Durch die Nutzung von Movement-Related Cortical Potentials (MRCPs) können die tatsächlichen Bewegungen zur Steuerung verwendet werden, um ein intuitives BCI zu implementieren. Auch die Monotonie der Kalibrierung eines BCIs und das Training können ermüdend und demotivierend sein, da die Aufgaben viele Male wiederholt werden müssen. Eine spielbasierte Trainingsstruktur könnte eine Option sein, um Teilnehmer zu motivieren und ihre Benutzererfahrung zu verbessern. In dieser Arbeit wurde ein BCI, basierend auf der Unterscheidung von MRCPs, mit einem Computerspiel als Paradigma implementiert und evaluiert. Diese Evaluierung wurde mittels eines Echtzeitexperiments mit 10 Teilnehmern durchgeführt. Dafür wurde ein Aufnahmeparadigma basierend auf dem BCI-Trainer-Spiel aus dem MoreGrasp-Projekt implementiert. Instanzen von drei Handbewegungsklassen, Palmargriff, Lateralgriff und Supination (rechts Drehung), der Hand wurden aufgenommen. Diese Instanzen wurden verwendet, um den idealen Klassifizierungszeitpunkt durch Kreuzvalidierung zu bestimmen und damit den Klassifikator zu trainieren. Jede Teilnehmerin und jeder Teilnehmer spielte nun mittels BCI das Spiel. Sie erhielten Rückmeldungen über ihre Leistung in Form eines Avatars, der die richtigen Bewegungen ausführte und der steigenden Punktzahl, wenn die Bewegungsklasse richtig detektiert wurde.

Die Punktzahlen und Resultate zeigten, dass jede teilnehmende Person signifikante Kontrolle über die drei Klassen hatte. Im Durchschnitt erreichten die Teilnehmer 67 von 135 Punkten, was eine Genauigkeit von zirka 50% bedeutet. Der Vergleich der Kalibrierungs- und Echtzeitresultaten deutet an, dass diese Leistungen mit weiterer Übung und besserem Timing noch verbessert werden könnten. Diese Resultate bestätigen die Eignung von MRCPs in Kombination mit dem BCI-Trainer-Spiel für die Anwendung in einem Echtzeit-BCI-System. Auch wenn das System in seiner derzeitigen Form keine vollständige Lösung für eine zuverlässige Dreiklassensteuerung ist, repräsentiert es trotzdem einen Startpunkt für die Entwicklung eines unabhängigen, vielseitig einsetzbaren Systems in der Zukunft.

Keywords: BCI, MRCPs, Classification, LDA, Game based

Contents

Abbreviations

BCI	Brain-Computer Interface
EEG	Electroencephalogram
SCI	Spinal Cord Injured
ALS	Amyotrophic Lateral Sclerosis
CAR	Common Average Reference
SSVEP	Steady State Visual Evoked Potentials
ERD	Event-Related Desynchronization
ERS	Event-Related Synchronization
SMR	Sensorimotor Rhythm
SCP	Slow Cortical Potential
MRCP	Motor Related Cortical Potential
BP	Bereitschaftspotential
sLDA	Shrinkage Linear Discriminant Analysis
LDA	Linear Discriminant Analysis
3D	Three Dimensional
USB	Universal Serial Bus
TCP/IP	Transmission Control Protocol/Internet Protocol
PCA	Principal Component Analysis
EOG	Electrooculogram
ECG	Electrocardiogram
STD	Standard Deviation
IIR	Infinite Impulse Response
TU	Technische Universität
EOF	End Of File
ROI	Region Of Interest

1

Introduction

1.1 Brain-Computer Interfaces

The idea of a brain-computer interface (BCI) is to enable users to control (assistive) devices only by intentional brain activity [1, 2]. Brain activity can be measured invasively using electrodes placed directly in the cortex [3, 4], or non-invasively, by for example recording the electroencephalogram (EEG) in realtime as it measures the electrical activity of the brain, which reflects the activity within. In this thesis, solely non-invasive recorded EEG will come to bear. Ultimately, BCIs should help severely motor impaired persons, like high spinal cord injured (SCI), people suffering from amyotrophic lateral sclerosis (ALS) or locked-in patients to gain more freedom and autonomy in their daily life.

Despite the different brain activities and their fundamental differences, the classical designs of brain computer interfaces are vastly similar to each other. The principle of each BCI can be categorized with these basic components (see Figure 1.1): signal acquisition, preprocessing, extraction of features, classification, application and feedback.

In the Graz BCI laboratory, signal acquisition is usually done in a non-invasive manner, utilizing EEG. The signal is eventually preprocessed to increase the signal to noise ratio, e.g. by applying spatial filters, such as Laplacian derivation or common average reference (CAR) filters [5, 6]. Thereafter, features, which describe the differences between the targeted conditions in the best possible way, are extracted. The extracted features are then used to train a classification model [7, 8] of which the output can be used to drive any connected application. BCIs work in a closed loop manner, this means for every action users set or intend the BCI must offer feedback usually by the application.
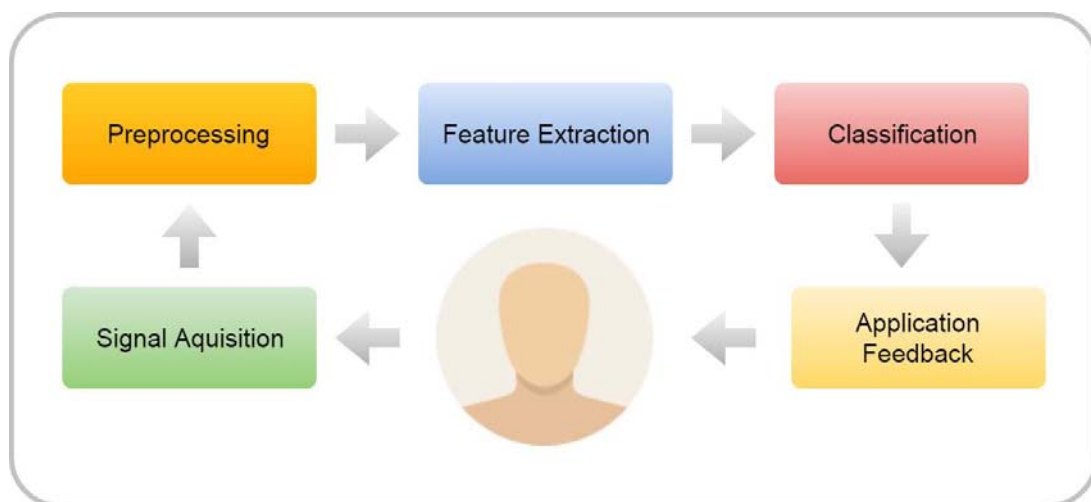

Figure 1.1: The basic components of a BCI.

BCIs can be driven by various kinds of brain signals, some of them are externally driven, like in P300 spelling systems, where with the help of a spelling matrix letters or musical notes can be selected [9,10]. In these systems, while fixating the attention on the targeted letter or note, rows and columns in the selection matrix start flashing, this way eliciting event-related potentials, such as the P300, which can later be used to discriminate between the targeted letter and all other elements in the matrix.

Another group of BCIs make use of steady-state visual evoked potentials (SSVEP), which are the natural response to a visual stimulus, for example lights flashing in a certain frequency range ($\sim$ 6 Hz to 30Hz). These designated flicker frequencies and its harmonics are mainly represented in occipital brain regions and have been used in BCIs for controlling many applications like [11] flight simulators or even in neuroprosthesis [12] [13]. But not only BCIs utilizing externally driven stimuli are used, the main research focus actually lies on internally driven or self-paced BCIs, where users are not dependent on flashes or flickering, rather than they attempt to modulate their brain signals on their own intention.

For the last decades the Graz-BCI approach was based on self modulated rhythms, which could be detected by EEG [14]. These self modulations were usually generated by mental imagery of different tasks like imagined repetitive plantar flexion/extension of both feet or imagined repetitive hand movements [15]. But also non-motor tasks like mental subtraction or [16, 17] or imagining singing a song were used for discriminating different states. These imagined tasks induce a change in power of the EEG in certain frequency bands relative to a rest period. These changes are called event-related desynchronization (ERD) and event-related synchronization (ERS). Users may trigger these modulations independently, but they can also perform this on an external demand like an instruction (cue). These so called sensorimotor rhythm based BCIs (SMR-BCIs) were largely investigated and applied for various control purposes like neuroprosthesis [13], selectors [18] and eventually playing and competing in video games [16, 19, 20].

1.2 Movement-related Cortical Potentials

Although SMR-BCI studies in healthy as well as in severely impaired persons show promising results, they still lack natural control modalities in most applications. While SMR-BCIs do detect the difference in various self modulated brain states, they do not recognize the actual intended movement. This means users may end up using repetitive motor imagination of foot movements for controlling the opening or closing of a hand neuroprosthesis, which is neither intuitive nor resembles any form of natural control.

Recently, the Institute of Neural Engineering at Graz University of Technology, in looking for ways to overcome this problem, became engaged in the investigation of slow cortical potentials (SCP) while performing movements [21]. Most prominent among those movement-related cortical potentials (MRCPs), an example is shown in Figure 1.2, is the so called Bereitschaftspotential (BP), which can be described as a negative peak in the EEG amplitudes imminent to the actual onset of a movement [22]. This negativity starts already before the movement onset, peaks around the movement onset and reverts back to normal niveau. It can manifest in different forms depending on the executed movements, like foot movements or upper limb movements. Studies have shown that utilizing these MRCPs, various upper limb movements [23] and even different grasps [24] can be discriminated. These findings could lead to a possible solution in order to use the actual intended movement as a control signal for the same movement performed by a robotic arm or a neuroprosthesis.
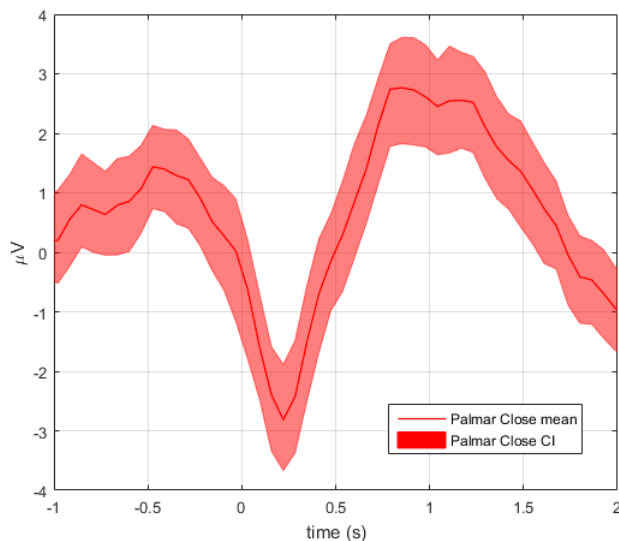
Figure 1.2: Example of an MRCP resulting from performing a palmar closing grasp, calculated by applying non parametric t-percentile bootstrap statistic using alpha of 0.05 and epoched on the detected movement onset at 0.

1.3 Games in BCI

BCI use is a skill, which users have to learn. A classification model usually has to be calibrated each new day before it can be used, since the variation in electrode position and impedance severely diminishes the performance of pre-trained or generalized classification models. In these calibration sessions users have to perform their training tasks repetitively and 60 to 80 repetitions per conditions are not uncommon. Instructions for those repetitions, also called trials, are usually given in an abstract form using crosses for fixating the gaze and pictograms (like a hand or feet) or arrows (for directions) instructing the user what to do. These recurrent calibration sessions can become fatiguing and moreover demotivating to a user.

Todays video game industry enlists more than 2.5 billion customers all over the globe with a total revenue (in 2017) of 78.61 billion dollars [25]. On a basic level, a video game demands similar actions from its user than the BCI calibration does: fixation of the gaze towards objects on a screen, timely performing actions according to instructions (classic: buttons, or movements, as in the Nintendo Wii) and full attention of its users. However, video games are able to engage its users for hours, often on daily basis.

With respect to these similarities, a number of game-based BCIs have been developed. There are systems using SSVEP features like a games to navigate in an 3D environment [26] or a 2D racing game [27]. Also there are P300 features based systems, one allows users to play space invaders [28] another Tetris [29]. Because both types of BCIs rely on external stimuli, they are not suitable for self paced systems which is an essential step towards natural control. There are self paced system based on SMR features to play games like pinball [30], Tic Tac Toe [31], maneuvering in 3D spaces [32] or even an international BCI competition game [16]. Even though these system enable self paced control, they often use very abstract tasks e.g. tongue movement imagination for navigation [31] and they usually suffer from a significant response time.

Towards building a system that offers more intuitive control the the GrazBCI lab developed

the so called BCI Trainer game as part of the MoreGrasp project [33], which incorporates elements of a video game to improve the experience of BCI calibration and training (see Figure 1.3). In this game users control a wheelchair bound avatar in a virtual environment who has to perform different actions like grasping a glass, opening doors or switching a radio on, which correspond to common movements of the upper extremity. The game was built to support eight different movements, of which three are relevant for this work, a palmar close gasp (palmar grasp) for picking up and drinking from a glass, a lateral close grasp (lateral grasp) for eating soup with a spoon, a supination of the wrist (supinate) for turning a radio louder. For each run the tasks and its number of repetitions that should be performed are set in advance. In the game the avatar moves around a normal room where objects corresponding to the tasks are placed in a typical manner. The avatar comes to a rest in front of them, reaches out the hand towards it and then stops, waiting for instructions. If the correct command is sent to the game, the hand performs the correct movement, if the wrong command is sent it shakes from left to right. In a run each object is visited in a random order as often as previously defined. After a run, users are presented with their reached score, which reflects how many movements were detected correctly.
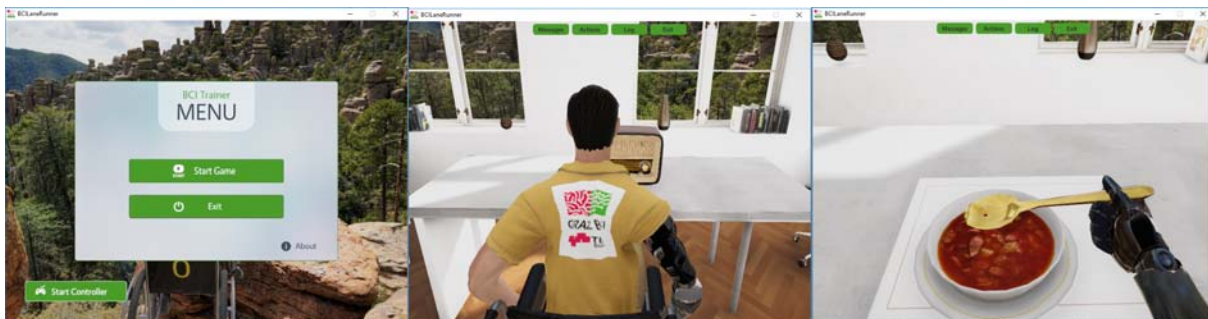

Figure 1.3: BCI Trainer Game.

1.4 Motivation and Aim

In the field of BCIs, there are many challenges and limitations that have to be considered. Some depend on external stimuli, others rely on mental tasks which do not correlate with the goals of the BCI and usually the experiments are very monotonous which can be boring and in turn exhausting for subjects. The idea behind this thesis was to build a BCI, which counteracts many of these issues, by decoding MRCPs of the actual task to generate a control signals and training users in a game-based scenario in order to improve their experience. The aim of this thesis was to build an intuitive multi-class BCI, by using the BCI Trainer game as basis for calibration and training. By combining the positive features of a computer game for the calibration for a BCI system, a less taxing and in turn more appealing way of setting up such a system should be reached. Additionally, using MRCPs as features, will allow using the same movements as in the game which will provide better natural control options for the BCI. To evaluate this system an experiment with ten healthy subjects will be performed and their performance evaluated. The following thesis will describe every aspect of the system and experiment in detail, as well as present the subsequent results and conclusions.

2
Methods

2.1 Concept

The concept of the proposed system and in turn for the experiment can be seen in Figure 2.1. It shows the steps and components for the three class MRCP BCI and its evaluation. First step of the BCI was to record calibration data trials for three selected hand movement classes: palmar grasp, lateral grasp and supination. Recorded was not only EEG, but also information about the hand movements of the subjects, as well as a photodiode signal for synchronization and the event informations from the BCI Trainer game which were stored synchronously to the other signals. In order to use these collected signals and information for calibration, data processing was performed in the next step. Its purpose was to find and align the game events to the EEG as well as the movement onset which had to be detected first. A classification model, a regularized linear discriminant analysis model (sLDA) was determined by cross validation.
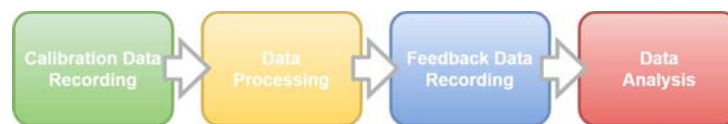

Figure 2.1: Concept of the experiment.

The online feedback data recording system, which was the main element of the BCI, can be seen in more detail in Figure 2.2. It shows the data processing steps of the built BCI. As one can see, the EEG was first band pass filtered, as well as CAR (common average reference) filtered in the preprocessing. Time domain features were extracted and classified by the sLDA. The continuous classification output was smoothed and transmitted to the game control block, which handled the timing of sending the triggered class to the BCI Trainer game. The game, which acted as the paradigm in this experiment, then displayed this trigger as a hit or a miss, presenting feedback to the subject.
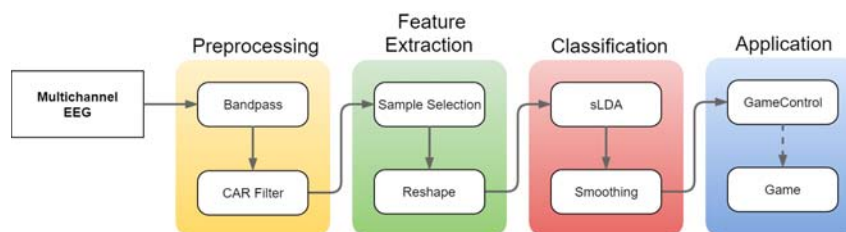

Figure 2.2: Overview of the concept of the feedback data recording system.

The final step of the experiment was to analyze and evaluate the recorded data and performance of the subjects. A number of statistical analyses were calculated, as well as EEG correlates and topographical overviews extracted.

2.2 Data Processing

2.2.1 Cue Detection and Management

Photodiode Flag Detection

The first step in the data processing part of this system, was the cue alignment of the game and the photodiode, as unwanted delays (e.g. network packet loss) could occur between the game event and the photodiode flag. To the subjects, the stopping of the hand was the cue to start their movement execution. This was accompanied by a flash (not visible to the subjects), which was recorded by a photodiode. The exact time point of this cue was extracted and aligned with the corresponding game event as follows:

The photodiode signal was cleaned of any trends, by subtracting the mean of the signal, and then subtracting the median filtered signal. This median filter had a window length of 332ms. After normalization of the signal between 0 and 1, a threshold of 0.4 was applied. For each relevant game event, the next second of the processed photodiode signal was searched for the first rising edge. If none was found, the correlating event was discarded, as correlation to the photodiode and in turn to the EEG could not be guaranteed any more. Additionally, the average time delay between the two was also calculated and saved for later use.

Movement Onset Detection

When working with MRCPs, the movement onset is the most important time point. For this purpose the movement onset was calculated separately for each trial and linked to a game event and its photodiode flag.

To do this, data from the data glove was analyzed. First, broken channels of the data glove had to be disregarded. The data glove is equipped with a number of stretch sensors, which would usually output values between 0 and 1, according to their state. But some of the sensor channels only deliver up to 5 discrete values, which suggest that they are not working correctly anymore. By disregarding any channel, that displayed this behavior, it was assured no irrelevant information attributed to the detection.

The next step, was to epoch all trials of each class from -3 to 3 seconds with respect to the photodiode cue. For each class of movements, a principal component analysis (PCA) was calculated, in an effort to reduce the dimensionality of the signal [34]. PCA is a tool, that tries to decorrelate the principal components of signals. It does this by finding weights to transform the input variables, in our case the data glove channels. The result is an output, where the first principle component is responsible for as much variance as possible. The second principal component explains as much of what is left, while being independent of the first and so on. This leads to uncorrelated components which explain all off the variance of the data. In this case the PCA was used to find the movement information in the data glove signals. The idea was, that when movement occurs, the resulting signal was correlated across all the sensor channels and was the source of the majority of variance in the signals. By calculating the first principal component, a single dimensional representation of the movement was reached.

To eventually extract the onset of this simplified movement, each trial was processed separately. First they were smoothed using a bidirectional mean filter, with a window size of 200ms. Then the signal was differentiated, squared and normalized between 0 and 1. The resulting curve, was now searched for gradients that exceeded 1.5. If any existed, the position of the first, in the range of -0.5 to 1.5 around the cue, was selected as the movement onset. This range was

chosen, as some subjects might have started too early and some might have started delayed. If no movement onset was found in the range, the trials was not used for further analysis. Finally, for each class and each subject, the average delay between photodiode cue and movement onset was also calculated and saved for later use.

2.2.2 Preprocessing

Dealing with Artifacts - Outlier Rejection

Artifacts are unwanted features in EEG recordings, whose source is not the intended measurement target, the brain. Since EEG records electrical potential on the scalp of humans, not only signals originating from the cortex are picked up. Due to volume conduction of the body and head, potential shifts can be transmitted all over. This is the reason, why physiological potentials like eye movements, muscle activity or even ECG (electrocardiogram) can sometimes be observed in EEG recordings [35]. But, not only physiological artifacts, as described, can influence a measurement. A number of technical artifacts like 50 Hz power line noise, impedance changes of electrodes or amplifier noise can be a problem. In every EEG experiment artifacts are a known issue that has to be addressed. While the best strategy for dealing with them is to avoid them, whenever possible, they cannot be fully prevented. Their presence can negatively impact performance of a BCI, or worse, lead to an artifact driven BCI. To prevent influences from artifacts, measures have to be taken to prevent and detect them.

In this experiment an outlier rejection, based on statistical parameters, was performed on the trials. The system was initially based on findings by Delorme et al. [36], but also successfully included by Faller et al. [37] and Schwarz et al. [15, 23, 24].

The rejection criteria were:

- **Amplitude**
  This method rejected any trial in which any channel or sample exceeded a threshold of +-125 μV.

- **Variance**
  This method rejected trials if the variance of a channel exceeded the threshold of 5 times the standard variance.

- **Probability**
  This method rejected trials based "unusual behavior". To do this the joint probability of the trial is compared to the one of all trials.

- **Kurtosis**
  This method also rejects trials based on unusual probability distributions. Here the kurtosis of a trial is calculated and compared to a threshold [38].

After the cue detection and the outlier rejection, on average 52 trials remained per class. Using similar methods, also artifact afflicted channels were identified to exclude channels showing power line noise or muscle artifacts. These were recognized and later not used in the spatial filtering.

Filtering and Downsampling

As previously discussed, MRCPs are features that occur in a low frequency band. To prepare the signals, a unidirectional, fourth order, IIR, band pass filter, between 0.3 and 3 Hz, was applied to all EEG channels which were recorded at 512 Hz sampling frequency.

To increase signal to noise ratio, a common average reference filter (CAR), was applied to the band pass filtered signals. CAR filtering works by subtracting the average amplitude over

all channels, from each channel at each time point. For calculation of this average amplitude, channels marked by the statistical outlier rejection were excluded. Channels with high noise would have a great impact on the average, thus spreading unwanted noise over the whole scalp. In this way a single noisy channel on outer scalp position might drive the classification model.

Downsampling to 16 Hz was performed on the resulting signal in an effort to facilitate online computational performance. As the upper frequency bound of 3 Hz of the used band pass, is still lower than 0.5 times the sampling frequency at 8 Hz, Nyquist's criterion is upheld.

From the resulting signals, trials were epoched from -3 to 3 seconds around the previously calculated movement onset for further calculations.

2.2.3 Feature Extraction

MRCPs are event related potentials in EEG, which can be observed alongside the onset of movement execution. Using these time domain features, requires the system to, not only see one sampling point, but a number of samples over time. The number of samples selected and their distribution over time is always a trade off. If too many samples are selected, computational effort for classification could cause the system to not perform in real time, which makes online classification impossible. Whereas, too few samples might not contain enough information to reliably distinguish between classes.

For this thesis, the feature extracting procedure used is shown in Figure 2.3. For each time point, a trailing window of one second was chosen. Of this window, every second sample was taken. In previous work of Schwarz et al. (Schwarz et al. 2018), this window delivers the best trade off between number of samples and performance. These resulting 8 samples were taken from every channel, combined and transformed into a one dimensional feature vector, as can be seen below. The result was vector of size 1x456 (57 channels times 8 timepoints). As a trial or data stream progresses, the next feature of the next time point is selected, by shifting the selection time point along the time axis for each sample. This allows for continuous feature extraction and subsequent classification.
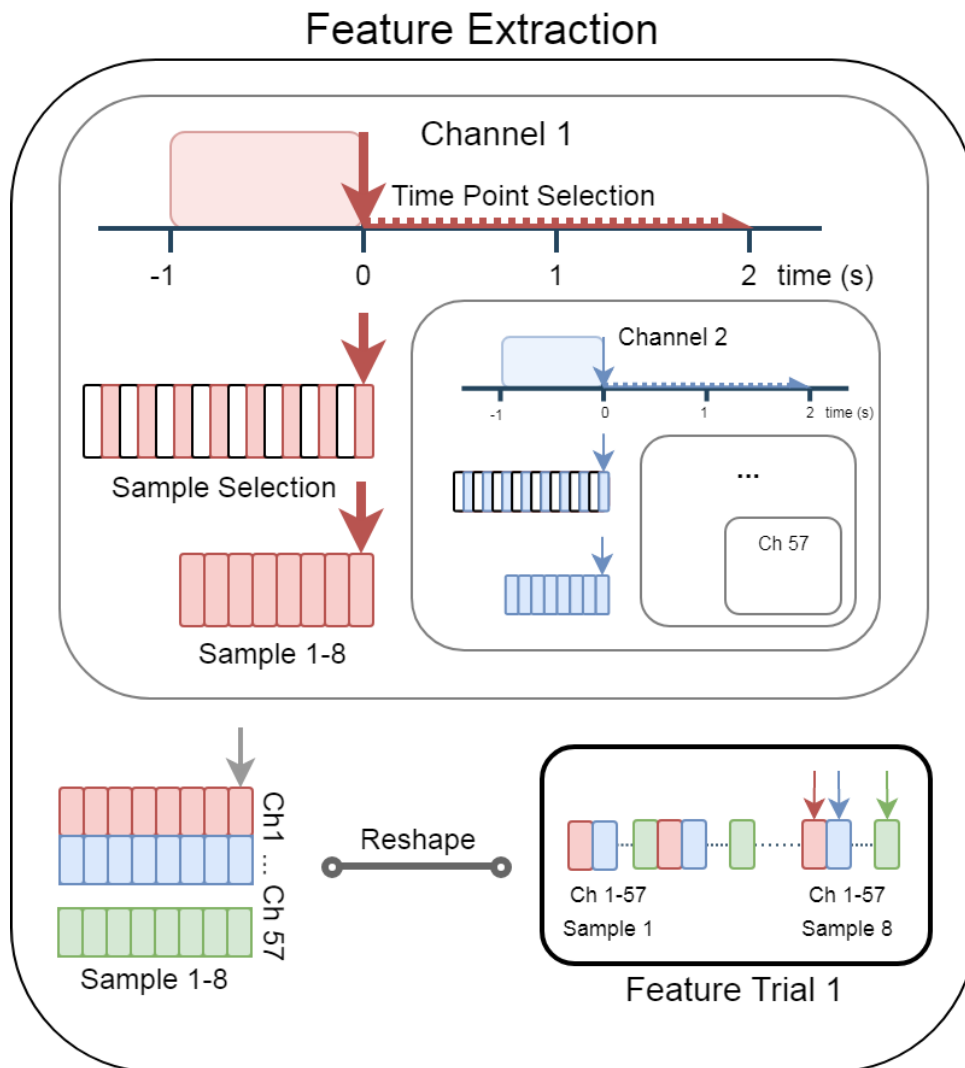
Figure 2.3: Overview of the time domain feature extraction process.

2.2.4 Classification

In this experiment a suitable multi-class classifier was required. A multi-class shrinkage linear discriminant analysis (sLDA) was chosen, as it showed promising results in previous studies [21, 23, 24].

Shrinkage Lineare Discriminant Analysis

A multi-class linear discriminant analysis is a common method of classification in, not only EEG experiments, but also many other machine learning tasks like distinguishing between facial expression [39] or for text classification [40]. It operates by finding linear combinations of features, which are characteristic for or separate, the chosen classes. The idea of an LDA, is to increase class separation, by reducing data variation within classes, through maximizing the ratio of "between-class variance" to "within-class variance" [41].

Looking at the theory behind it, a set of samples are given by x1,....,xn and their class labels

as y1,...,yn. The within-class scatter matrix, where μ_k is the sample mean of the k-th class:

$$S_w = \sum_{i=1}^{n} (x_i - \mu_{y_i}) - (x_i - \mu_{y_i})^T \tag{2.1}$$

The between-class scatter matrix, an estimation of the covariance matrix, where m is the number of classes, μ is the overall sample mean and n_k is the number of samples in the k-th class:

$$S_b = \sum_{k=1}^{m} n_k(\mu_k - \mu) - (\mu_k - \mu)^T \tag{2.2}$$

This allows us to formulate the multi-class LDA as an optimization problem, by maximizing the ratio of between-class scattering to within-class scattering:

$$\widehat{w} = arg \max_{w} \frac{w^T S_b w}{w^T S_w w} \tag{2.3}$$

The result is a generalized eigenvalue problem:

$$S_b w = \lambda S_w w \tag{2.4}$$

A problem, calculating the weights for LDA, occurs with high data dimensionality and few data points. Which was the case in this experiment, as the dimensionality is high, due to the number of channels and samples as described in the feature selection. Additionally, in comparison, the trial number is relatively low. A decrease in classification performance is the result of imprecise estimated covariance matrices, as large and small eigenvalues are scaled incorrectly. To counteract this, regularization called shrinkage is a common tool to compensate the systematic bias [7]. The covariance estimation is redefined, to counteract this error. A factor γ is introduced and μ is the average eigenvalue trace:

$$\widetilde{S} = (1 - \gamma)S + \gamma\mu I \tag{2.5}$$

As S is a positive semi-definite, the eigenvalue decomposition is applied:

$$S = VDV^T \tag{2.6}$$

Due to orthogonality of V we get the eigenvalue decomposition and $\widetilde{S}$ as:

$$\widetilde{S} = (1 - \gamma)VDV^T + \gamma\mu I = V((1 - \gamma)D + \gamma\mu I)V^T \tag{2.7}$$

As a result S and $\widetilde{S}$ have the same eigenvector, while too large and too small eigenvectors are now moderated. The parameter γ is calculated analytically and is described by Blankertz et. al 2011 [7].

Cross Validation and Classifier Selection

In order to find the best time point to train the classifier, a cross validation was performed. The cross validation is of importance, as every subject performs the tasks slightly differently and in turn, the signals may show variations. Although it might be possible that through extensive calculations an even better classifier might be found, due to the experiment boundaries, of recording the calibration trials followed by the feedback trials, a trade-off between good results and calculation time had to be found. For this reason, a five times five cross validation was chosen. Also the trial was restricted region of interest (ROI), from the movement onset to two

seconds later.

The cross validation was performed for each time point in this defined region of interest by repeated training of an sLDA with features of one time point from the majority of the trials, and testing it on the same time point of the remaining trials. This was repeated for all time points until the end of the region of interest was reached.

The result of this calculation was an overview of which time point in the MRCP contains the most differentiating information between classes. From this result the time point with the best performance was selected. With all features of this time point the final classifier was calculated and saved.

Individual Classification Time Point Selection

In the online system, the classifier determined a class for every sample. Selecting the time point, at which the classification is taken for the trials, had to take all delays into consideration as well as the uniqe behaviour of each subject and their ideal classification time point calculated by the cross validation. Each subject performed the given tasks slightly differently, which lead to varying delays for each class as well. As a compromise, the average delay of the movement onset for all classes of a subject was calculated.

The final classification delay was the sum of:

1. The average delay between game events and photodiode

2. The average delay between the movement onset and the photodiode

3. The delay between the movement onset and the ideal classification time point

4. Additional 100 ms, half the averaging window of 200ms of the online system

The resulting delay was saved alongside the sLDA, for further use by the online feedback system.

2.2.5 Data Analysis

Confidence Interval Calculation

In order to show the characteristics and statistical significant differences between EEG correlates of the movement classes, the approach of calculating a confidence interval was chosen. To determine this, all EEG channels were preprocessed as in the online system. They were band pass filtered between 0.3 and 3 Hz as well as CAR filtered. Also, they were downsampled to 16 Hz. All trials were then epoched -1 to 2 seconds around the movement onset. For each class a confidence interval with an alpha of 0.05 over all trials was calculated by using a nonparametric t-percentile bootstrap statistic. This was performed for each channel individually. The approach was chosen, to find an meaningful approximation of the distribution of each time point in a trial, with regard to the movement onset.

Chance Level Calculation

Part of the results of this study were the scores reached by the subjects. In order to determine if a subject was able to successfully control the BCI, the scores had to be evaluated for significance. In this experiment three classes were distinguished. From a statistical point of view, each class had a probability of 33.3% of being classified correctly. Taking into account the number of measurements, the confidence interval for a chance classification, had also been taken into

account [42]. In the experiment 135 trials, 45 per class, were recorded. For this experiment the significance level, for positive classification, was at 40,41% (or 55 out of 135 correct classified trials) with an alpha of 0.05.

2.3 System Setup

For this experiment, two systems were built in, one for calibration data recording and one for feedback data recording. Both systems were based on the standard GrazBCI system. They were implemented using the following software and libraries:

- TOBI Signal Server and Client [43–45]

- MATLAB 2015b

- Simulink

- TCP/UDP/IP Toolbox 2.0.6 [46]

- GrazBCI libraries

All recorded data was saved via MATLAB as .mat files.

2.3.1 Calibration Data Recording

For training data recording a basic model was implemented in Simulink. Its main purpose was to receive and save all incoming data streams as well as collecting and translating events from the BCI Trainer game. For the model the signal server receives and unifies the data streams from the amplifiers and the data glove, and makes it available for applications, like the scope or the TiA/TiD Client which provides the data streams to the Simulink models. The model was first setup using a Matlab script: dev_startup. This script manages the recording runs, initializes the TiA/TiD Client and includes all run relevant data like subject codes or the IP address and port of the game. To start recording a run, it must be executed. During execution, it will ask for the number of the run. This number was later used, in combination with a timestamp, to save the recordings. The initialization script also started the Simulink model for recording the calibration data. In the model, as seen in Figure 2.4, the data was acquired by the TiA/TiD Client from the signal server. It divided the streams into EEG, EOG and data glove data. At the recording stage, the photodiode stream was still part of the EEG. These streams were then unbuffered, as they are handled by the signal server in batches. Additionally, a rate transfer is performed on the data glove signals, as they are recorded at a lower rate. This led to repeated samples which did not impact the functionality of further processing.

An important part of the system was the sfGameControl block. It will be explained in detail later on. In this system it was connected to one of the streams via a placeholder, as it was programmed to function with the classification data in the feedback system as well. In the dev_startup the feedback was set inactive for the recording. The GameControl block was responsible for establishing the connection to the game paradigm, receiving events, translating them and providing them as output to save them. Finally, all the data streams, as well as the event stream, were written to the workspace using the Simulink block. As the model was stopped by the received corresponding event from the game, the data in the workspace was then saved to file.
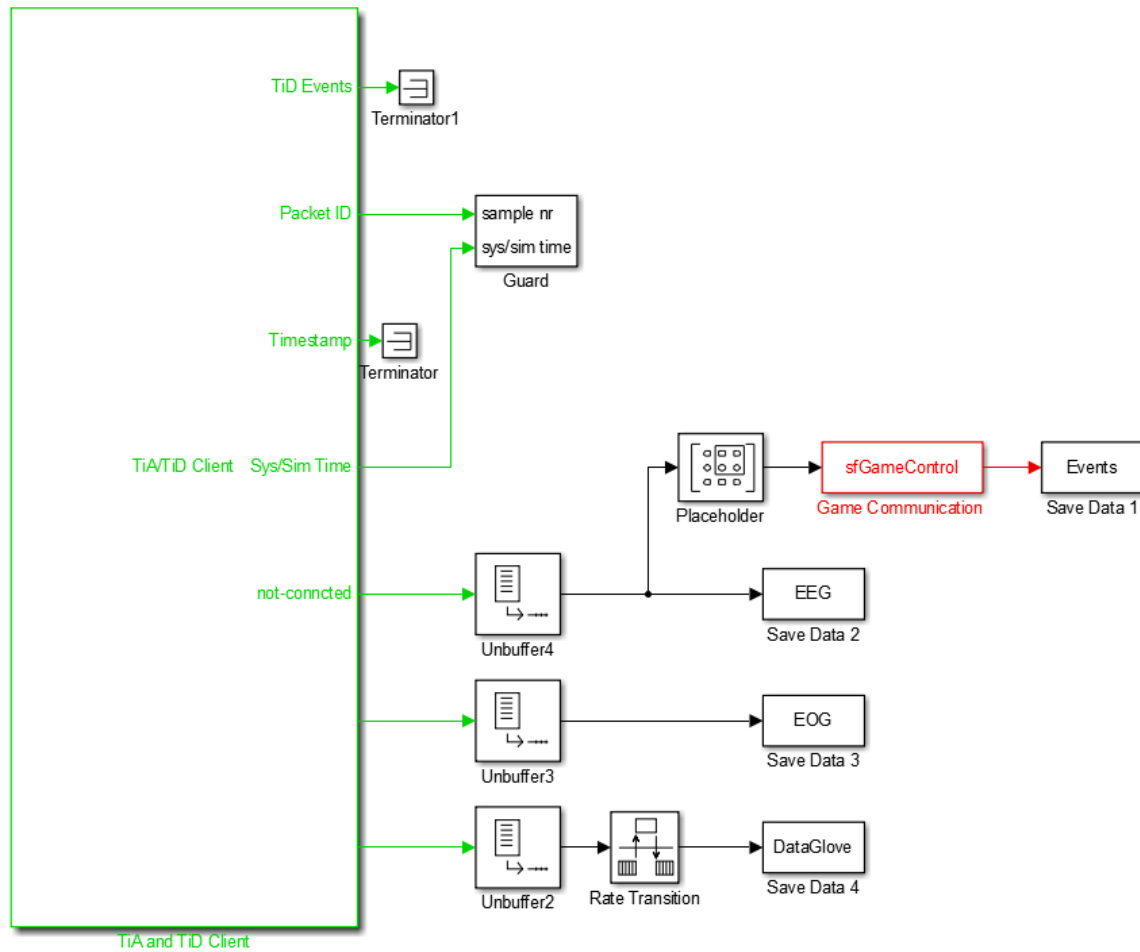
Figure 2.4: Simulink model of the calibration data recording system.

2.3.2 Feedback Data Recording

The online feedback data recording model was basically an extension of the training data recording system. The structure and interactions with other applications like the signal server were the same. For initialization and starting of a feedback recording run, again a dev_startup script was used. Here the functionalities were basically the same, with the exception that all additional information for the online Simulink model, like the sLDA loading or block parameters, were set here as well for easy access.

Figure 2.5: Simulink model of the feedback data recording system.

Lookin at the Simulink feedback system shown in Figure 2.5, it can be seen that the basic recording structure did not change. Only the classification branch off the EEG stream was extended by the classification proceedings. The implementation of the data processing of feedback system started with the submatrix block, which replaced the placeholder from the training recording system. It selected only the EEG channels from the stream which still contained the photodiode channel. The EEG was then treated exactly in the same way, as in the offline preprocessing. First it was band pass filtered between 0.3 and 3 Hz by a fourth order IIR filter. Then the common average reference filter was applied on all EEG channels. Of importance here was, that the same channels which got rejected by the outlier rejection, were not part of the average calculation. In this system the data was also reduced by downsampling to 16 Hz, in order to reduce the computational effort.

After this the features were extracted for each channel. This was realized by implementing an Matlab function, which contained a buffer of all the samples of the last second. With each new sample as an input, it appended the new one and discarded the oldest one. The function then took every second sample in its buffer, as described in the feature extraction, and reshaped them into a feature vector of length 456. The features were then passed along as the output of this block and on to the classification.

In the sLDA block processing, as seen in Figure 2.6, a constant 1 was added to the feature vector. The reason for this was, that the sLDA matrix was designed in a way that the bias did not have to be subtracted separately. This extended feature vector was then multiplied by the sLDA matrix. The result was a vector with the three distances to the hyperplane of the sLDA. Their value indicated how certain the classifier is. To determine the classification, the class with the highest value was found by the maximum block. Through this procedure a classification for every sample was reached. These classifications were then smoothed, with a window of 200ms, by the sfSmoothing function. It operated by buffering the results and calculating the class which occurred the most in the window of 200ms. Additionally, it also reported the percentage of occurrence in the window for the class, as a kind of probability for the class. The output of the sLDA block was the two dimensional vector of class and its probability, as well as the classification output before smoothing, for recording purposes.
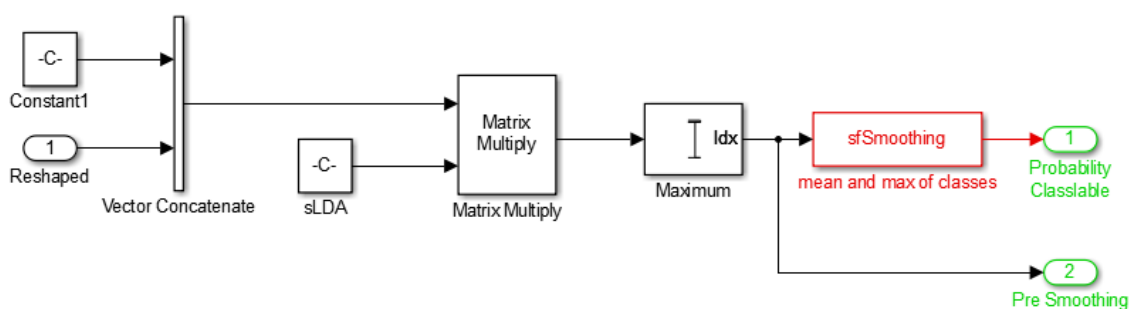

Figure 2.6: Overview of the Classification in the feedback data recording system.

Finally, all resulting signals were brought back to the sampling frequency of 512 Hz by repeating samples. This signal was then monitored by the GameControl block. Depending on the game events, it selected and sent the classification result to the game, if the specified delay after the start movement cue had expired. Also, this event was saved alongside the game events. The

data saving process was the same as in the training recording system.

2.3.3 Game Control Block

One of the most essential parts of the system was the GameControl block. When the Simulink model was loaded, the block first established the connection to the game via TCP/IP, using pnet() from the TCP/UDP/IP Toolbox 2.0.6. Tough MATLAB also includes functions for this purpose, these are part of toolboxes which require a license to be available to work. As these licenses tend to not be free in the TU Graz network, the more robust version via pnet() was chosen. If the connection could not be established an error was shown to the user and the model stopped.

With a working connection, the next step was to set paradigm parameters for the game. This was done by sending the predefined messages as described in the documentation of the game.

These parameters included:

- The number of trials for each class (15 trials per class)

- The seconds per task (set to 3 second)

- Setting the game mode to "Minimal Interaction" (restricting the movement of the avatar to a desk)

- Enabling "Debug View" (enabling the photodiode square)

- Disabling the "Success Gesture" (an additional thumbs up would be performed which would increase recording time dramatically)

Also recording status flags were initialized for later use during the recording. Finally, the command was sent to the game to start the run. During the recording the block performed two major roles. On the one hand, it received and translated the events from the game and on the other hand it decided if and when to send a true or false trigger event back to the game.

The first functionality was triggered by checking if any data was being received. If this was the case, the message was read in letter by letter until the defined delimiter of $''<EOF>''$ was reached. In some programming languages, such as C# in which the game was written, this delimiter could be detected automatically, but this was not possible with the tools of Matlab 2015b. After the message was read in, it was checked for its context and translated to its corresponding event. Each detected event resulted in an output of the block, which contained the event code. For some events additional functionality of the system applied. When a "End of Run" event was received, the recording system would be stopped and all files saved. In case an movement execution event was registered an additional flag in the block was set indicating that a classification would be required. Alongside this flag also the time when it was triggered and the class information was saved.

The second functionality, of sending triggers to game, depended on this flag. If it was set, the system checked it the delay for the classification had passed. As soon as it did, the system compared the classification result at this sample and the open class. If they were identical, a correct classification trigger was sent to the game. If not, an incorrect trigger was sent. Additionally, to the game triggers, also the corresponding events for each class were provided as output and the flags were reset.

2.4 Experiment Setup

The experiment setup for this thesis can be seen in Figure 2.7. Subjects were seated in a comfortable chair in a shielded measurement box. Comfort is important, as subjects are not supposed to move during recording runs. Also, the shielding consisted of a faraday cage and sound suppression material. In front of the subjects, in a distance of 70 centimetres, a computer screen with the paradigm was placed on a table. Right hand movements were also recorded, using a data glove (manufactured by 5DT), as well as synchronization information, recorded by a photodiode attached to the screen.

Figure 2.7: Experiment setup in a shielded measurement box.

2.4.1 Paradigms

Paradigms in BCI systems are commonly very straight forward. First subjects are usually given some kind of point to focus on, then they are presented with some kind of cue after which they are supposed to perform a certain task. While doing this, they are supposed to avoid generating physiological artifacts, like blinking, eye movements and swallowing. One of the issues with this standard approach is that doing this over and over leads to subjects getting bored or tired with the task which leads to worse quality of the recorded data.

Recording Calibration and Feedback Data

The paradigm for the experiment was based on the BCI Trainer game which was developed for the MoreGrasp project [33]. As can be seen in Figure 2.8, it features an avatar in a wheelchair in a normal everyday environment of a living space. Goal of the game is to perform a set of specified movements on correlating ordinary objects. Playing the game, subjects see the avatar driving to the object, reaching for it, with a prosthetic arm, and stopping before the corresponding movement is performed. At this point the game awaits the corresponding command from the BCI. If the game receives the correct input at this time, the hand will perform the correct movement and the score increases. If a wrong input is given, the avatar will shake his hand horizontally and move to the next object.

Figure 2.8: Overview of the game used as paradigm for this experiment.

For the experiment three movement tasks for the right hand were chosen: palmar grasp, lateral grasp and supination. The corresponding objects, or cues in this case, can be seen in Figure 2.9. A glass was shown as cue for the palmar grasp, a spoon for the lateral grasp and the radio knob for the supination. For each of the tasks subjects were instructed to wait until the avatars hand stopped, then perform the movement in one continuous motion, and then hold the end position of it until the object disappeared.

Figure 2.9: Objects which act as cues indicating the task which should be performed.

As the experiment consisted of two parts, recording and feedback, two slightly different paradigms were applied for them. In Figure 2.10 an overview of the recording paradigm for a trial can be seen. The paradigm was nearly the same for the calibration and feedback sessions. The only difference was the 'Feedback' period which only occurred in the feedback sessions. In the calibration sessions, nothing happens additionally to the movement execution.

Steps, timings and instructions of the paradigm were:

- **Object on Screen** (-2 to 3 s)
  While any object was on the screen, subjects were instructed to avoid causing any physiological artifacts, as described before. For this they should always focus their eyes on the same spot of an object to prevent eye movements. They also were instructed, to try to sit still and avoid any unnecessary muscle activity, like swallowing or movements, during this time. And finally, they were told to keep blinking confined to the break period after each trial.

- **Avatar Hand moves towards Object** (-2 to 3 s)
  In this first phase, as the cue object appears on the screen and the game avatars hand of the avatar moved towards the object, subjects were instructed to keep their hand still, not moving in any preparation, and wait until the game avatars hand stopped.

- **Movement Execution** (0 to 3 s)
  After the hand stopped (at 0s), subjects were instructed to perform the indicated task, in one continuous movement, and then hold the end position until the object disappears (at second 3).

- **Break** (3 to 6 s)
  After the object disappeared and the table was empty, subject were free to blink or swallow if necessary.

- **Feedback**
  This part of the paradigm was only part of the feedback sessions. First subjects were again instructed to perform the corresponding movement after the hand had stopped as before. But now, after an individually calculated ideal classification time, feedback was introduced. The hand on the screen either performed the indicated task, if it was classified correctly, or it indicated a wrong classification by shaking from horizontally.
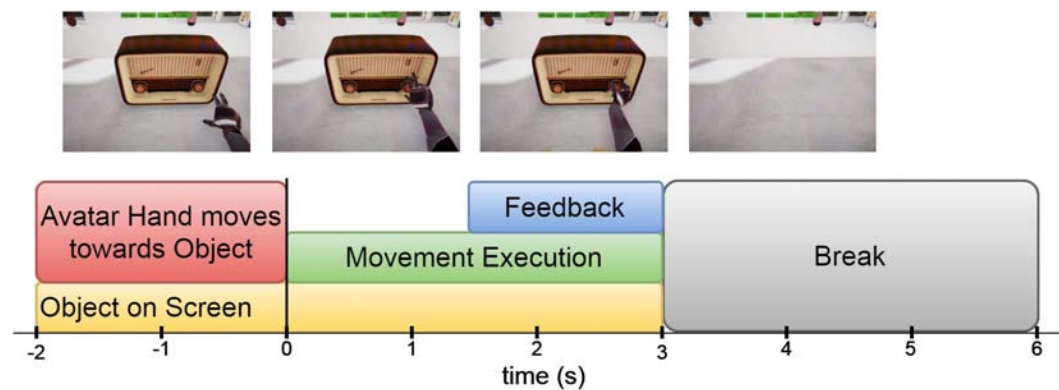
Figure 2.10: Overview of the paradigm in combination with what is shown to the subject at any time.

Rest

In addition to the movement execution, trial of resting EEG were also recorded. Even though for this thesis, the data was not used, for possible further work with this data, it was also collected.

Resting EEG was recorded using a simple paradigm:

1. First the paradigm screen turned black for ten seconds, indicating the start of the recording to help subjects settle down and to give possible filters time to adjust.

2. A small white dot appeared in the middle of the screen for 180s. While this dot was on the screen, subjects were instructed to sit still, avoid swallowing, focus their eyes on the dot and try to keep blinking to a minimum. Their goal was to try to maximize the time between blinks, without forcing their eyes to stay open.

3. Finally, the dot disappeared and 10s more were recorded, where subjects were allowed to blink and swallow but should remain still.

Eye Movements

Artifacts caused by eye movements and blinking have a big influence on EEG data and may drive any classification model instead of actual brain signals. In an effort to remove them, instances

of them can be recorded and later used in processing. In this thesis, this was not done, but as a precaution for possible further work with this data they were recorded as well. The first and the last step of this paradigm are the same as in the rest recording.

The paradigm for eye movement recording:

1. First the paradigm screen turned black for ten seconds, indicating the start of the recording to help subjects settle down and give possible filters time to adjust.

2. Now three different tasks would be instructed. Each of them would last 10 s and be repeated three times in a random order. While any cue was on the screen, subject were asked to sit still and avoid swallowing. After it disappeared, they had 2 to 3 s, in which they were allowed to do this, if they needed to. The different task were:

   a) A small white dot appeared on the screen and it would jump either up and down or left and right in the middle of the screen, with a frequency of about 1 Hz. Subjects were instructed to follow it with their eyes until it disappeared.

   b) Text would appear in the middle of the screen saying "Blinzeln". Here subjects were asked to perform a number of distinct blinks while this was presented.

3. Finally, the dot disappeared and 10s more were recorded, where subjects were allowed to blink and swallow but should remain still.

2.4.2 Signal Recording

All data was recorded and saved at a sampling frequency of 512 Hz. As in this experiment MRCPs were the main signals, timing and synchronicity were of great importance. Especially, the actual time of the movement onset in each trial was of essence. In order to synchronize all data and find the movement onset, not only EEG signals, but also photodiode impulses, data glove signals and of course the event information the game provided were recorded.

EEG

For EEG recording, an active electrode system, from g.tec medical engineering GmbH g.GAMMAsys, was used in combination with four g.USBamps. Using the intrinsic methods of the amplifier a 8th order chebyshev bandpass filter in the range of 0.1 to 200 Hz was applied, as well as a notch filter with the center at 50 Hz. An extended 10-20 system electrode cap, equipped with 57 active ladybird electrodes was used. The electrode positions can be seen in Figure 2.11 where they were positioned according to Oostenveld et al. 10-5% electrode setup [47–49]. Additionally the 3D electrode positions were recorded using an ELPOS system [50] by Zebris medical GmbH.
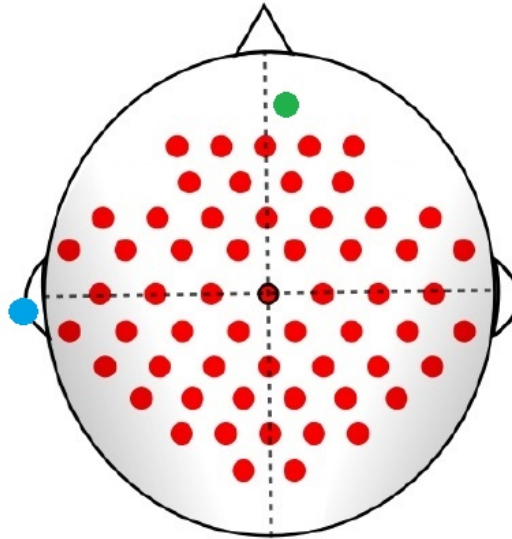
Figure 2.11: Placement of the EEG electrodes, according to the 10-5% system with referece in blue and ground in green.

Electrooculogram

Six lady bird electrodes were placed above, below and next to the eyes as seen in Figure 2.12. Their purpose was to record any signals originating from movements (horizontal or vertical eye movements) or blinks of the eyes.
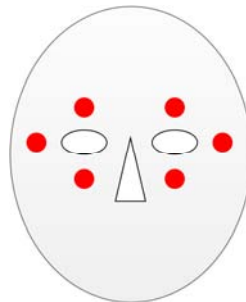
Figure 2.12: Placement of the EOG electrodes around the eyes of the subjects.

Photodiode

One of the main uncertainties in experiments like this, is that due to computation time, signal filters and network transmissions, finding the actual time point of when a subject sees a cue is of essence. To do this, a photodiode system was used. This system worked by placing a photodiode, as a sensor, onto the paradigm screen, where one of the corners is programmed to be black, as a default, and flash white, for 150 ms, as an important event occurs in the paradigm. When this increased light level reaches the photodiode, a potential flag is triggered. This resulting voltage is used as an output signal, which was recorded by connecting it to an empty channel in the USBAmp. There it was transmitted to the recording computer and saved synchronously to the EEG. The result was an additional signal channel that showed distinct flags, at important time points of the paradigm, in the EEG. In Figure 2.13 the photodiode measurement setup can be seen, with the green and yellow cable connecting the photodiode on the screen to the circuit and the black y shaped cable connecting the output of the circuit to the amplifier.
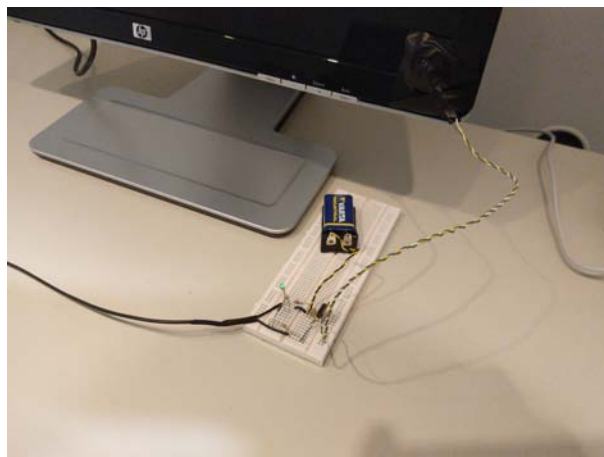
Figure 2.13: Photodiode measurement setup.

Data Glove

In this experiment, the timing of the movement onset for the grasping tasks play an important role in the training data recording, as the classifier was calculated in respect to it. To detect it, information about the right hand movement was recorded, using a 5DT data glove. It measures 14 channels of information about each finger flexure, as well as the abduction between fingers. The information output of these channels was a value proportional to average flexure of each sensor between 0 and 1. These extreme points were defined automatically in the beginning by a calibration, where subjects were asked to perform movements of their hand, in their full range of motion of it. The glove was connected to the recording computer via a medical USB photocoupler. This preventive measure was applied to ensure, no electrical interferences from the data glove would influence the EEG measurement. In the recording computer the data was also handled by the signal server. In Figure 2.14 the data glove and the photocoupler (red) can be seen.

Figure 2.14: Data glove with photocoupler.

Game Data

The game, as seen in the paradigm section, sent a range of information about events occurring in real time to the recording computer. This was done via a previously established TCP/IP connection between them. More information about this data transfer and its implementation can be found in the later chapter System Setup, Game Control Block. Here, we will focus mainly on the game data that is stored with the EEG. As the system received an event from the game, it translated it into an event code which made the data processing later more efficient. Stored events provided general information about each run, like its start and stop event. Also, they hold general timing and information about each trial and its class, like its animation start, the movement execution trigger and the stop event.

Table 2.1: General run event codes, translated and saved by the system.

Event Name	Start of Run		End of Run	
	hex code	dec code	hex code	dec code
	0x300	768	0x8300	33536

Table 2.2: Class specific event codes, translated and saved by the system.

Event Name	Start Movement Execution		Start Class Animation		Class Classified	
Class	hex code	dec code	hex code	dec code	hex code	dec code
Palmar Grasp	0x039D	925	0x139D	5021	0x239D	9117
Lateral Grasp	0x039E	926	0x139E	5022	0x239E	9118
Supinate	0x0308	776	0x1308	4872	0x2308	8968

In tables 2.1 and 2.2 an overview can be seen over the events translated and saved. An important note here is, that while the event code is chosen as an hexadecimal code, as is usually done in the basic GrazBCI, the event code stored is its decimal equivalent.

2.4.3 Experiment Procedure

Subjects

The experiment was performed with ten healthy subjects. Their ages ranged from 24 to 35 with a mean of 27 years. Four of them are male and six female. All of the subjects participated in some kind of EEG or BCI experiment before. All subject were previously informed about the aim and the experimental flow and gave their written consent.

Sessions

Each subject participated in one measurement session, which lasted 2.5 hours on average. Bevore the recording started, participants were shown the paradigms and had the chance to practice performing the movements. This assisted in familiarizing them with the task and helped to insure they would perform the movements consistently the same throughout the recording.

Table 2.3: Overview of the paradigms used and trials recorded for a recording session.

Run Nr	Paradigm Type	Number of Classes	Trials per Class	Number of Trials
1	Rest	1	1	1
2	Eyes	3	3	9
3	Recording	3	15	45
4	Recording	3	15	45
5	Rest	1	1	1
6	Eyes	3	3	9
7	Recording	3	15	45
8	Recording	3	15	45
9	Rest	1	1	1
10	Eyes	3	3	9
11	Feedback	3	15	45
12	Feedback	3	15	45
13	Feedback	3	15	45

As can be seen in table 2.3, one session consisted of 13 runs, of which three runs were recorded using the rest paradigm, three using the eye movement paradigm, four using the recording paradigm and finally three using the feedback paradigm. This resulted in: three recordings of 180s, each, of resting EEG and three trials of 10s, each, of vertical and lateral eye movement as well as blinking. This data was not used for this thesis, it was recorded for possible future work with the recorded EEG data.

The relevant data trials for palmar grasp, lateral grasp and supination class resulted in:

- Calibration Recording Paradigm
  - 60 trials per class
  - 180 trials in total

- Feedback Recording Paradigm
  - 45 trials per class
  - 135 trials in total

3
Results

3.1 Preliminary Testing

In order to test the feasibility of this experiment, a preliminary pilot recording was performed. The goal of this pilot was to evaluate, whether the built data recording system in combination with the game was suitable for recording MRCPs. For this purpose, 80 trials per class of six different movement types of the right hand of one subject were recorded. The six classes (movement types) were: supination, pronation, palmar open, palmar grasp, lateral open, lateral grasp, pincer open, and pincer close.

3.1.1 Movement-related Cortical Potentials

The data processing for the preliminary study was performed as described, with the exception that no common average filter was applied to the data. Figure 3.1 shows the general overview of the recorded MRCPs of all classes, along with the calculated confidence interval shown as the shaded area. In the Figure the, for MRCPs characteristic, strong negative shift at the movement onset can be seen for all classes. Also, an increased negative (compare C1 versus C2) contralateral amplitude can be observed.

Towards building the system, the three classes: palmar grasp, lateral grasp and supination were selected in Figures 3.2, 3.3 and 3.4 the calculated MRCPs are compared against each other.

In Figure 3.5 the topographical overview over of the MRCPs of all six classes of the pilot recording are shown. The selected time points, again centered on the detected movement onset, were distributed to focus on the movement onset.
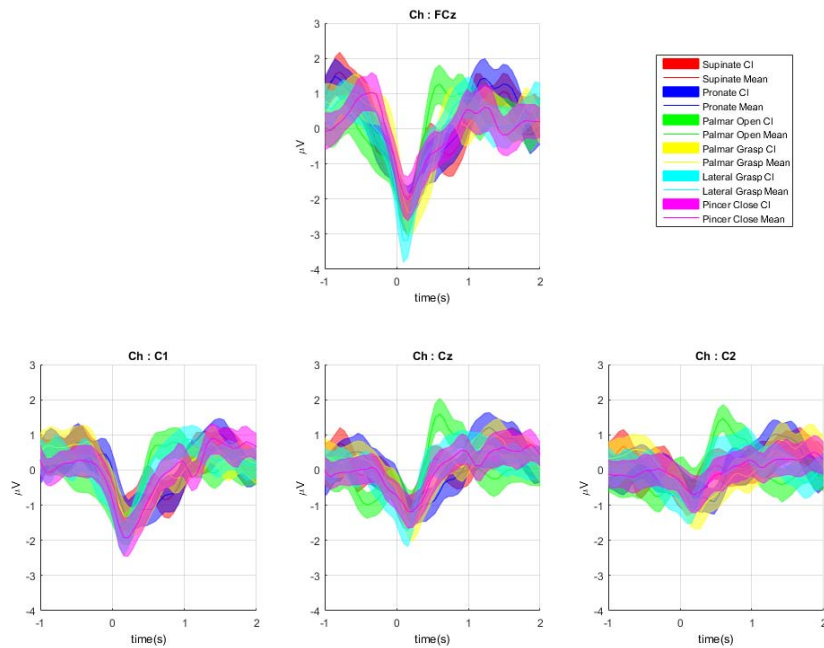
Figure 3.1: *Overview of the MRCPs of supinate, pronate, palmar open, palmar grasp, lateral grasp and pincer close classes, epoched around the movement onset over the central electrodes: FCz, C1, Cz and C2. The continuous lines show the grand average while the shaded areas present the mean confidence intervals.*
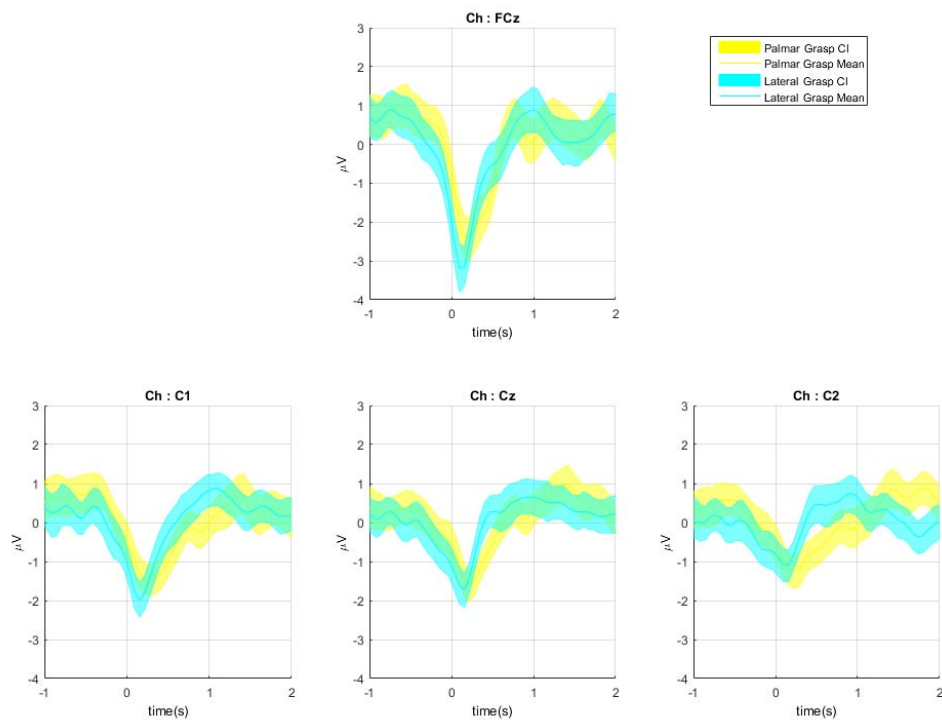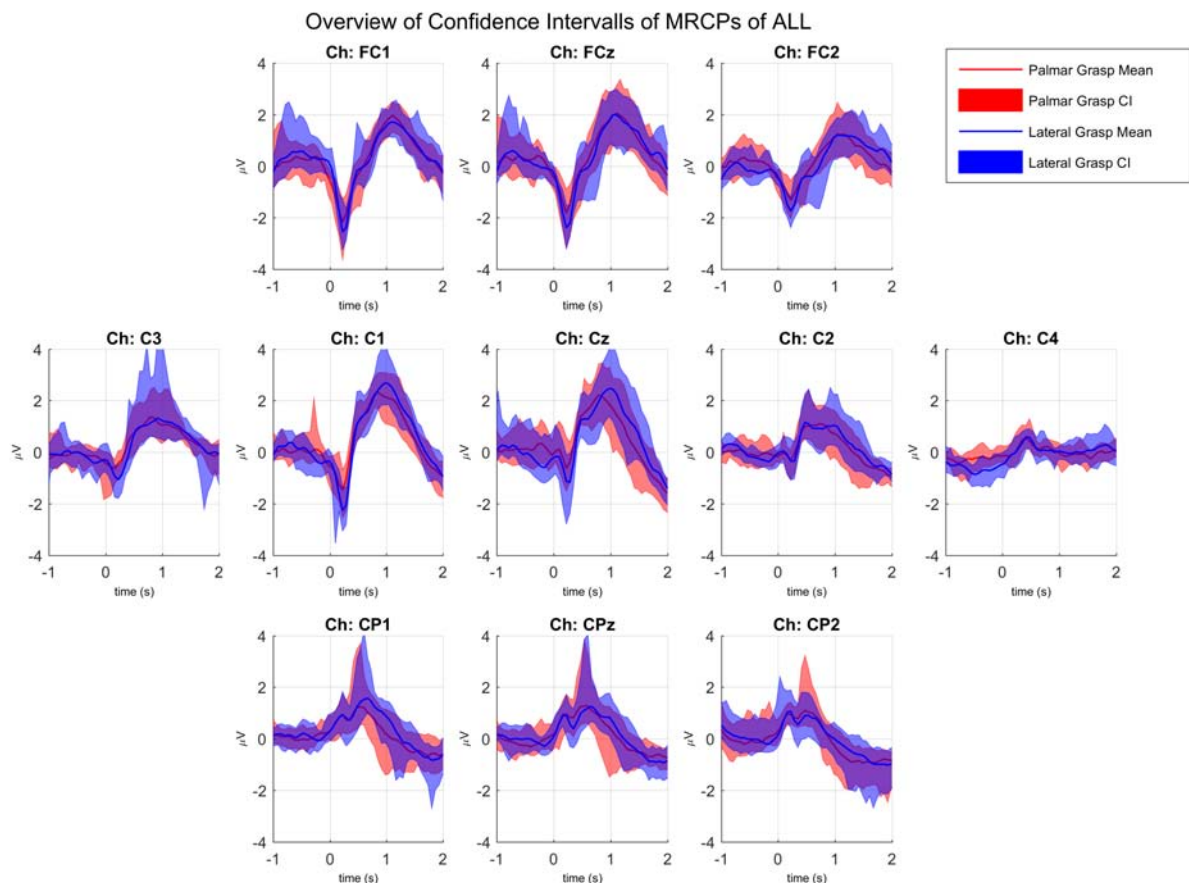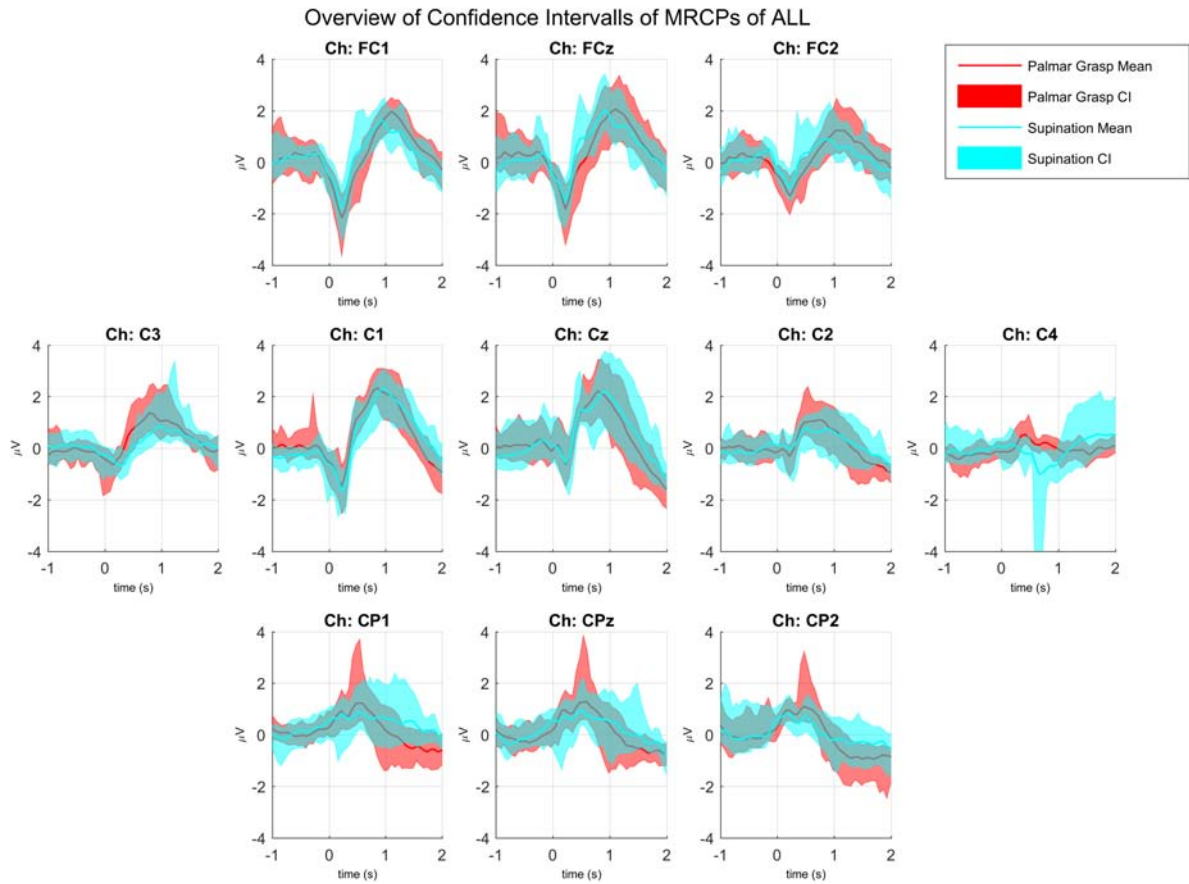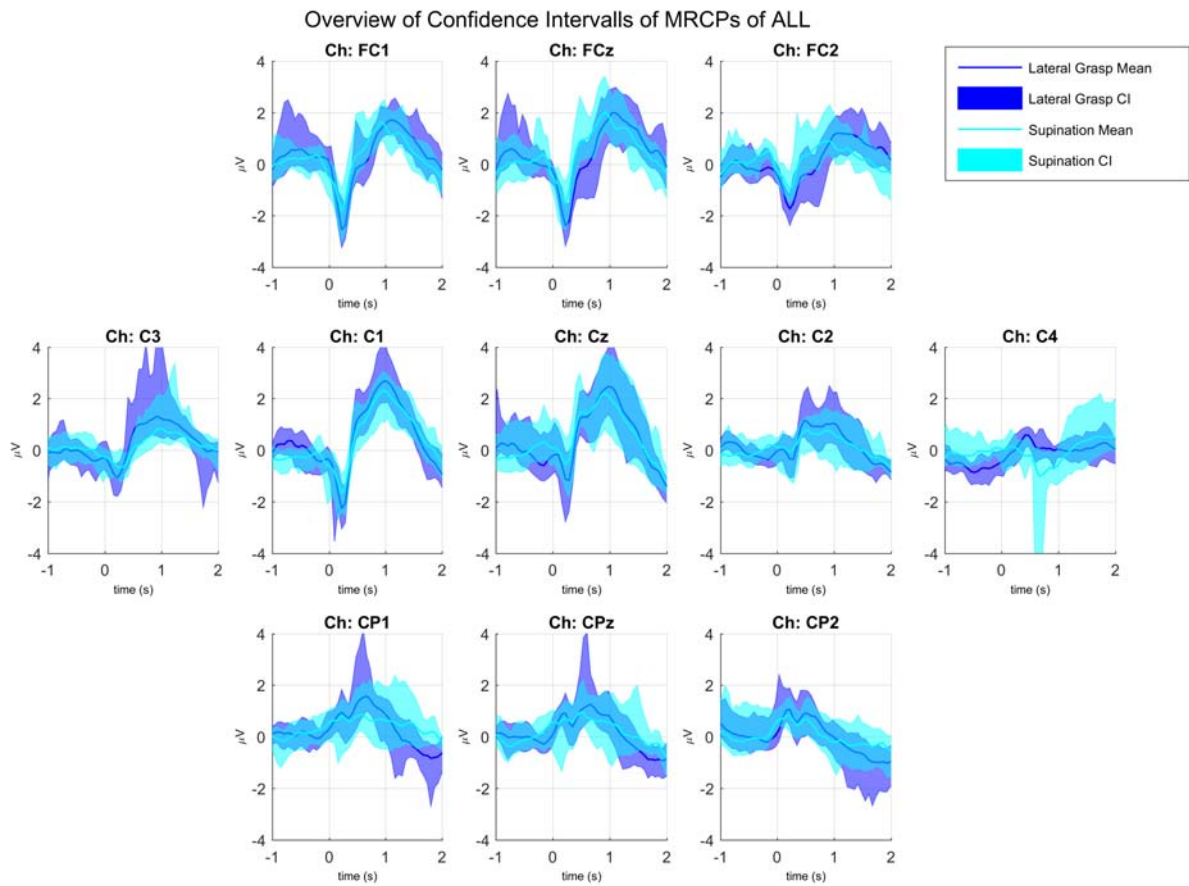

Figure 3.2: *Overview of the MRCPs of palmar and lateral grasp, epoched around the movement onset over the central electrodes: FCz, C1, Cz and C2. The continuous lines show the grand average while the shaded areas present the mean confidence intervals.*
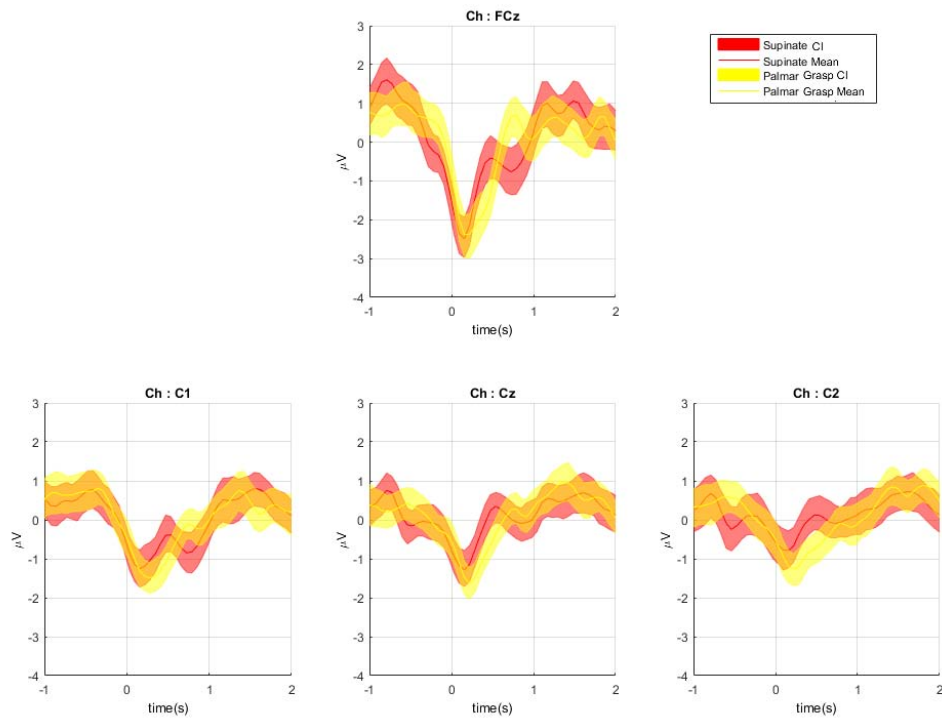
Figure 3.3: Overview of the MRCPs of palmar grasp and supination, epoched around the movement onset over the central electrodes: FCz, C1, Cz and C2. The continuous lines show the grand average while the shaded areas present the mean confidence intervals.
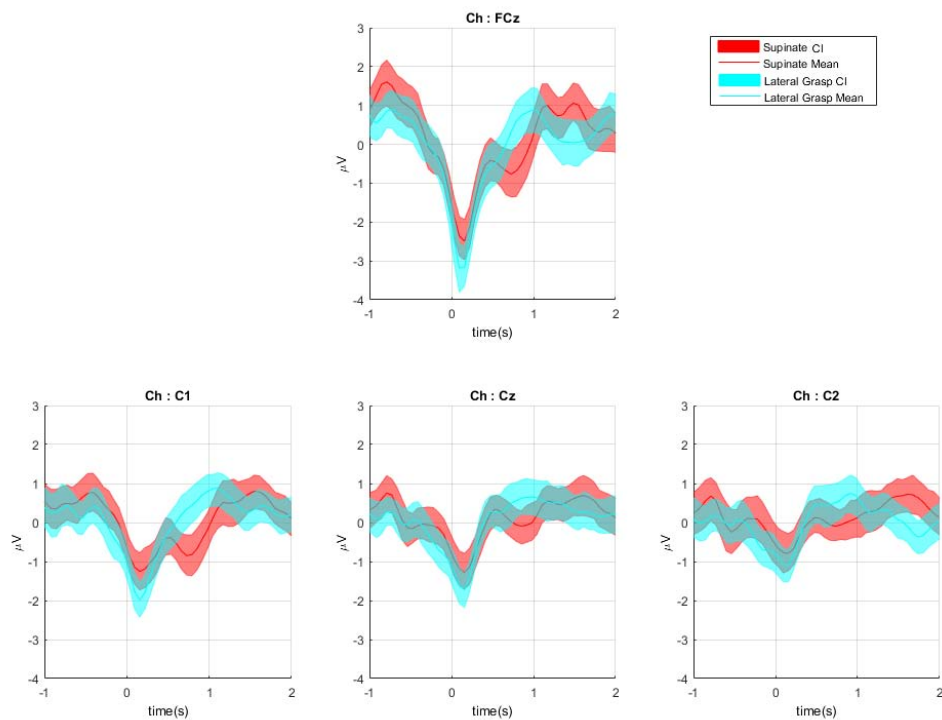
Figure 3.4: Overview of the MRCPs of lateral grasp and supination, epoched around the movement onset over the central electrodes: FCz, C1, Cz and C2. The continuous lines show the grand average while the shaded areas present the mean confidence intervals.
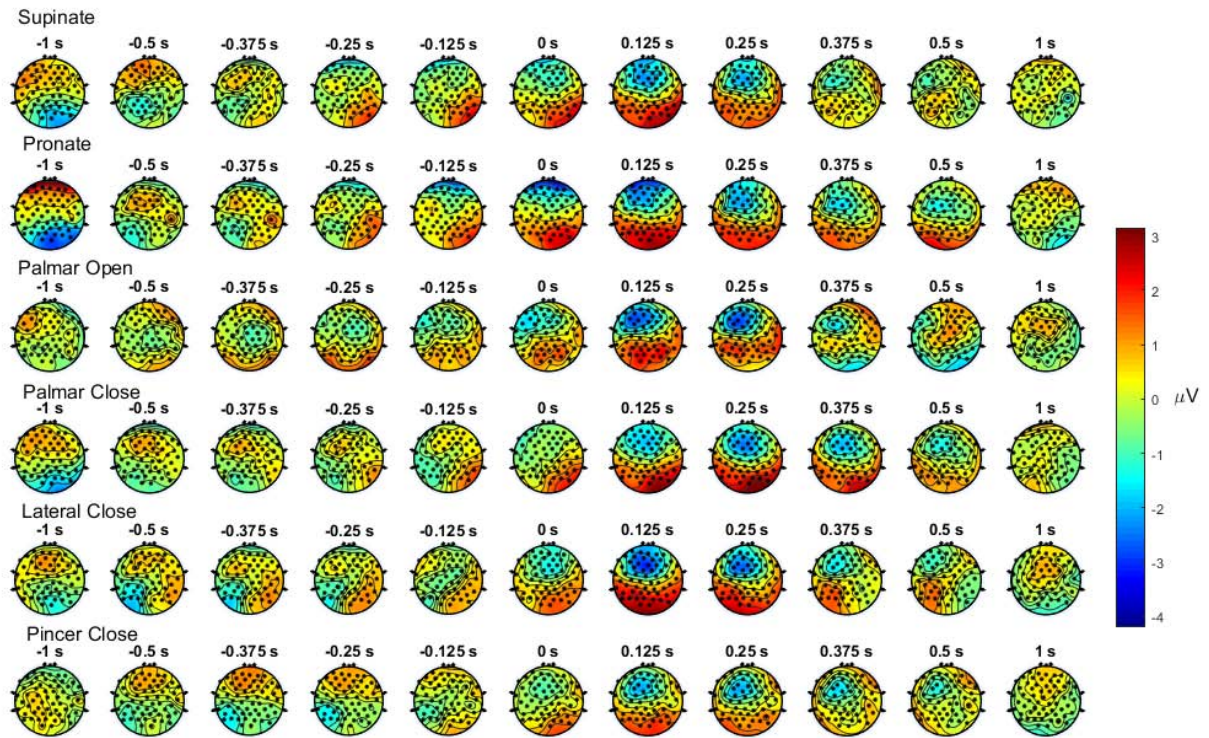
Figure 3.5: *Topographical overview of the MRCPs of all classes in the preliminary test. Time points are distributed from -1 to 1 s around the movement onset, with a focus on the MRCP.*

3.1.2 System Time Delays

In Figure 3.6 the box plot gives an overview over the time differences between the received game event triggers and the photodiode flags in the pilot measurement. The mean delay was 108,2 ms. In Figure 3.7 the time delays between the photodiode and the movement onset are shown for each class.
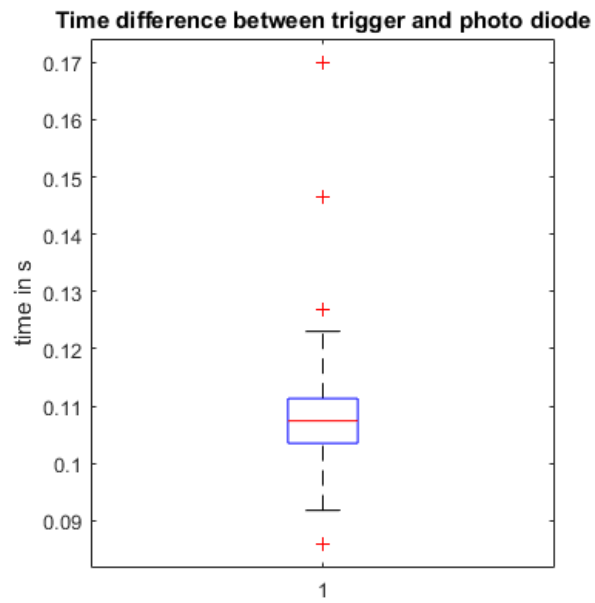
Figure 3.6: Time delay between the game event trigger and the detected photodiode flag.
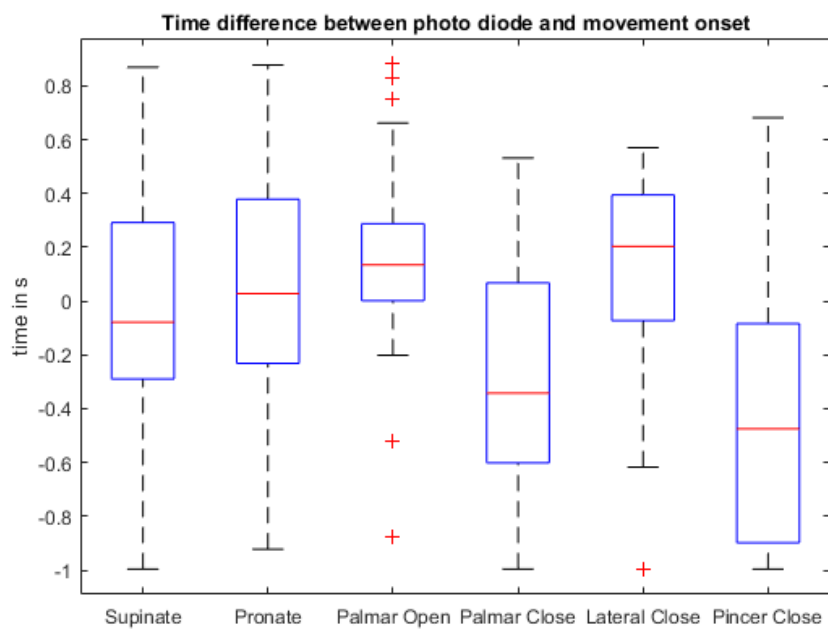
Figure 3.7: Overview of time delays between the photodiode flags and the movement onset for each class.

3.2 Feedback Experiment

The results of the feedback experiment are the ones collected measuring ten subjects using the three chosen classes of: palmar grasp, lateral grasp and supination.

3.2.1 Offline Analysis

Here the calculated results for the recorded training data are shown. For each class 60 trials were recorded, but on average 52 were used in the calculations after the cue alignment, movement onset detection and outlier rejection as described in the methods.

Movement-related Cortical Potentials

In Figures 3.8 to 3.10 the average MRCPs and their confidence interval are shown comparing each of the classes. The combination over all subjects was calculated, the same way as the confidence interval, using a nonparametric t-percentile bootstrap statistic with an alpha of 0.05.

Figure 3.8: Overview of the MRCPs of palmar and lateral grasp, epoched around the movement onset over the central electrodes: FCz, C1, Cz and C2. The continuous lines show the grand average while the shaded areas present the mean confidence intervals.

Figure 3.9: Overview of the MRCPs of palmar grasp and supination, epoched around the movement onset over the central electrodes: FCz, C1, Cz and C2. The continuous lines show the grand average while the shaded areas present the mean confidence intervals.

Figure 3.10: Overview of the MRCPs of lateral grasp and supination, epoched around the movement onset over the central electrodes: FCz, C1, Cz and C2. The continuous lines show the grand average while the shaded areas present the mean confidence intervals.

In Figure 3.11 the average topographical overview of the grand average MRCPs over all subjects for palmar grasp, lateral grasp and supination is shown.
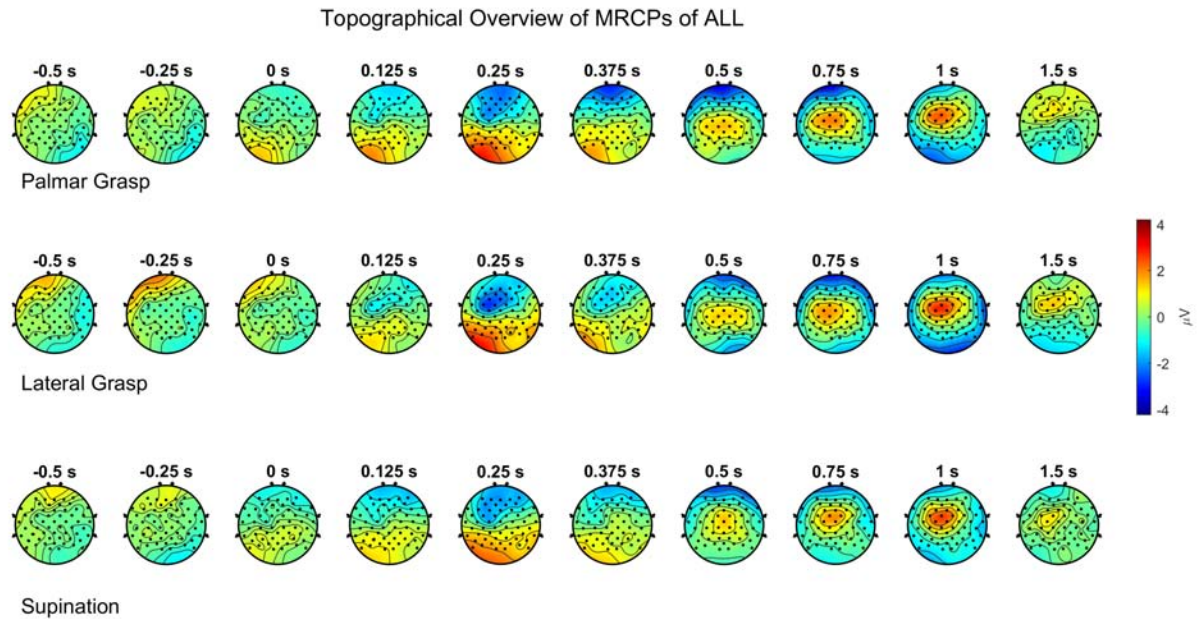
Figure 3.11: Topographical overview of the grand average MRCPs of all subjecs of palmar grasp, lateral grasp and supination classes. Time points are distributed from -0.5 to 1.5 s around the movement onset, with a focus on the MRCP.

The individual plots for each subject can be found in the appendix.

Cross Validation Results

In table 3.1 as well as Figures 3.12 and 3.13, the results of the offline cross validation of each subject are shown. For each time point the cross validated accuracy is shown in blue. The highest accuracy is marked with an red x. Also, the chance level in black and the significance level in magenta are shown.

Table 3.1: Accuracy and chosen time point of cross validation.

Subject	Accuracy in %	Time Point in s
CC2	63,63	1,23
DA1	59,54	0,77
DA4	70,89	0,58
DJ7	55,71	1,35
DQ9	76,53	0,97
EA6	57,53	1,16
EA9	64,47	1,1
ED4	49,11	1,1
ED7	53,51	0,71
ED8	61,63	0,52
Average	61,26	0,95
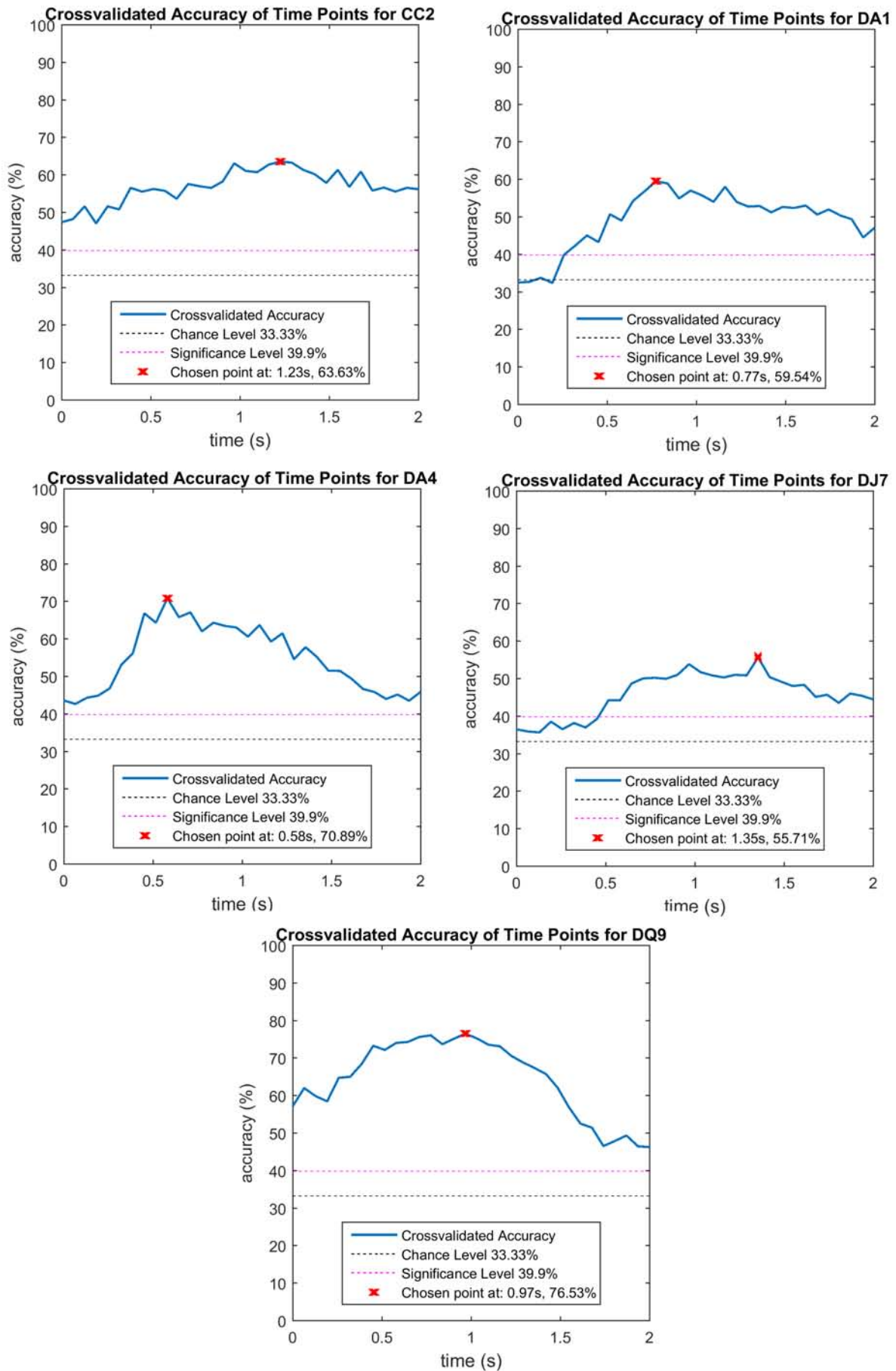
Figure 3.12: Cross validated accuracy of recording data trials from 0 to 2 seconds after the movement onset of subjects CC2, DA1, DA4, DJ7 and DQ9.
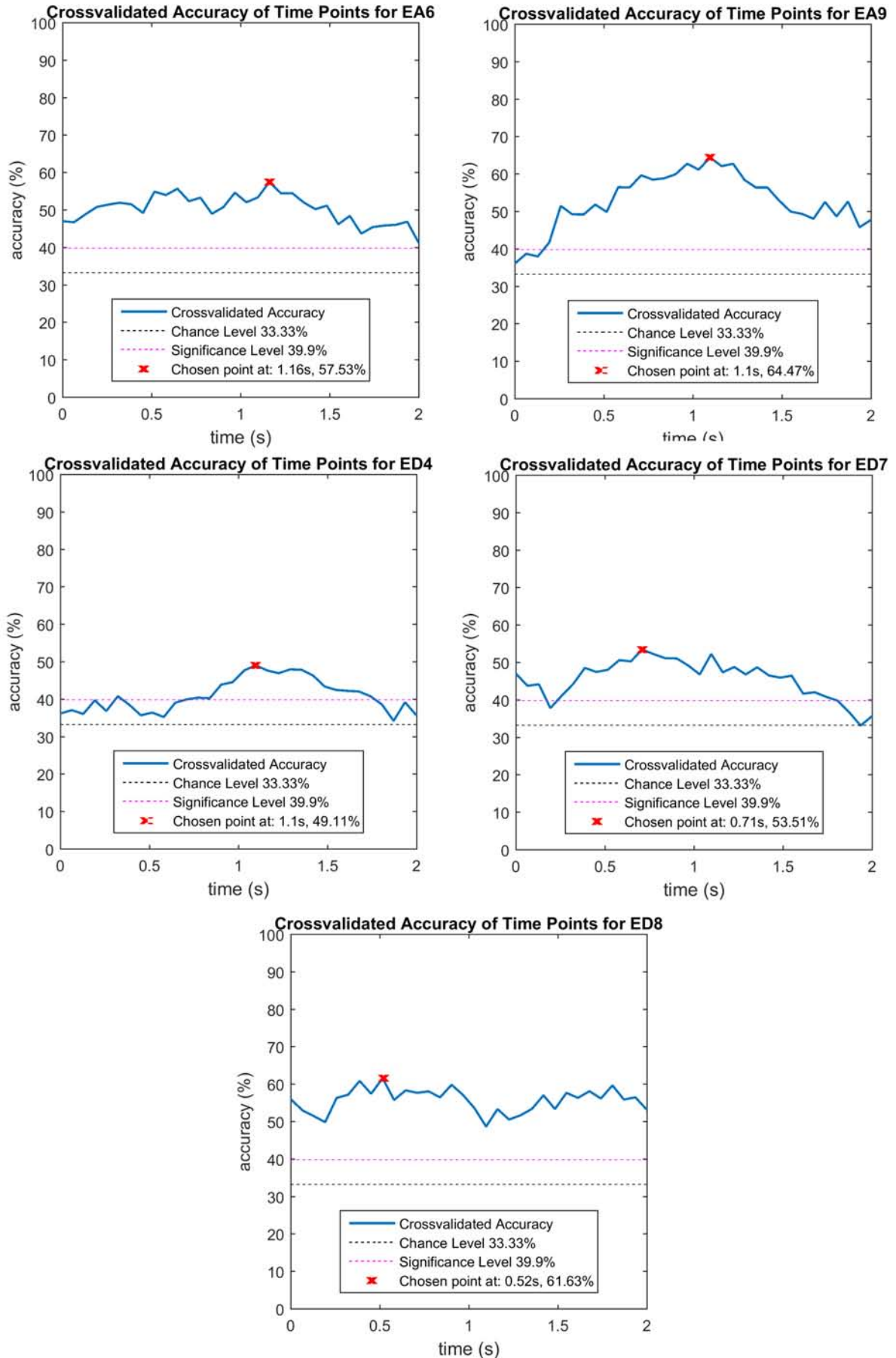
Figure 3.13: Cross validated accuracy of recording data trials from 0 to 2 seconds after the movement onset of subjects EA6, EA9, ED4, ED7 and ED8.

3.2.2 Online Analysis

Here the results for the online recorded feedback data is shown. In three runs, 45 trials per class were recorded, 15 per run.

Scores and Accuracys per Run

The reached scores and accuracys, for each run and overall, of all subject are shown in table 3.2. For the three classes the chance level is at 33,33% and the significance level overall for 135 trials, 45 per class, is at 40,41%. Additionally, also the average result over all subjects are shown.

Table 3.2: Scores and accuracy of all subject for each run and over all.

Subject	Run 1		Run 2		Run 3		Over All	
	score of 45	in %	score of 45	in %	score of 45	in %	score of 135	in %
CC2	20	44,44	24	53,33	19	42,22	63	46,67
DA1	22	48,89	27	60,00	22	48,89	71	52,59
DA4	25	55,56	22	48,89	31	68,89	78	57,78
DJ7	19	42,22	25	55,56	22	48,89	66	48,89
DQ9	20	44,44	23	51,11	22	48,89	65	48,15
EA6	21	46,67	31	68,89	22	48,89	74	54,81
EA9	16	35,56	25	55,56	22	48,89	63	46,67
ED4	24	53,33	22	48,89	18	40,00	64	47,41
ED7	20	44,44	21	46,67	22	48,89	63	46,67
ED8	20	44,44	20	44,44	23	51,11	63	46,67
Average	20,70	46,00	24,00	53,33	22,30	49,56	67,00	49,63

Single Trial Classification Overview

To give an overview or the performance of the classifier, in Figures 3.14 to 3.23, the classifier output for each trial and class are shown for all subjects. The trials are shown for each class, marked yellow is when the classier output matches the trial class and marked blue when it classified another. The red line shows the individual point of trial classification for each subject, which is a result of the offline cross validation.

Single Trial Online Classification Output per Trial of CC2
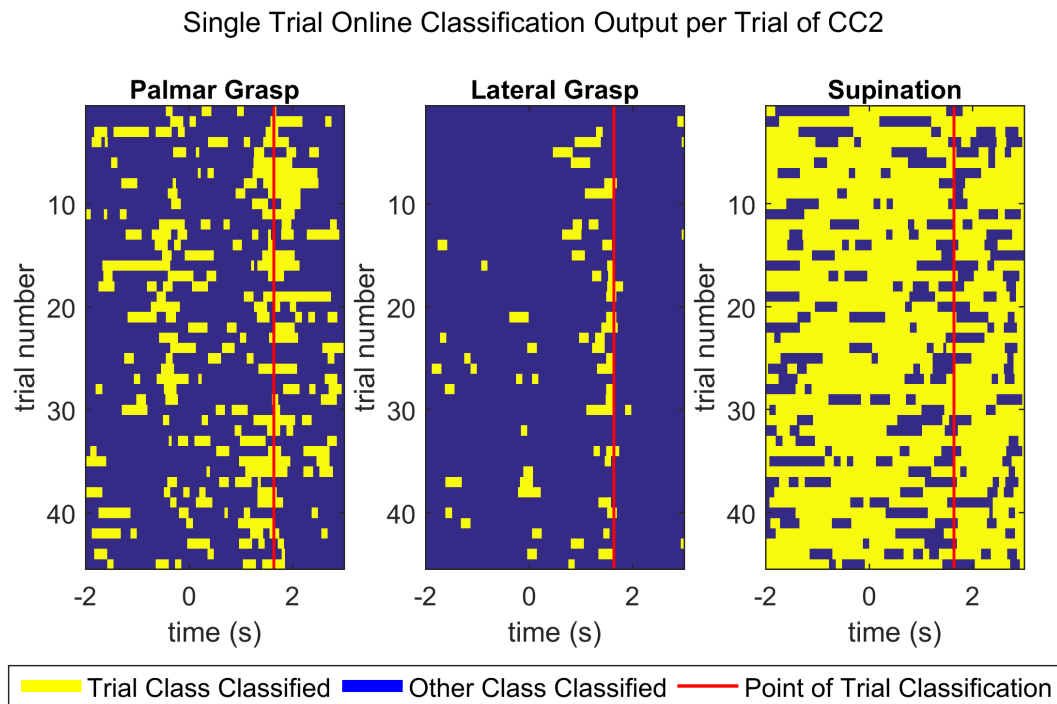
Figure 3.14: Classifier output for each trial and class of subject CC2. Matching trial class and classifier output is shown in yellow, differing in blue. The point of online trial classification in the is shown in red.

Single Trial Online Classification Output per Trial of DA1
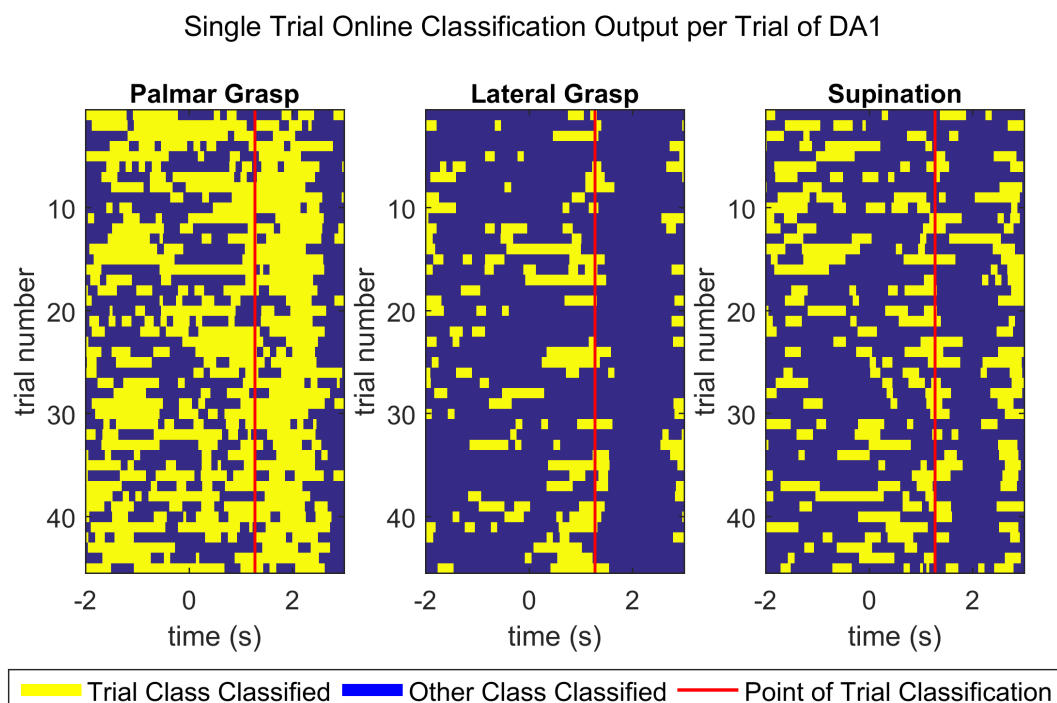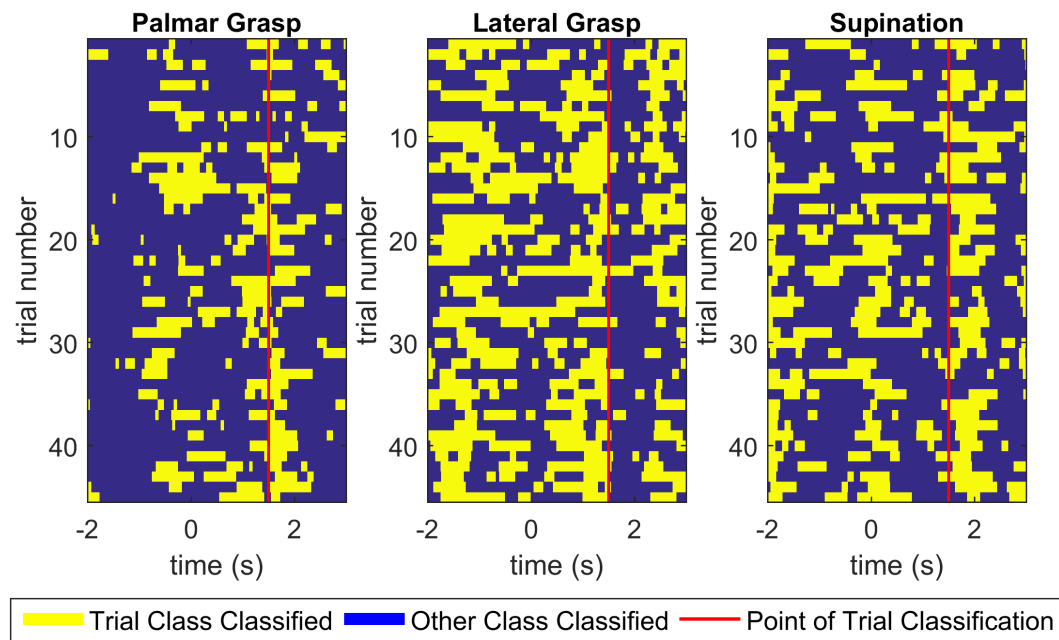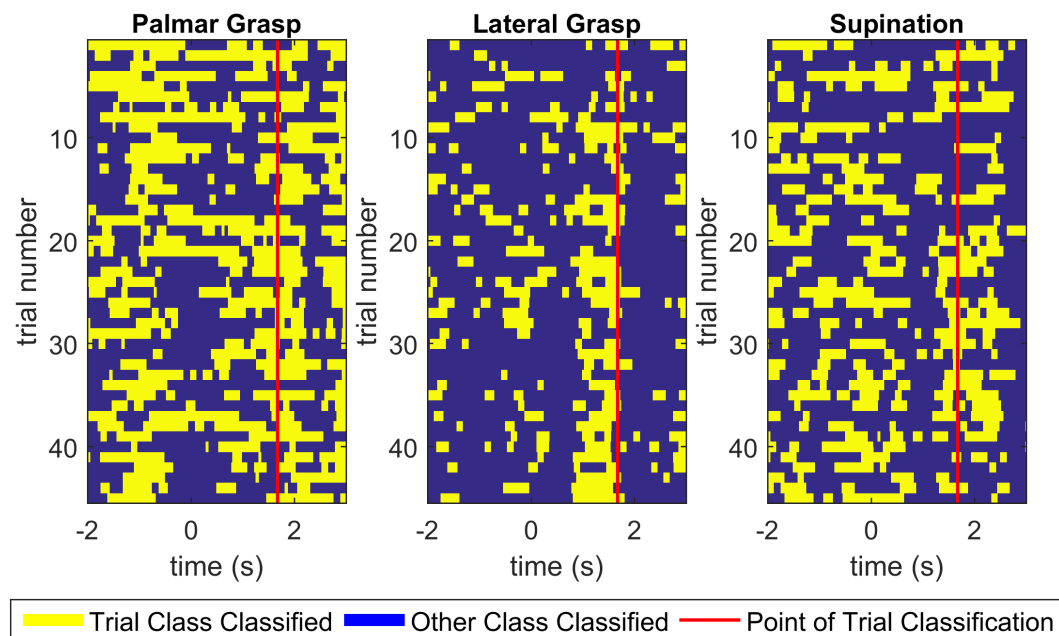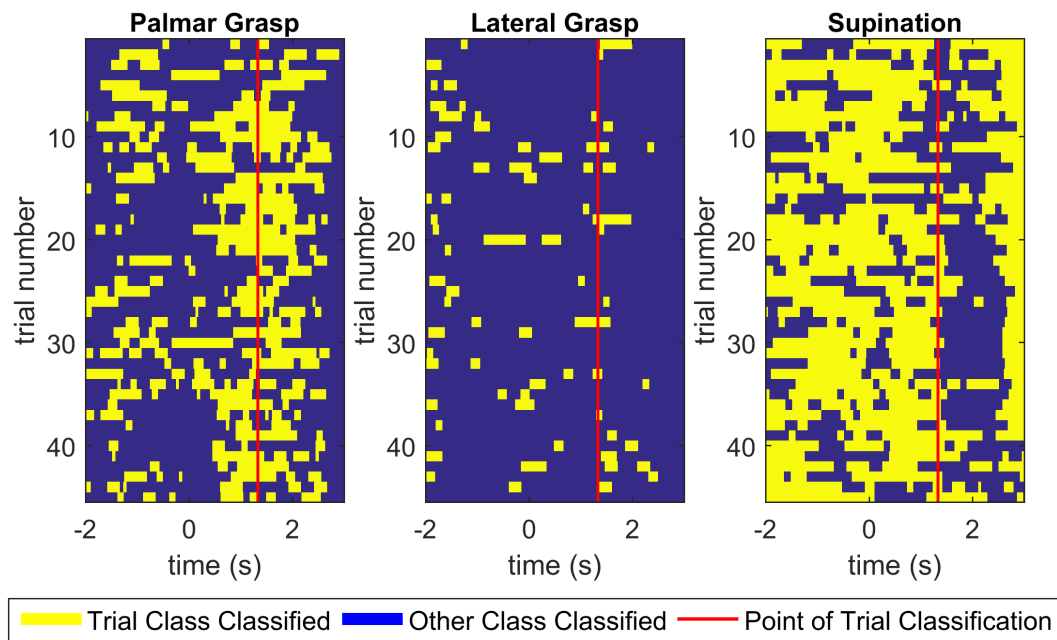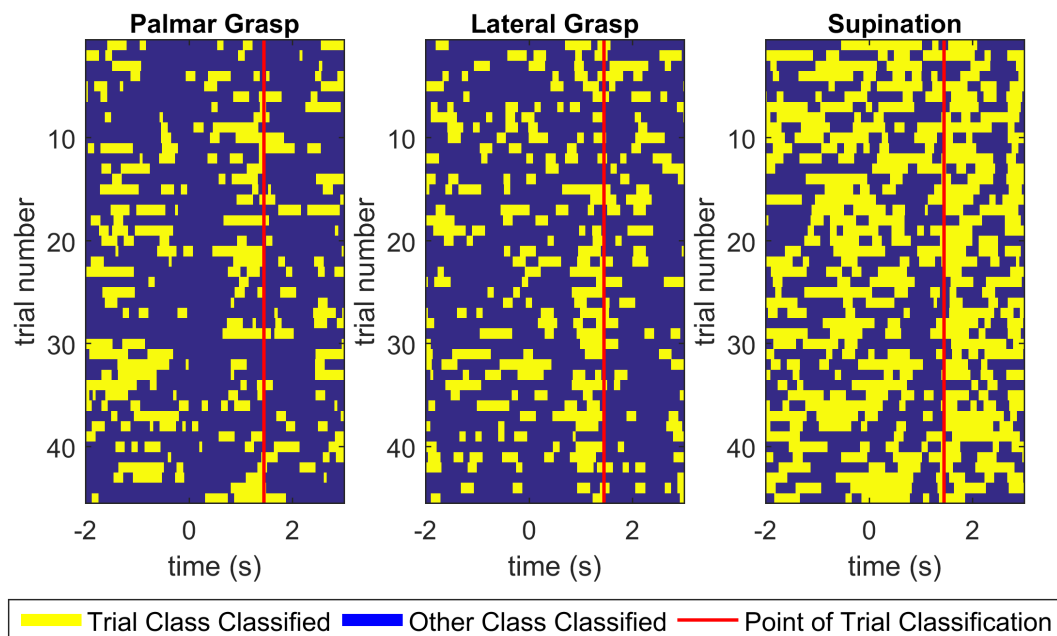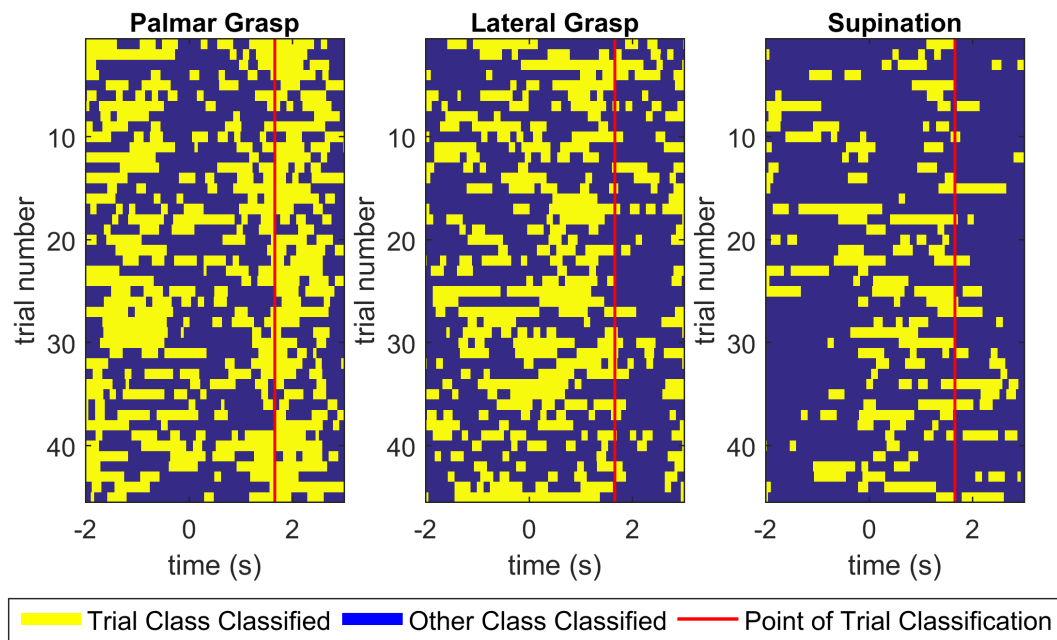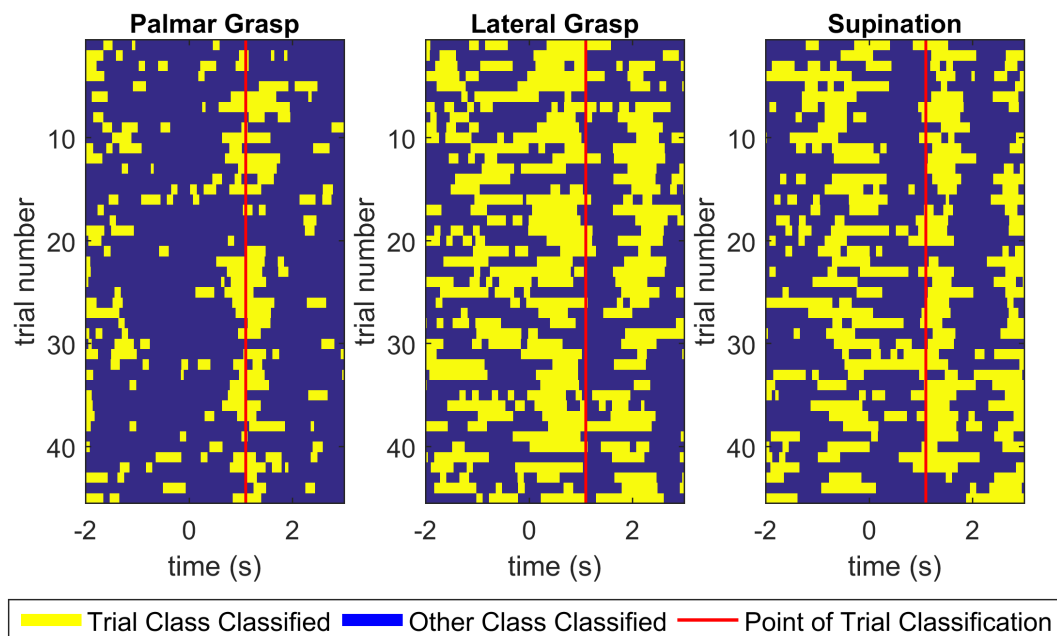

Figure 3.15: Classifier output for each trial and class of subject DA1. Matching trial class and classifier output is shown in yellow, differing in blue. The point of online trial classification in the is shown in red.

Single Trial Online Classification Output per Trial of DA4
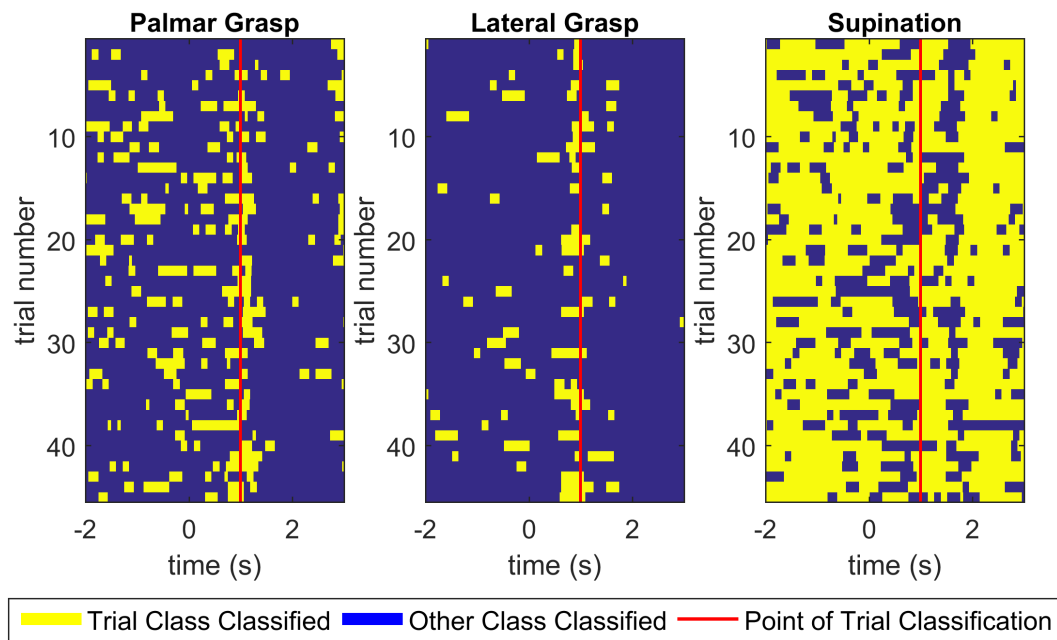
Figure 3.16: *Classifier output for each trial and class of subject DA4. Matching trial class and classifier output is shown in yellow, differing in blue. The point of online trial classification in the is shown in red.*

Single Trial Online Classification Output per Trial of DJ7
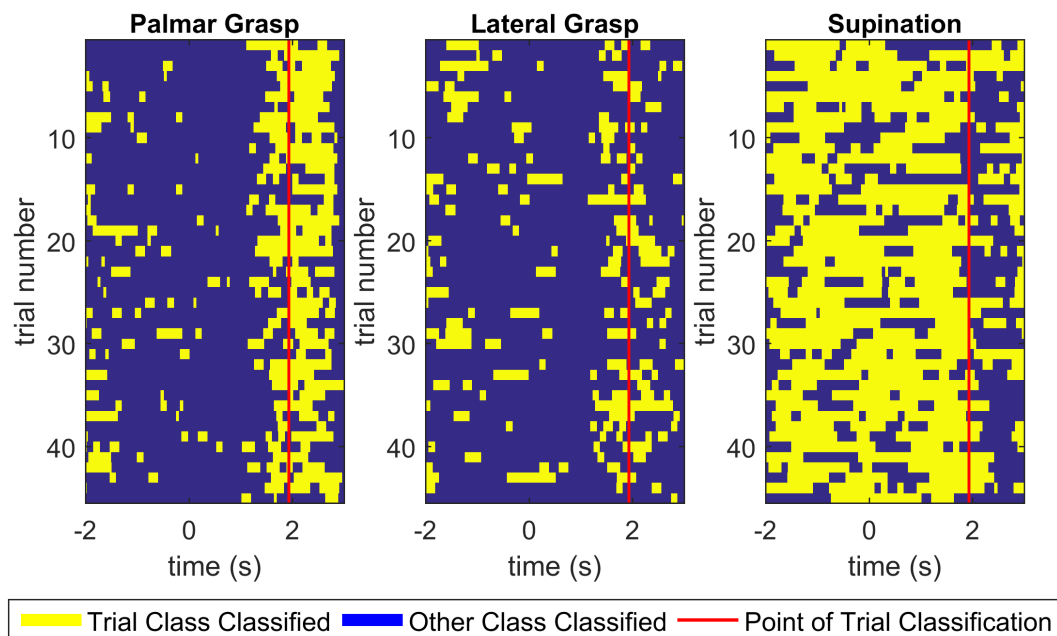
Figure 3.17: *Classifier output for each trial and class of subject DJ7. Matching trial class and classifier output is shown in yellow, differing in blue. The point of online trial classification in the is shown in red.*

Single Trial Online Classification Output per Trial of DQ9

Figure 3.18: Classifier output for each trial and class of subject DQ9. Matching trial class and classifier output is shown in yellow, differing in blue. The point of online trial classification in the is shown in red.

Single Trial Online Classification Output per Trial of EA6

Figure 3.19: Classifier output for each trial and class of subject EA6. Matching trial class and classifier output is shown in yellow, differing in blue. The point of online trial classification in the is shown in red.

Single Trial Online Classification Output per Trial of EA9

Figure 3.20: *Classifier output for each trial and class of subject EA9. Matching trial class and classifier output is shown in yellow, differing in blue. The point of online trial classification in the is shown in red.*

Single Trial Online Classification Output per Trial of ED4

Figure 3.21: *Classifier output for each trial and class of subject ED4. Matching trial class and classifier output is shown in yellow, differing in blue. The point of online trial classification in the is shown in red.*

Single Trial Online Classification Output per Trial of ED7

Figure 3.22: *Classifier output for each trial and class of subject ED7. Matching trial class and classifier output is shown in yellow, differing in blue. The point of online trial classification in the is shown in red.*

Single Trial Online Classification Output per Trial of ED8

Figure 3.23: *Classifier output for each trial and class of subject ED8. Matching trial class and classifier output is shown in yellow, differing in blue. The point of online trial classification in the is shown in red.*

3.2.3 Overview Offline and Online Results

To get an overview of the results, offline and online data were compared. These included the accuracies, the confusion matrices and the timings of the movement onset.

Accuracys Offline Online

The comparison between the offline cross validation and online score accuracy for each subject can be seen in Figure 3.24. It also visualizes the chance level of 33.33% for a three class classification in black, as well as the, as in the methods described, calculated significance level of 40,41% in magenta for the online accuracy and the 39,9 significance level for the offline cross validated accuracy.
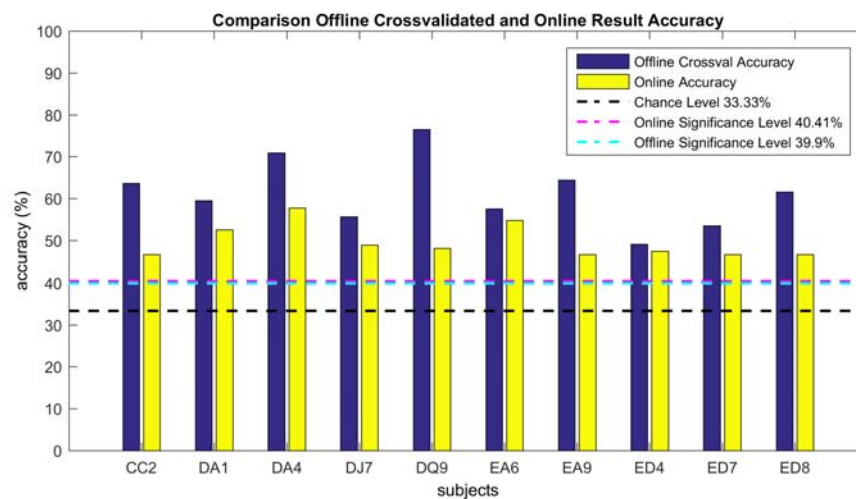
Figure 3.24: *Comparison of the offline recording data cross validated and the online scored accuracy of each subject.*

Confusion Matrices Offline Online

In order to get an overview of the performance of the classifier in respect to each class, in Figures 3.25 to 3.34 the confusion matrices of the cross validated offline and the online score results are shown for all subjects.
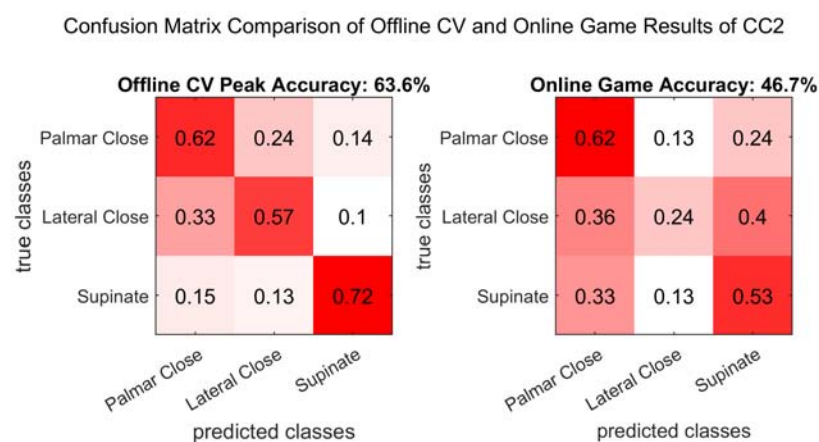
Figure 3.25: *Overview of confusion matrices of cross validated offline recording and online score results of CC2.*
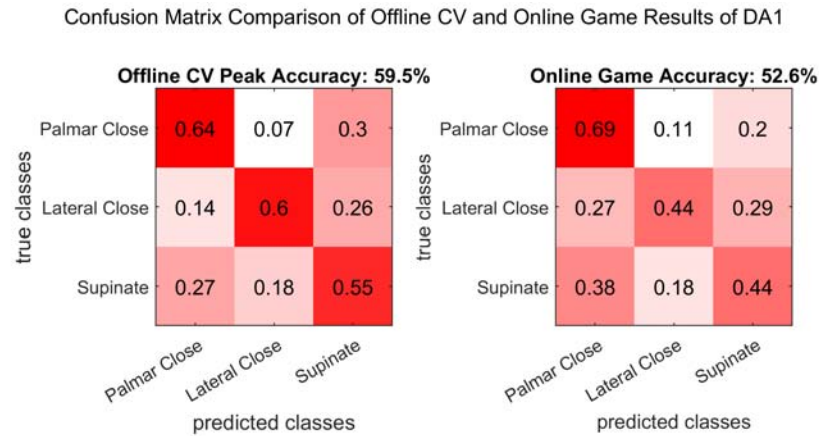
Figure 3.26: Overview of confusion matrices of cross validated offline recording and online score results of DA1.
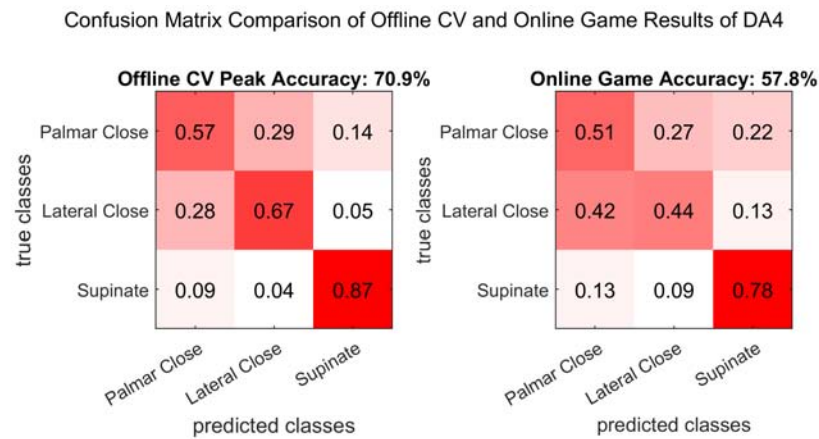
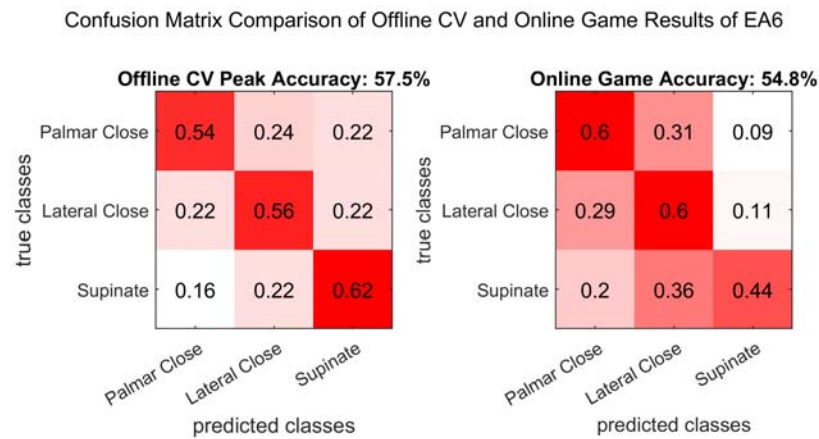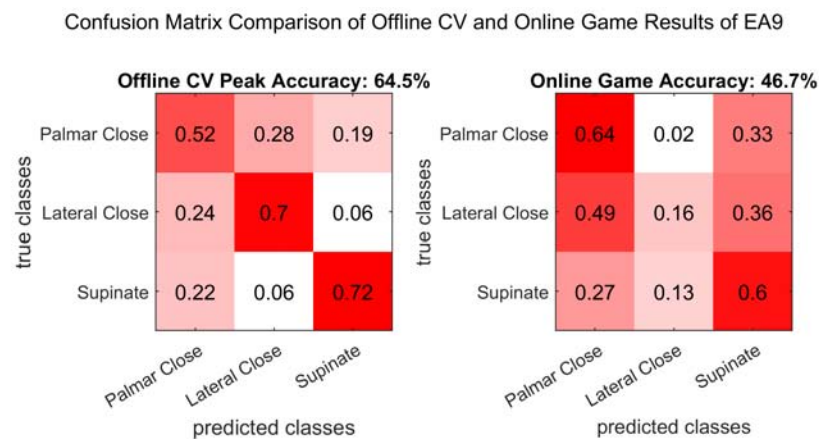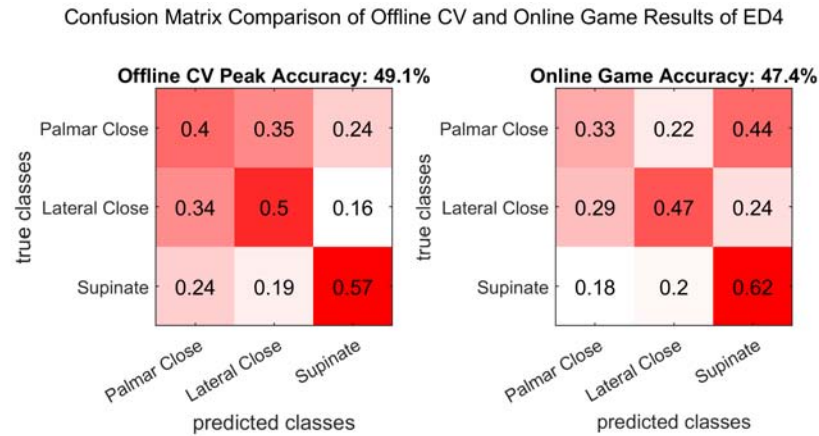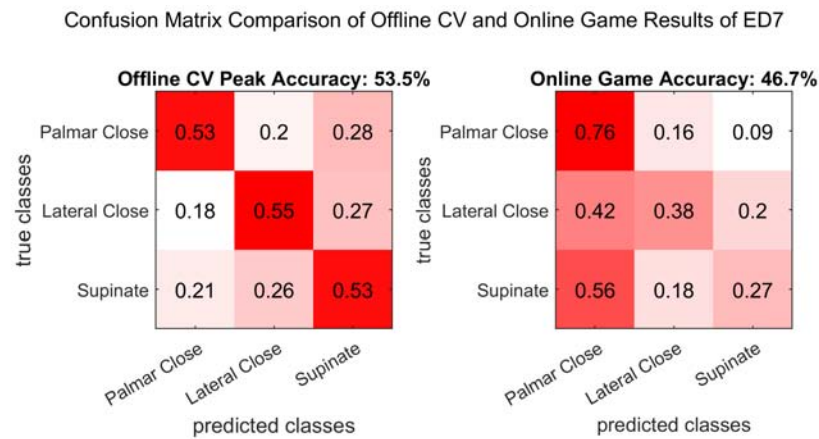*Figure 3.27: Overview of confusion matrices of cross validated offline recording and online score results of DA4.*
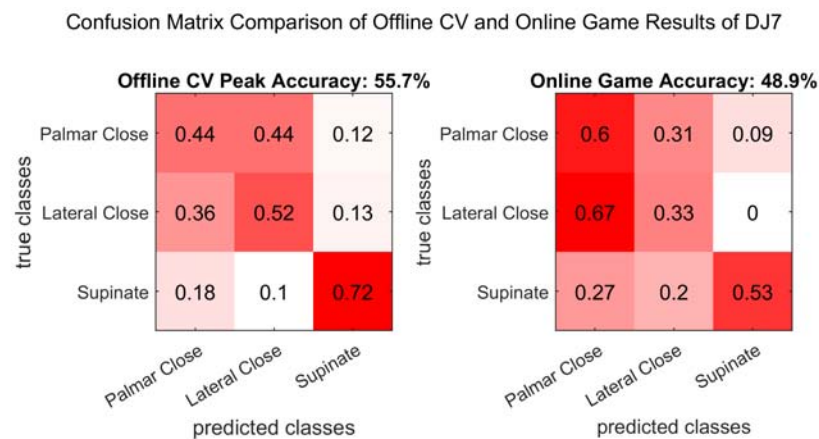
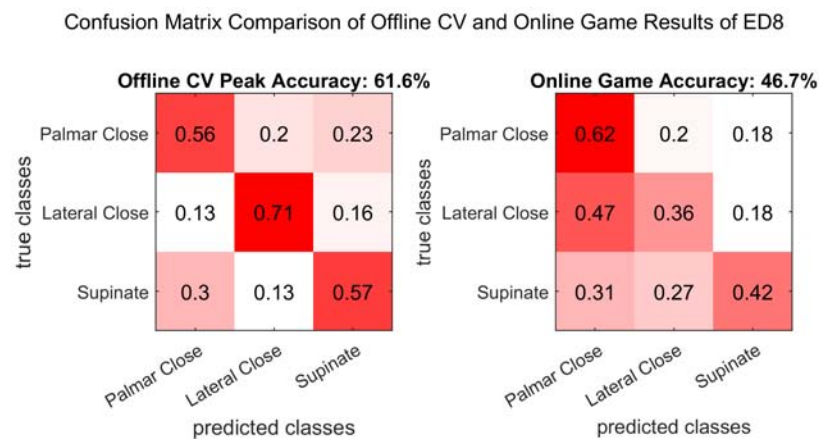*Figure 3.28: Overview of confusion matrices of cross validated offline recording and online score results of DJ7.*
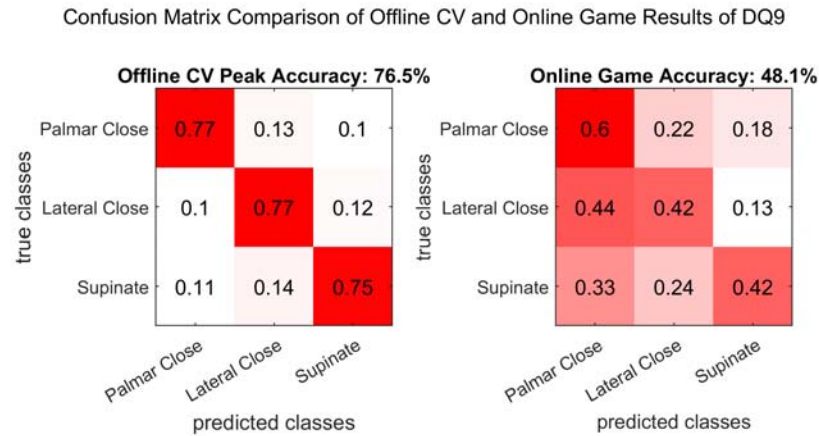
Figure 3.29: Overview of confusion matrices of cross validated offline recording and online score results of DQ9.

Figure 3.30: Overview of confusion matrices of cross validated offline recording and online score results of EA6.

Figure 3.31: Overview of confusion matrices of cross validated offline recording and online score results of EA9.

Confusion Matrix Comparison of Offline CV and Online Game Results of ED4

Offline CV Peak Accuracy: 49.1%

	Palmar Close	Lateral Close	Supinate
Palmar Close	0.4	0.35	0.24
Lateral Close	0.34	0.5	0.16
Supinate	0.24	0.19	0.57

Online Game Accuracy: 47.4%

	Palmar Close	Lateral Close	Supinate
Palmar Close	0.33	0.22	0.44
Lateral Close	0.29	0.47	0.24
Supinate	0.18	0.2	0.62

Figure 3.32: *Overview of confusion matrices of cross validated offline recording and online score results of ED4.*

Confusion Matrix Comparison of Offline CV and Online Game Results of ED7

Offline CV Peak Accuracy: 53.5%

	Palmar Close	Lateral Close	Supinate
Palmar Close	0.53	0.2	0.28
Lateral Close	0.18	0.55	0.27
Supinate	0.21	0.26	0.53

Online Game Accuracy: 46.7%

	Palmar Close	Lateral Close	Supinate
Palmar Close	0.76	0.16	0.09
Lateral Close	0.42	0.38	0.2
Supinate	0.56	0.18	0.27

Figure 3.33: *Overview of confusion matrices of cross validated offline recording and online score results of ED7.*

Confusion Matrix Comparison of Offline CV and Online Game Results of ED8

Offline CV Peak Accuracy: 61.6%

	Palmar Close	Lateral Close	Supinate
Palmar Close	0.56	0.2	0.23
Lateral Close	0.13	0.71	0.16
Supinate	0.3	0.13	0.57

Online Game Accuracy: 46.7%

	Palmar Close	Lateral Close	Supinate
Palmar Close	0.62	0.2	0.18
Lateral Close	0.47	0.36	0.18
Supinate	0.31	0.27	0.42

Figure 3.34: *Overview of confusion matrices of cross validated offline recording and online score results of ED8.*

An overview of how the participants adjusted their behavior using the feedback BCI, Figure 3.35 shows the average movement onset of each class for each subject, along with the standard deviation, for the offline training trials, as well as the online feedback trials.
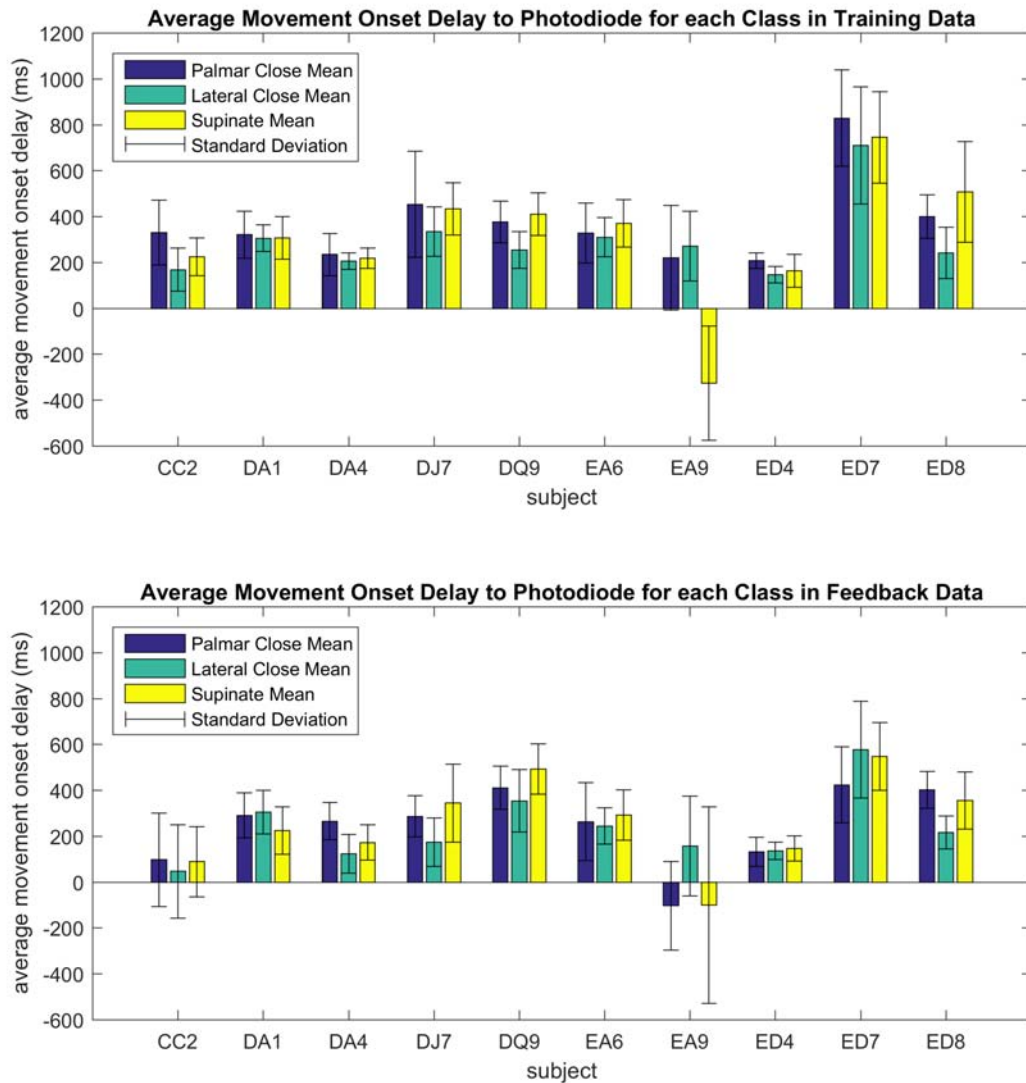
Figure 3.35: Overview of the delay between movement onset and the photodiode flag in the offline training trials and the online feedback trials.

4

Discussion

In this work, we were able to show the suitability of using the BCI Trainer game, developed for the MoreGrasp project, in an MRCP based online BCI. The scores and accuracies of the online experiment showed promising results above chance level for all subjects. They were able to control the three class online BCI with an accuracy of 50% on average, where the chance level is at 33,33% and the chance level at 40,41%.

4.1 Preliminary Tests

Analysis of the MRCPs recorded in the preliminary tests show the characteristic negativity around the movement onset is clearly visible in all six classes recorded. Furthermore, clearly observable is the lower, contralateral negative expression as can be seen in Figure 3.1. When comparing the chosen classes of palmar close, lateral close and supinate, as seen in Figures 3.2 to 3.4, significant differences in selected channels can be observed for any combination. These significant differences suggest the suitability of these features to be used to train a classifier and use them towards control in an online BCI. In the topographical overview the differences, though not their significances, can be seen in Figure 3.5. They show the expression of the MRCP close to the movement onset distributed around the head in very similar but slightly different ways for each class.

An important aspect of the preliminary test were the system time delays. In order to assess and manage these, the game included an event signaling, flashing patch, which was recorded as a flag, registered by a photodiode. As shown in Figure 3.6 the delay between the game trigger and the photodiode flag, showed values around the mean of 108 ms. The region spanned by most of the samples in the four quartiles spanned from 95 to 115ms with a few outliers outside of that. This suggests a relatively stable, constant time delay, which, nonetheless should be monitored. The reason for this delay was not determined but it was probably an accumulation of network delays and interfering processes of the recording computer in combination with the recording filters. Through detecting, quantifying and considering it, it had no influence on the experiment.

Additionally, also the delay between the photodiode flag and the movement onset were taken into account. For each class this delay differs not only in range but also in center of distribution in comparison to the photodiode flag. This suggests that even though the same person performs each movement, the behavior for each movement is slightly different. Further analysis of the data and the game revealed that the animations for each class differed in length, before the cue to start the movement execution. This in combination with feedback from the subject, who reported uncertainty in the cue, probably lead to the high range of delays. In order to be able to use the movements and in turn their to the movement onset time locked features for an online BCI, differences in delays and their ranges had to be minimized. In an effort to archive this, subjects were more carefully instructed in the tasks and were trained in the movements before recording started. Also the developer of the game was asked to change the game, so every animation had the same lenght.

In summary this preliminary test, confirmed the suitability of using the game as the paradigm for the online BCI, as it allowed for recording distinguishable MRCPs, through a system with manageable technical and subject specific delays.

4.2 Feedback Experiment

In the experiment, first data was recorded for offline analysis in order to find an individually ideal classifier. For each subject the ideal time point for classification was found using an cross validation, where the average accuracy across subjects reached 61,16%, with the best at 76,53% and the lowest at 49,11%. Using this calculated classifiers, subject reached online accuracy on average around 49,63 % with the best at 57,78 and the lowest 46,67%.

4.2.1 Offline Results

For the offline part of the experiment, next to the cross validation, the results were also analyzed from a neurophysiological point of view for each subject. All subjects showed accuracies above the chance level of 40,41% as well as the expected MRCP patterns.

Movement-Related Cortical Potentials

Towards building the online BCI, 60 trials of palmar close, lateral close and supination were recorded of each subject. Using the statistical method of calculating a nonparametric t-percentile bootstrap statistic, the mean and distribution of each time point around the movement onset of each class, a representation of the MRCPs for each subject were calculated. These individual results and comparisons between classes can be found in the appendix. In order to show an overview, the same statistical tool was applied over the result for each subject to reach an general estimation for all subjects. The resulting plots in Figures 3.8 to 3.10 show the characteristic negative shift at the movement onset, which is more prominent in the contralateral hemisphere to the moving hand, in the accumulated results of all subjects. In these plots a difference is visible between the classes, though they are not significant in the results over all subject. When looking at the individual results, the same pattern is visible to some degree. As opposed to the combined result, individual subject do show significant differences, in selected channels, between classes at different time points after the movement onset. This variation shows the necessity of the individual time point selection for training the classifier, as no single time point shows significant differences for all subjects. As in the preliminary testing, the topographical overview of the combined MRCP of all subjects underlines these results.

Cross Validation

The cross validation was performed in order to find the time point with the best discriminability between classes, in order to train the sLDA classifier. Results, in table 3.1 and Figures 3.12 and 3.13, show that on average an accuracy of 61,26% were reached with selected time points distributed around 950 ms after the detected movement onset. Similar results were shown in [24]. For the offline cross validated accuracy, the subject with the highest value reached 76,53% whereas the lowest scoring subject reached 49%. For most subjects the accuracy results were shaped as a curve, of which the peak was selected, clearly indicating an ideal classification time point exists and was selected.

4.2.2 Online Results

The online, with feedback recorded data, shows promising results as each subject was able to perform above significance level of 40,41%, on average at 49,63% accuracy. Considering these results in combination with the classifier output suggests that the subjects did have a degree of control, which might be increased with further training.

Accuracy

In the online experiment, performance of each subject can easily be assessed by the score they reached in the game which can directly be translated into accuracy. For every subject 45 trials per class with feedback were recorded in three runs. Over all subjects, an average score of 67 of 135, an 49,63% accuracy, was reached. Each subject individually was able to perform better than the significant chance level of 40,41%. The best accuracy reached was at 57,78% with a score of 78 of 135 while the lowest was at 46,7% at a score of 63 of 135. Looking at the individual runs, in the first the average accuracy was lowest at 46%, in the second the best result with 53,33% was reached and in third 49,56%. In scores this is a average score of 20,7 for the first, 24 for the second and 23,3 for the third, each of 45 possible. As in this part of the experiment, subjects received feedback, they had the chance to adjust their behavior in order to reach a higher score. Though they were specifically instructed to not change their movements, they could try to adjust their timing slightly. Because of this the accuracies of the individual runs suggest that between the first and the second and third run, subject were able to improve their timing in order to increase their score. While on average the best run was the second, this can be explained as subjects were still trying to improve and as a result had no fixed behavior yet. If the experiment had continued for longer, the results would probably improve as subjects learned better control over the system.

Classifier Output

The visualized classifier output, which can be seen in Figures 3.14 to 3.23, gives an overview of the actual performance of each subject at not only the classification time point. In nearly all classes of all subjects, these results show clearly identifiable clusters of correct classifications close to or at the point of classification. This shows that the classifier was capable of successfully differentiation between classes. But, this also clearly shows the greatest challenge for the subjects in this experiment, the timing. Even though the correctly classified clusters can span around 500 to 1000 ms, like it can be seen in the results of ED8, for others only a small very time locked cluster emerges, e.g. DA4. These two subjects especially show the importance of timing, as DA4 scored highest, with 57%, even though the classification output shows narrow clusters, while subject ED8 showed rather broad clusters, but was not able to find the correct timing for all classes, only reaching 46%. As can be expected, in the results also clearly visible are biases for certain classes for most subjects. But while they are present and might enhance the performance of this class, the other classes are clearly classified as well around correct time which suggests that the classifier actually performs quite well. Overall these results suggest, that with training, subjects might be able to perfect their timing which would lead to significantly better scores.

4.2.3 Comparisons, Overview

Generally comparing the accuracies of the offline and online part of the experiments shows, that a good result in the offline recording, does not necessarily lead to a higher score in the online part of the experiment. Also, the class with the best prediction accuracy might change for the online experiment. This might be attributed to the differences in behaviour as most subjects showed changes in timing for the movement onset between the offline and online recording. Overall the

timing of performing each class has such a high impact that through training the results could be significantly improved.

Accuracies

The comparison of accuracies in Figure 3.24 shows, there does not seem to be any correlation between the offline cross validation and the online score accuracies. Overall all calculated accuracies, of the offline recorded, cross validated time point, and the online reached score, were well over the chance level of 33,33 % of three classes, as well as the calculated significance level of 40,41%. No subject was able to reach the same accuracy as in the cross validation, most dropped by approximately 10%, which is consistent with other studies (Statthaler et al. 2017). Subjects whose offline accuracies were high, could generally not perform better than those with lower offline scores. Results suggest that while a well performing classifier increases the chance of a good performance, the result mainly depends on the individual subjects timing. If they were not able to find and repeat the movements at a good time point, the potential of the classifier could not be explored.

Confusion Matrices

The confusion matrices of classification for the offline cross validation results and the online score results in Figures 3.25 to 3.34, give an overview over the classification accuracy for each class. In the offline accuracies a clear diagonal trend, meaning predominantly correct classifications, can, to a certain degree, be seen in all subjects. One example would be DA4 where this can be seen clearly. Like for DA4, most uncertainties between two classes can be seen for the palmar close and lateral close grasp, in form of a visible intense 2 by 2 square, as can be expected as the tasks are very similar. For some subjects a bias for certain classes can be seen in form of a highlighted vertical strip. In the offline results, an increased general uncertainty over all classes can be observed for most subjects. For example DQ9 showed very good accuracy for all classes in the offline data, but in the online recordings lateral close was often misclassified for palmar close and supinate showed general uncertainty, while palmare close trials were classified as before. These results suggest that through the offline cross validation, classifiers for each subject could be found, which maximize the separability of the classes without favoring any specific class. While the online results on the other hand, show more biases for certain classes and more general classifier uncertainty, in most subjects the diagonal correct classification trend can be observed. When comparing offline and online, results of subjects with higher scores, like DA4 or EA6, seem to resemble the most between offline and online. This suggests that those subjects were able to utilize the potential of their classifier better than the other subjects.

Movement Onset

The comparison of movement onsets, in Figure 3.35 show the different behavior for each subject in the offline trial recording and the online feedback trial recording. The offline movements show that even though the behavior of the subjects show a nuber of differences between each other, the detected movement onsets for the different movement classes, are more similar, as the average onsets and their means overlap for most subjects. The online timings show similar results between subjects and classes. In comparison, however, subjects did adjust their behavior and timing, generally performing the movements earlier than in the training. This probably impacted the online performance, but due to the broad spectrum of classification as seen in the classification output they still had control.

Feedback of the Subjects

One of the goals of the experiment was to show the suitability of using the BCI Trainer game as a paradigm, in order to prevent fatigue in subjects and boost motivation for the experiment. While no scientific evaluation was performed to assess the impact of the game in this regard, most subjects remarked, that they liked the game, and were looking forward to the feedback recordings. Also, as all participating subjects had taken part in some kind of EEG study before, they reported this paradigm as more enjoyable than others they had been part of. Finally, at the end of the experiment, most subjects reported, despite still high rates of wrong classification, that they felt some control over the system.

4.3 Limitations and Future Work

In the application of the CAR filter manual inspection was necessary to check for symmetry shifts in the electrode layout, as it may theoretically happen that a whole scalp region with many electrodes could be excluded due to high noise, thus severely affecting the symmetry of the setup. In this experiment on average 2 channels (+/- 1 channel) were excluded due noise and therefore no symmetry problems occurred.

While the built system shows promise by discrimination between three classes at peak performance of 57,8%, in its current form is not suitable for use in real life. To improve performance, the classifier could be to retrained on the data collected in the online recording, thus adjusting to the changed behaviors of the participants when they are presented with feedback. While this might lead to an increase in in performance, it could also lead to more variation in the features, as subject might have been adjusting their behavior during the feedback experiment recording while learning to use the BCI. Another way to improve performance would be further training with the BCI. In order to move towards this ultimate goal of a reliable BCI controlled real life application, another step would be to find a way to use the principle shown in an asynchronous way. To do that, the greatest challenge would be to build a system to recognize when an MRCP occurs and translate it in real time. Additionally, the recording of the EEG should be simplified by finding a setup with fewer electrodes that does not lose too much information as to impact classification. Still, with all these adjustments a user would still have to train in using the BCI, for which at least the here shown game is a good option.

5
Conclusion

The aim of this work was to build a multi-class BCI based on MRCPs to demonstrate the feasibility of using these features in an online application. Secondarily, the suitability of the BCI Trainer game built for the MoreGrasp project, as a paradigm for such experiments was to be shown. For this purpose a system using the game as paradigm in the offline and online recording was built.

Ten subjects participated in the experiment, where an ideal classification time point of the MRCP for each subject was calculated and an sLDA classifier trained. The offline results showed the potential performance of this classifier with an average accuracy of 61% and top results of 76% for three classes. While in the online experiment, not all subjects managed to reach these potential scores, they reached a very promising average of 49% with a top score of 57% accuracy. Additionally, all subjects showed significant control. The reason for the difference between the offline and online score can found in the timing of each subject, which could possibly be improved by more training or retraining of the classifier with the online data.

Overall these results show that the game is suitable to record and classify MRCPs. Further they show the feasibility of a multi-class BCI using MRCP features for real-time control. Though further research and work is necessary for building a real life application, the results of this thesis prove a successful further development and implementation.

Bibliography

[1] J. R. Wolpaw, "Brain-computer interfaces (BCIs) for communication and control," in *Proceedings of the 9th international ACM SIGACCESS conference on Computers and accessibility - Assets '07*, 2007.

[2] J. D. R. Millán, R. Rupp, G. R. Müller-Putz, R. Murray-Smith, C. Giugliemma, M. Tangermann, C. Vidaurre, F. Cincotti, A. Kübler, R. Leeb, C. Neuper, K.-R. Müller, and D. Mattia, "Combining Brain-Computer interfaces and assistive technologies: State-of-the-Art and challenges," *Front. Neurosci.*, vol. 4, Sep. 2010.

[3] E. M. Maynard, C. T. Nordhausen, and R. A. Normann, "The utah intracortical electrode array: a recording structure for potential brain-computer interfaces," *Electroencephalogr. Clin. Neurophysiol.*, vol. 102, no. 3, pp. 228–239, Mar. 1997.

[4] M. J. Vansteensel, D. Hermes, E. J. Aarnoutse, M. G. Bleichner, G. Schalk, P. C. van Rijen, F. S. S. Leijten, and N. F. Ramsey, "Brain-computer interfacing based on cognitive control," *Ann. Neurol.*, vol. 67, no. 6, pp. 809–816, Jun. 2010.

[5] H. Ramoser, J. Müller-Gerking, and G. Pfurtscheller, "Optimal spatial filtering of single trial EEG during imagined hand movement," *IEEE Trans. Rehabil. Eng.*, vol. 8, no. 4, pp. 441–446, Dec. 2000.

[6] D. J. McFarland, L. M. McCane, S. V. David, and J. R. Wolpaw, "Spatial filter selection for EEG-based communication," *Electroencephalogr. Clin. Neurophysiol.*, vol. 103, no. 3, pp. 386–394, Sep. 1997.

[7] B. Blankertz, S. Lemm, M. Treder, S. Haufe, and K.-R. Müller, "Single-trial analysis and classification of ERP components—a tutorial," *Neuroimage*, vol. 56, no. 2, pp. 814–825, 2011.

[8] D. Steyrl, R. Scherer, J. Faller, and G. R. Müller-Putz, "Random forests in non-invasive sensorimotor rhythm brain-computer interfaces: a practical and convenient non-linear classifier," *Biomed. Tech.*, vol. 61, no. 1, pp. 77–86, Feb. 2016.

[9] A. Pinegger, H. Hiebel, S. C. Wriessnegger, and G. R. Müller-Putz, "Composing only by thought: Novel application of the P300 brain-computer interface," *PLoS One*, vol. 12, no. 9, p. e0181584, Sep. 2017.

[10] S. Halder, A. Pinegger, I. Käthner, S. C. Wriessnegger, J. Faller, J. B. Pires Antunes, G. R. Müller-Putz, and A. Kübler, "Brain-controlled applications using dynamic P300 speller matrices," *Artif. Intell. Med.*, vol. 63, no. 1, pp. 7–17, Jan. 2015.

[11] M. Middendorf, G. McMillan, G. Calhoun, and K. S. Jones, "Brain-computer interfaces based on the steady-state visual-evoked response," *IEEE Trans. Rehabil. Eng.*, vol. 8, no. 2, pp. 211–214, 2000.

[12] G. R. Muller-Putz and G. Pfurtscheller, "Control of an electrical prosthesis with an SSVEP-Based BCI," *IEEE Transactions on Biomedical Engineering*, vol. 55, no. 1, pp. 361–364, 2008.

[13] G. R. Müller-Putz, R. Scherer, G. Pfurtscheller, and R. Rupp, "EEG-based neuroprosthesis control: a step towards clinical practice," *Neurosci. Lett.*, vol. 382, no. 1-2, pp. 169–174, Apr. 2005.

[14] G. Pfurtscheller, G. R. Müller-Putz, A. Schlögl, B. Graimann, R. Scherer, R. Leeb, C. Brunner, C. Keinrath, F. Lee, G. Townsend, C. Vidaurre, and C. Neuper, "15 years of BCI research at graz university of technology: current projects," *IEEE Trans. Neural Syst. Rehabil. Eng.*, vol. 14, no. 2, pp. 205–210, Jun. 2006.

[15] A. Schwarz, R. Scherer, D. Steyrl, J. Faller, and G. R. Muller-Putz, "A co-adaptive sensory motor rhythms Brain-Computer interface based on common spatial patterns and random forest," *Conf. Proc. IEEE Eng. Med. Biol. Soc.*, vol. 2015, pp. 1049–1052, Aug. 2015.

[16] K. Statthaler, A. Schwarz, D. Steyrl, R. Kobler, M. K. Höller, J. Brandstetter, L. Hehenberger, M. Bigga, and G. Müller-Putz, "Cybathlon experiences of the graz BCI racing team mirage91 in the brain-computer interface discipline," *J. Neuroeng. Rehabil.*, vol. 14, no. 1, p. 129, Dec. 2017.

[17] E. V. C. Friedrich, C. Neuper, and R. Scherer, "Whatever works: a systematic user-centered training protocol to optimize brain-computer interfacing individually," *PLoS One*, vol. 8, no. 9, p. e76214, Sep. 2013.

[18] R. Scherer, M. Billinger, J. Wagner, A. Schwarz, D. T. Hettich, E. Bolinger, M. Lloria Garcia, J. Navarro, and G. Müller-Putz, "Thought-based row-column scanning communication board for individuals with cerebral palsy," *Ann. Phys. Rehabil. Med.*, vol. 58, no. 1, pp. 14–22, Feb. 2015.

[19] A. Schwarz, D. Steyrl, and G. R. Muller-Putz, "Brain-computer interface adaptation for an end user to compete in the cybathlon," in *2016 IEEE International Conference on Systems, Man, and Cybernetics (SMC)*, 2016.

[20] R. Scherer, A. Schwarz, G. R. Muller-Putz, V. Pammer-Schindler, and M. L. Garcia, "Game-Based BCI training: Interactive design for individuals with cerebral palsy," in *2015 IEEE International Conference on Systems, Man, and Cybernetics*, 2015.

[21] G. R. Müller-Putz, A. Schwarz, J. Pereira, and P. Ofner, "From classic motor imagery to complex movement intention decoding: The noninvasive Graz-BCI approach," *Prog. Brain Res.*, vol. 228, pp. 39–70, May 2016.

[22] H. Shibasaki and M. Hallett, "What is the bereitschaftspotential?" *Clin. Neurophysiol.*, vol. 117, no. 11, pp. 2341–2356, 2006.

[23] P. Ofner, A. Schwarz, J. Pereira, and G. R. Müller-Putz, "Upper limb movements can be decoded from the time-domain of low-frequency EEG," *PLoS One*, vol. 12, no. 8, p. e0182578, Aug. 2017.

[24] A. Schwarz, P. Ofner, J. Pereira, A. I. Sburlea, and G. R. Müller-Putz, "Decoding natural reach-and-grasp actions from human EEG," *J. Neural Eng.*, vol. 15, no. 1, p. 016005, Feb. 2018.

[25] "2018 video game industry statistics, trends & data - the ultimate list," https://www.wepc.com/news/video-game-statistics/, May 2018, accessed: 2018-9-14.

[26] E. C. Lalor, S. P. Kelly, C. Finucane, R. Burke, R. Smith, R. B. Reilly, and G. McDarby, "Steady-State VEP-Based Brain-Computer interface control in an immersive 3D gaming environment," *EURASIP J. Adv. Signal Process.*, vol. 2005, no. 19, p. 706906, Nov. 2005.

[27] P. Martinez, H. Bakardjian, and A. Cichocki, "Fully online multicommand brain-computer interface with visual neurofeedback using SSVEP paradigm," *Comput. Intell. Neurosci.*, p. 94561, 2007.

[28] M. Congedo, M. Goyat, N. Tarrin, G. Ionescu, L. Varnet, B. Rivet, R. Phlypo, N. Jrad, M. Acquadro, and C. Jutten, "" brain invaders": a prototype of an open-source p300-based video game working with the OpenViBE platform," in *5th International Brain-Computer Interface Conference 2011 (BCI 2011)*, 2011, pp. 280–283.

[29] G. Pires, M. Torres, N. Casaleiro, U. Nunes, and M. Castelo-Branco, "Playing tetris with non-invasive BCI," in *2011 IEEE 1st International Conference on Serious Games and Applications for Health (SeGAH)*, Nov. 2011, pp. 1–6.

[30] M. Krauledat, K. Grzeska, M. Sagebaum, B. Blankertz, C. Vidaurre, K.-R. Müller, and M. Schröder, "Playing pinball with non-invasive bci," in *Advances in neural information processing systems*, 2009, pp. 1641–1648.

[31] R. Scherer, A. Schwarz, G. R. Müller-Putz, V. Pammer-Schindler, and M. L. Garcia, "Lets play Tic-Tac-Toe: A Brain-Computer interface case study in cerebral palsy," in *2016 IEEE International Conference on Systems, Man, and Cybernetics (SMC)*, Oct. 2016, pp. 003 736–003 741.

[32] R. Scherer, F. Lee, A. Schlogl, R. Leeb, H. Bischof, and G. Pfurtscheller, "Toward Self-Paced Brain–Computer communication: Navigation through virtual worlds," *IEEE Transactions on Biomedical Engineering*, vol. 55, no. 2, pp. 675–682, Feb. 2008.

[33] MoreGrasp Project, "The MoreGrasp project," http://www.moregrasp.eu/, accessed: 2018-9-15.

[34] M. X. Cohen, *Analyzing Neural Time Series Data: Theory and Practice.* MIT Press, Jan. 2014.

[35] M. Fatourechi, A. Bashashati, R. K. Ward, and G. E. Birch, "EMG and EOG artifacts in brain computer interface systems: A survey," *Clin. Neurophysiol.*, vol. 118, no. 3, pp. 480–494, Mar. 2007.

[36] A. Delorme and S. Makeig, "EEGLAB: an open source toolbox for analysis of single-trial EEG dynamics including independent component analysis," *J. Neurosci. Methods*, vol. 134, no. 1, pp. 9–21, Mar. 2004.

[37] J. Faller, C. Vidaurre, T. Solis-Escalante, C. Neuper, and R. Scherer, "Autocalibration and recurrent adaptation: towards a plug and play online ERD-BCI," *IEEE Trans. Neural Syst. Rehabil. Eng.*, vol. 20, no. 3, pp. 313–319, May 2012.

[38] A. Delorme, T. Sejnowski, and S. Makeig, "Enhanced detection of artifacts in EEG data using higher-order statistics and independent component analysis," *Neuroimage*, vol. 34, no. 4, pp. 1443–1449, Feb. 2007.

[39] J. H. Shah, M. Sharif, M. Yasmin, and S. L. Fernandes, "Facial expressions classification and false label reduction using LDA and threefold SVM," *Pattern Recognit. Lett.*, Jun. 2017.

[40] M. Pavlinek and V. Podgorelec, "Text classification method based on self-training and LDA topic models," *Expert Syst. Appl.*, vol. 80, pp. 83–93, Sep. 2017.

[41] J. Friedman, T. Hastie, and R. Tibshirani, *The elements of statistical learning.* Springer series in statistics New York, NY, USA:, 2001, vol. 1.

[42] G. Müller-Putz, R. Scherer, C. Brunner, R. Leeb, and G. Pfurtscheller, "Better than random: a closer look on BCI results," *Int. J. Bioelectromagn.*, vol. 10, no. EPFL-ARTICLE-164768, pp. 52–55, 2008.

[43] G. R. Müller-Putz, C. Breitwieser, F. Cincotti, R. Leeb, M. Schreuder, F. Leotta, M. Tavella, L. Bianchi, A. Kreilinger, A. Ramsay, M. Rohm, M. Sagebaum, L. Tonin, C. Neuper, and J. D. R. Millán, "Tools for Brain-Computer interaction: A general concept for a hybrid BCI," *Front. Neuroinform.*, vol. 5, p. 30, Nov. 2011.

[44] C. Breitwieser, C. Neuper, and G. R. Müller-Putz, "A concept to standardize raw biosignal transmission for brain-computer interfaces," *Conf. Proc. IEEE Eng. Med. Biol. Soc.*, vol. 2011, pp. 6377–6380, 2011.

[45] "tools4BCI," http://tools4bci.sourceforge.net/, accessed: 2018-9-14.

[46] "TCP/UDP/IP toolbox 2.0.6 - file exchange - MATLAB central," https://de.mathworks.com/matlabcentral/fileexchange/345, May 2015, accessed: 2018-9-14.

[47] R. Oostenveld and P. Praamstra, "The five percent electrode system for high-resolution EEG and ERP measurements," *Clin. Neurophysiol.*, vol. 112, no. 4, pp. 713–719, Apr. 2001.

[48] "Report of the committee on methods of clinical examination in electroencephalography," *Electroencephalogr. Clin. Neurophysiol.*, vol. 10, no. 2, pp. 370–375, 1958.

[49] G. H. Klem, H. O. Lüders, H. H. Jasper, and C. Elger, "The ten-twenty electrode system of the international federation. the international federation of clinical neurophysiology," *Electroencephalogr. Clin. Neurophysiol. Suppl.*, vol. 52, pp. 3–6, 1999.

[50] "ELOS system zebris," http://www.soniber.com/documentos/e_Elguide_l.pdf, accessed: 2018-9-14.

6

Appendix

In the following Figures additional result for all subjects are shown. For every subject the average MRCPs and their confidence interval are shown comparing each of the classes. The combination over all subjects was calculated, the same way as the confidence interval, using a nonparametric t-percentile bootstrap statistic with an alpha of 0.05.

Also for every subject the average topographical overview of the MRCPs over all subjects for palmar close, lateral close and supination is shown.
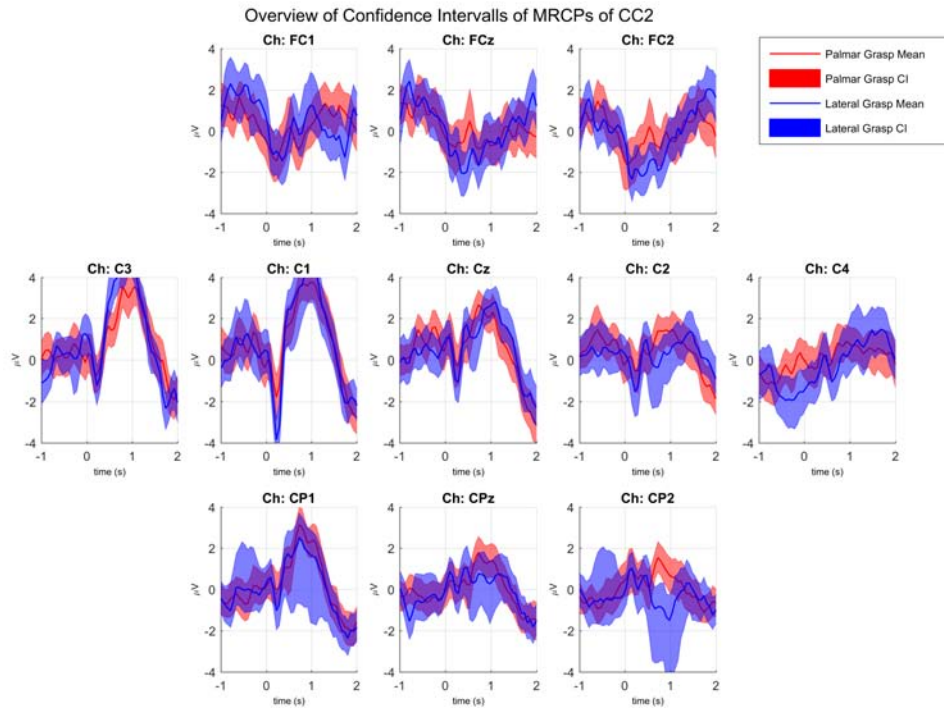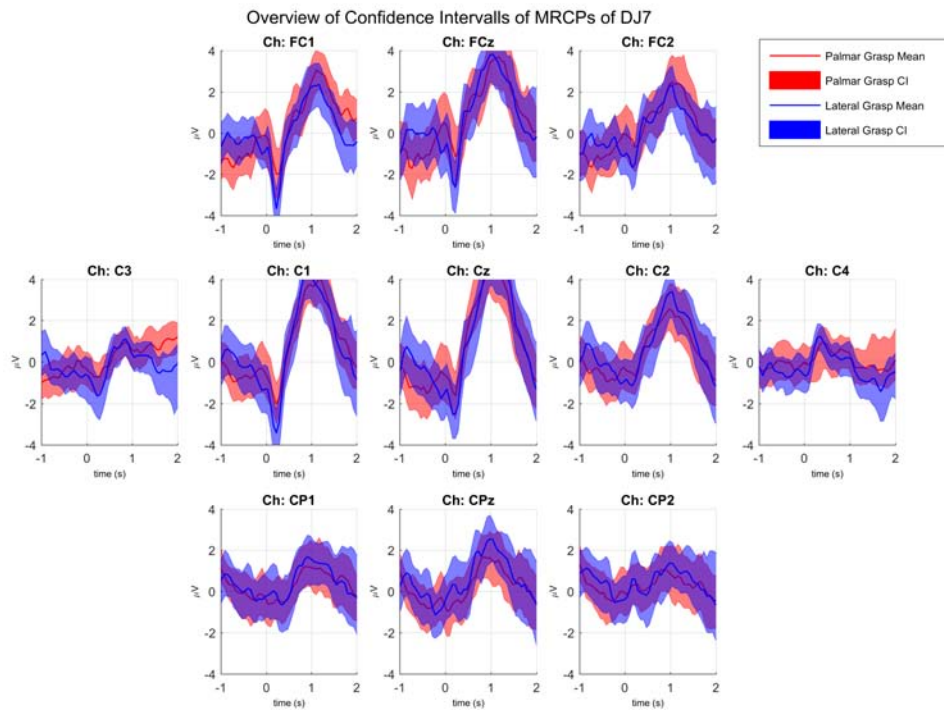
Figure 6.1: *Overview of the MRCPs of Subject CC2 of palmar and lateral grasp, epoched around the movement onset over the central electrodes: FCz, C1, Cz and C2. The continuous lines show the grand average while the shaded areas present the mean confidence intervals.*
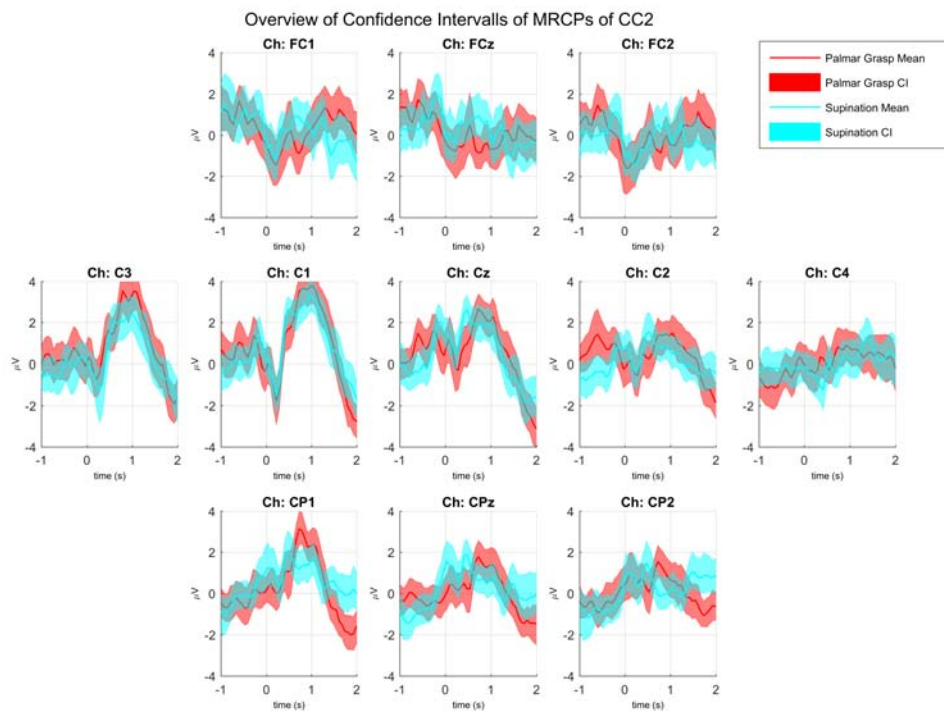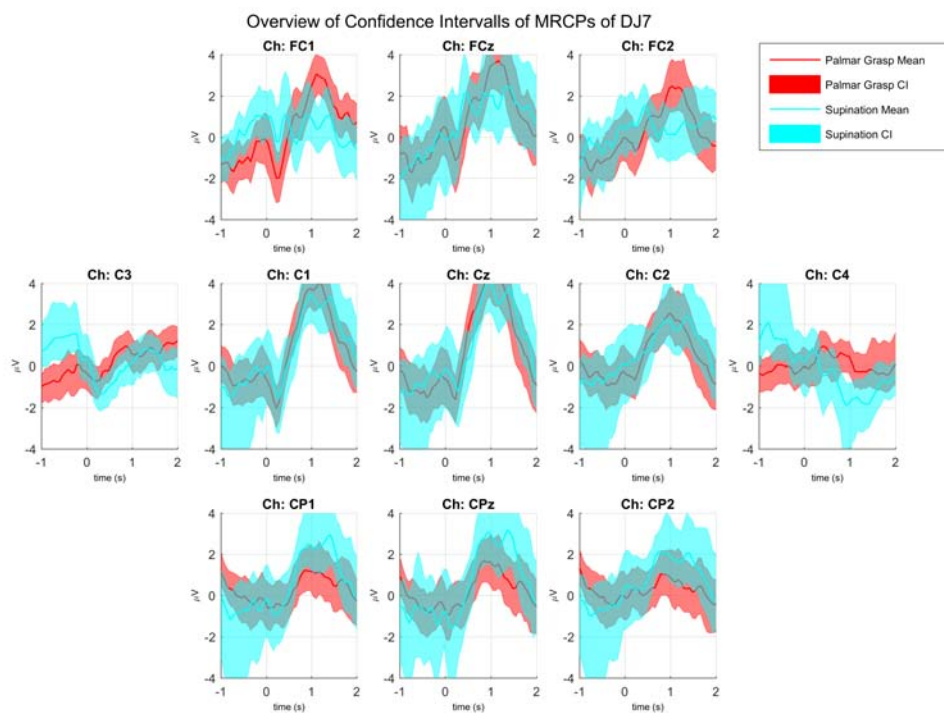

Figure 6.2: *Overview of the MRCPs of Subject CC2 palmar grasp and supination, epoched around the movement onset over the central electrodes: FCz, C1, Cz and C2. The continuous lines show the grand average while the shaded areas present the mean confidence intervals.*
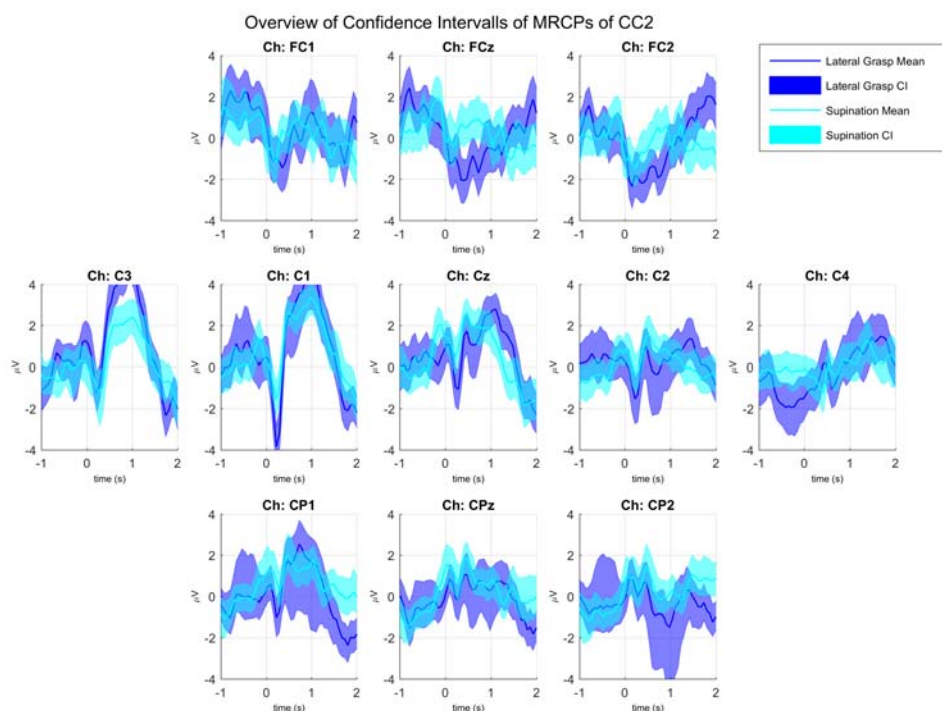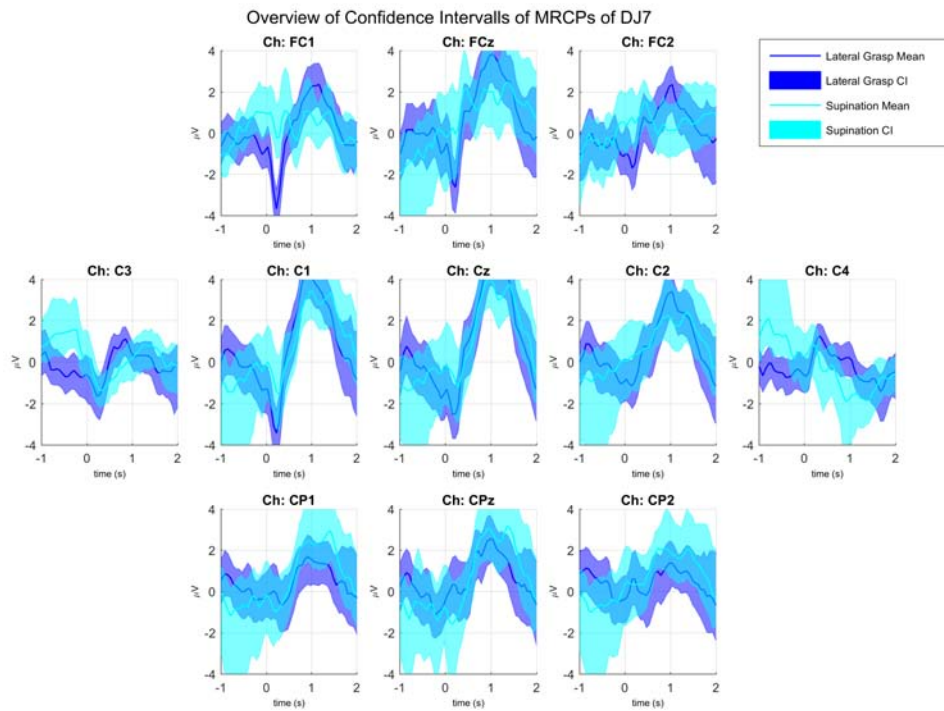
Figure 6.3: *Overview of the MRCPs of Subject CC2 lateral grasp and supination, epoched around the movement onset over the central electrodes: FCz, C1, Cz and C2. The continuous lines show the grand average while the shaded areas present the mean confidence intervals.*
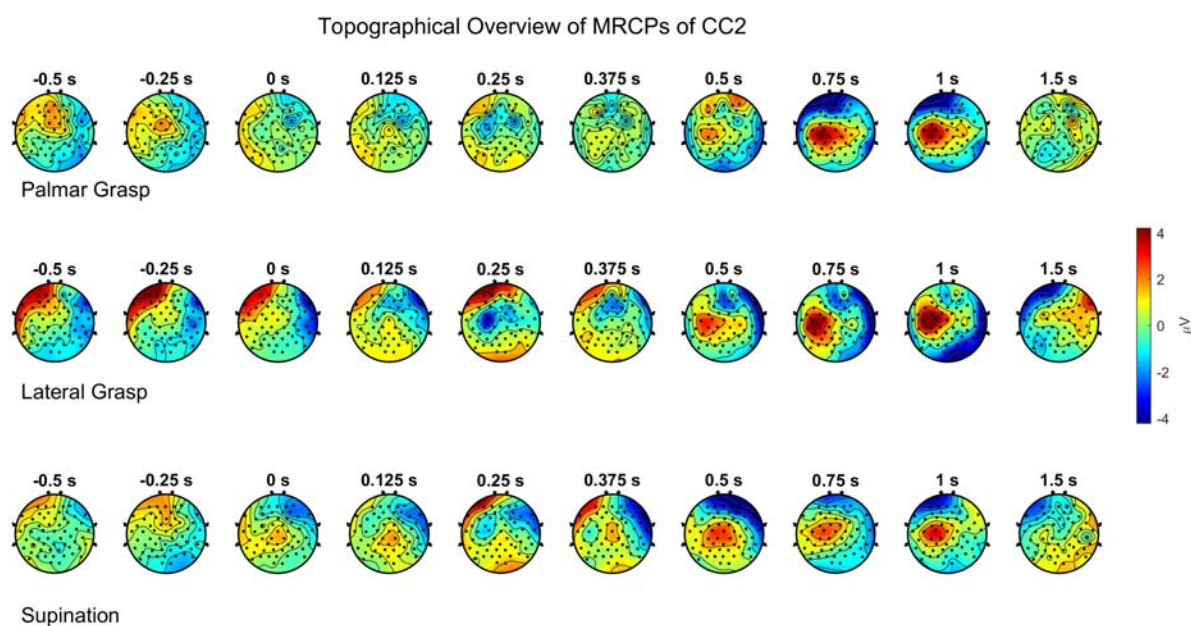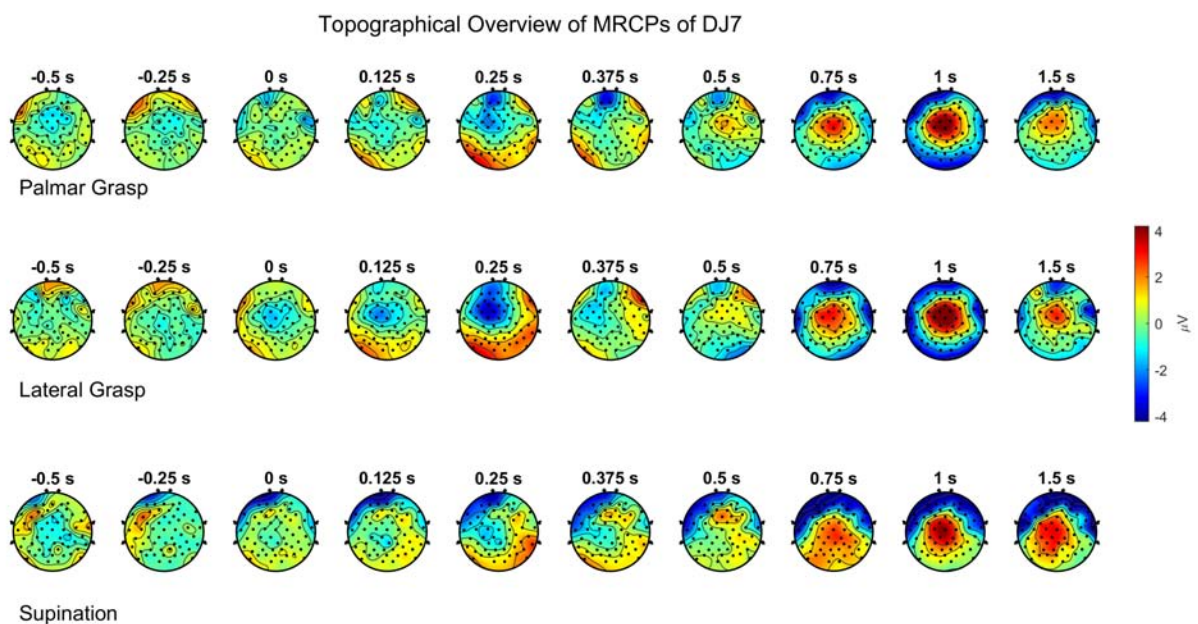

Figure 6.4: *Topographical overview the MRCPs of Subject CC2 of palmar close, lateral close and supination classes. Time points are distributed from -0.5 to 1.5 s around the movement onset, with a focus on the MRCP.*
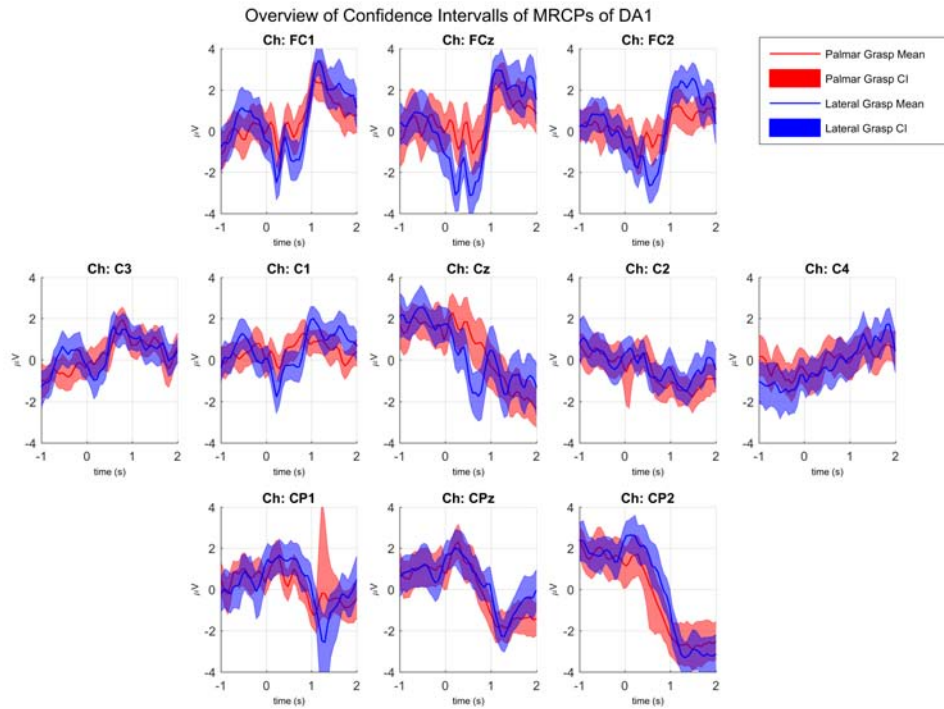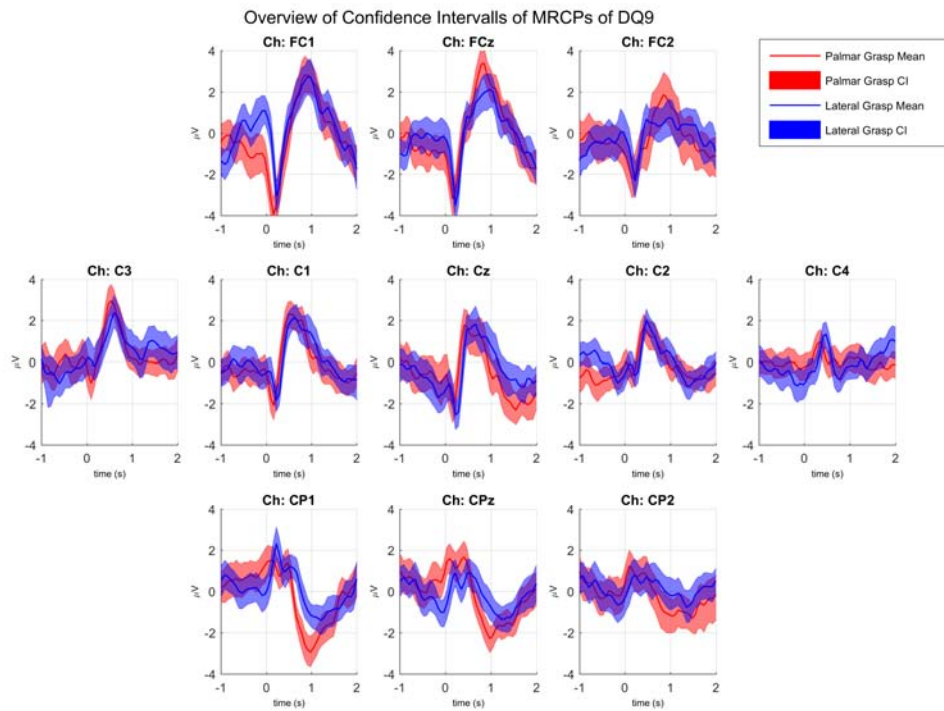
Figure 6.5: *Overview of the MRCPs of Subject DA1 of palmar and lateral grasp, epoched around the movement onset over the central electrodes: FCz, C1, Cz and C2. The continuous lines show the grand average while the shaded areas present the mean confidence intervals.*
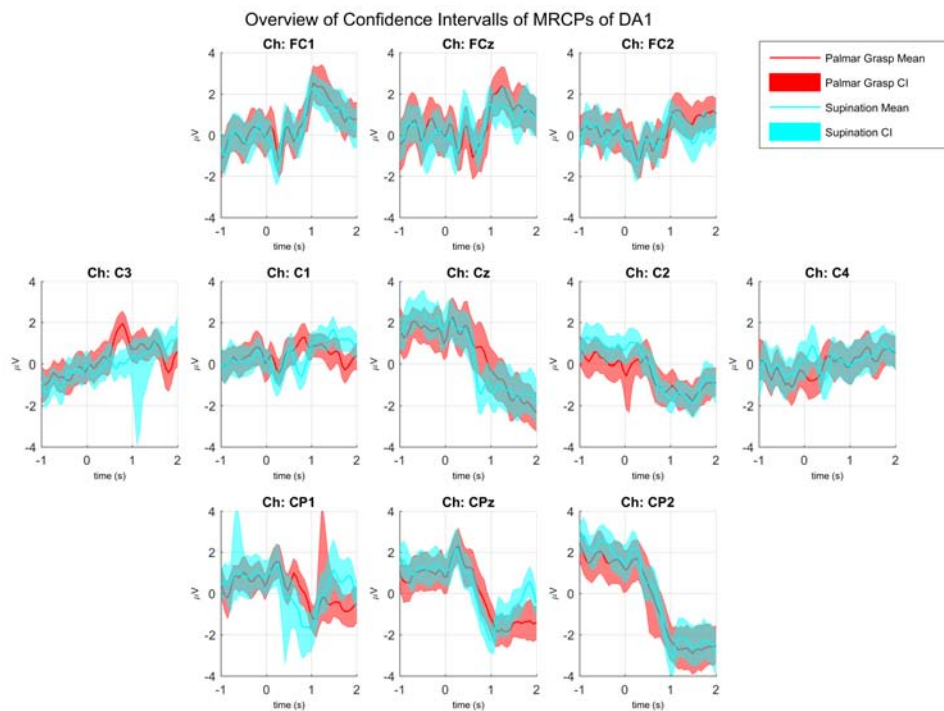
Figure 6.6: *Overview of the MRCPs of Subject DA1 palmar grasp and supination, epoched around the movement onset over the central electrodes: FCz, C1, Cz and C2. The continuous lines show the grand average while the shaded areas present the mean confidence intervals.*
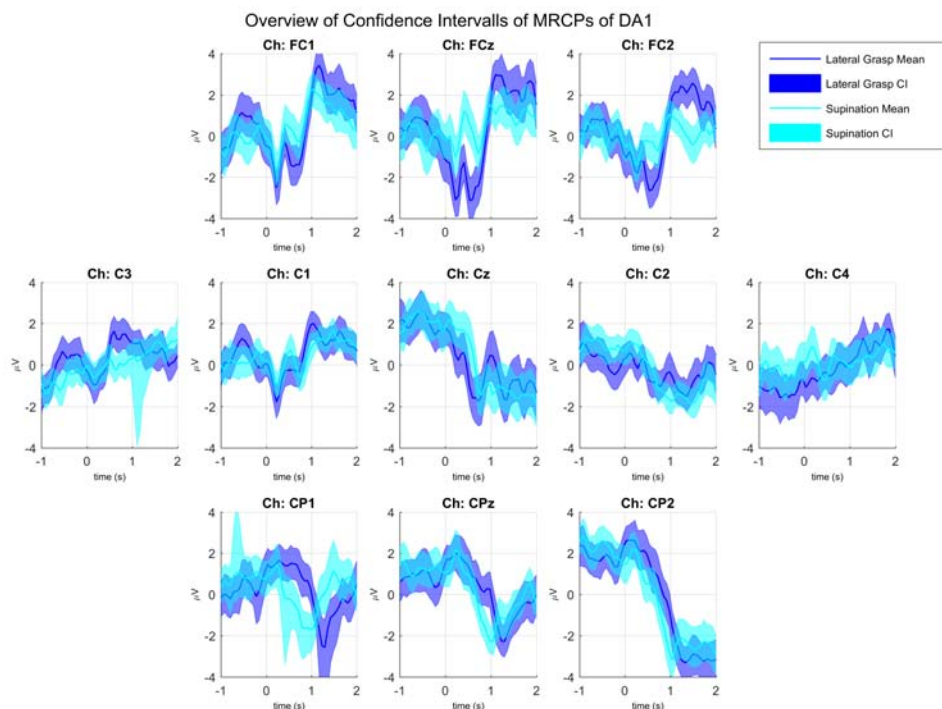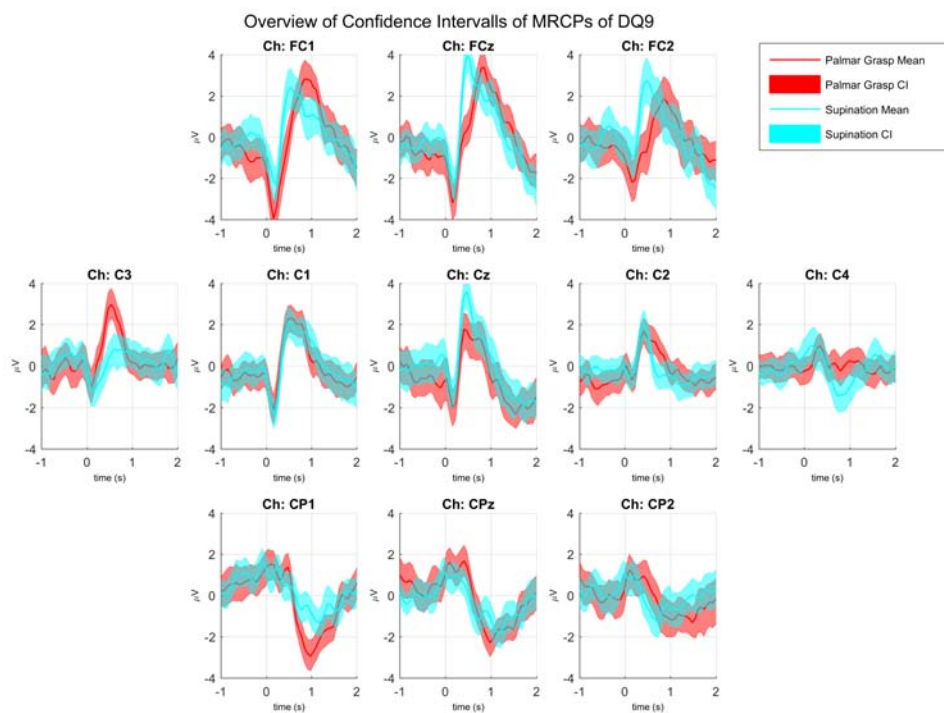
Figure 6.7: Overview of the MRCPs of Subject DA1 lateral grasp and supination, epoched around the movement onset over the central electrodes: FCz, C1, Cz and C2. The continuous lines show the grand average while the shaded areas present the mean confidence intervals.
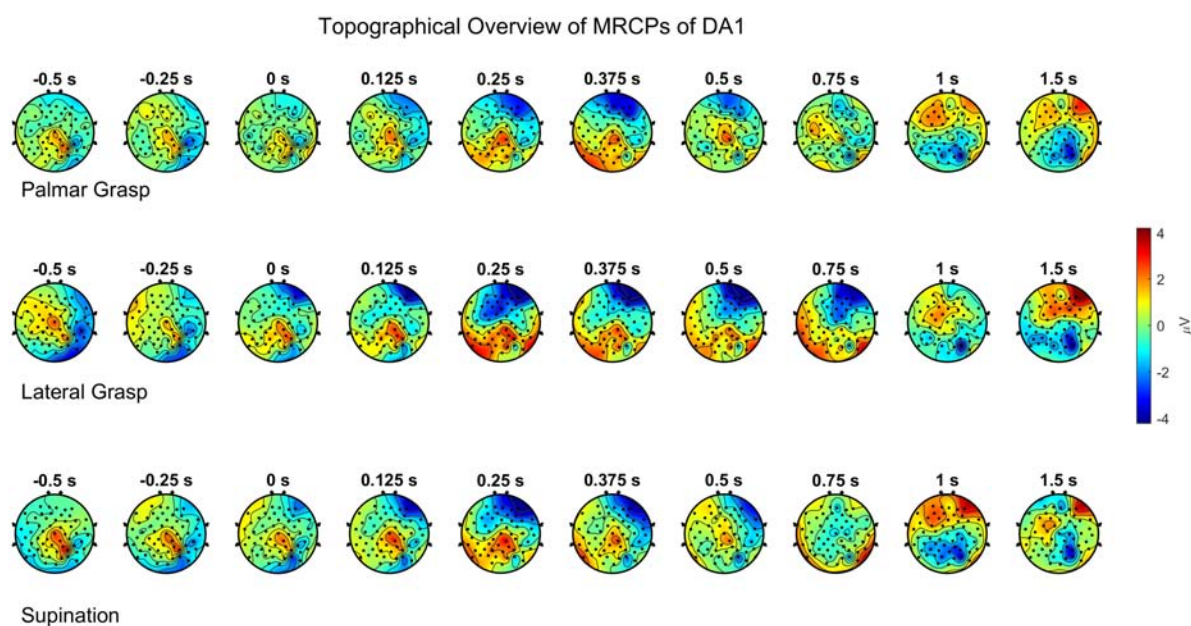
Figure 6.8: Topographical overview the MRCPs of Subject DA1 of palmar close, lateral close and supination classes. Time points are distributed from -0.5 to 1.5 s around the movement onset, with a focus on the MRCP.
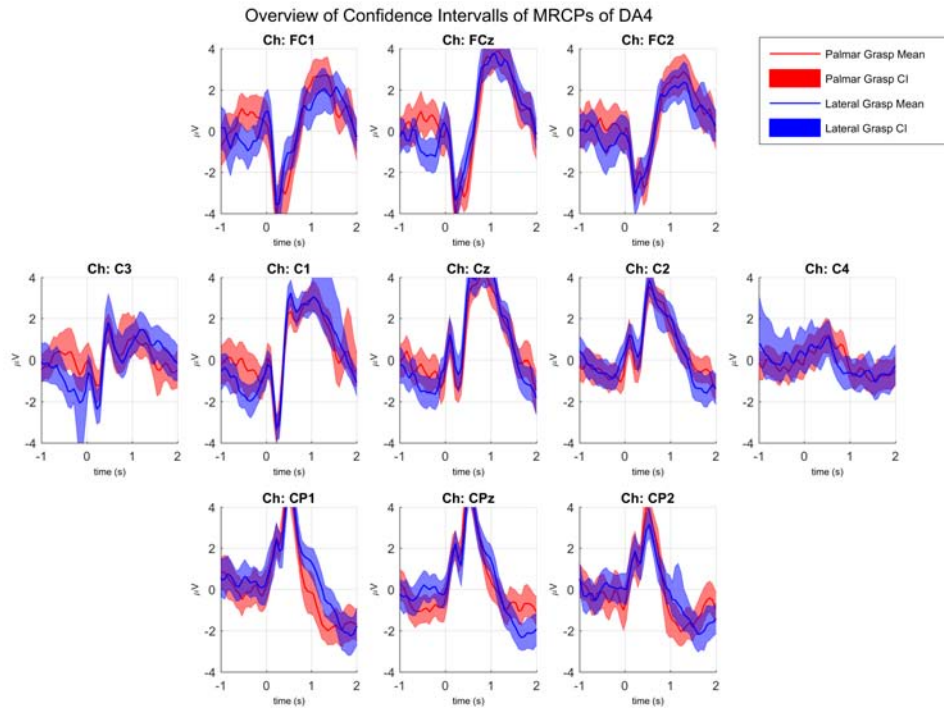
Figure 6.9: Overview of the MRCPs of Subject DA4 of palmar and lateral grasp, epoched around the movement onset over the central electrodes: FCz, C1, Cz and C2. The continuous lines show the grand average while the shaded areas present the mean confidence intervals.
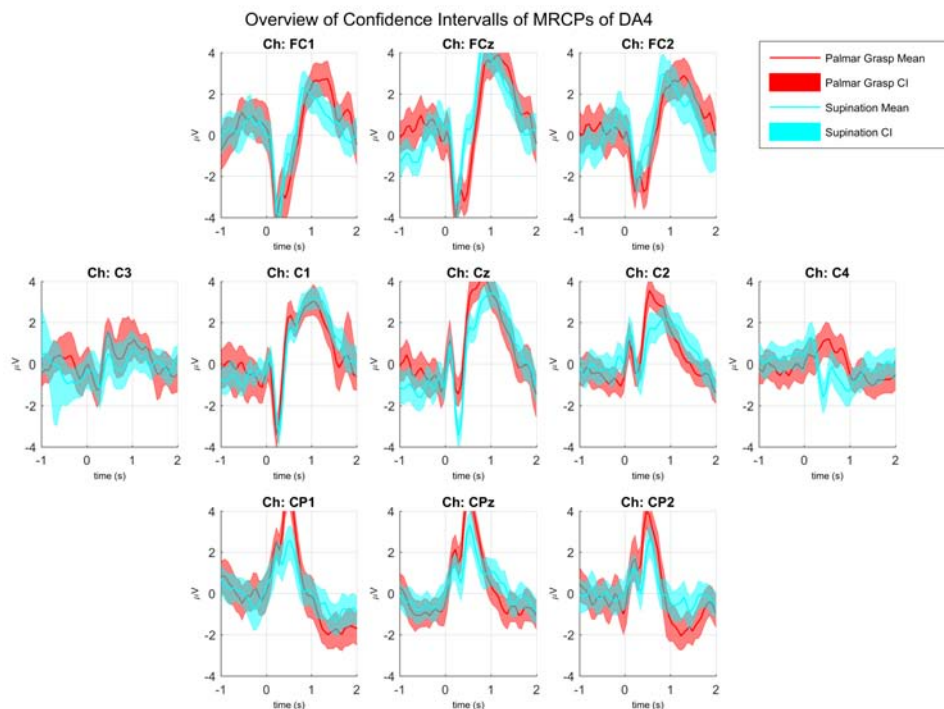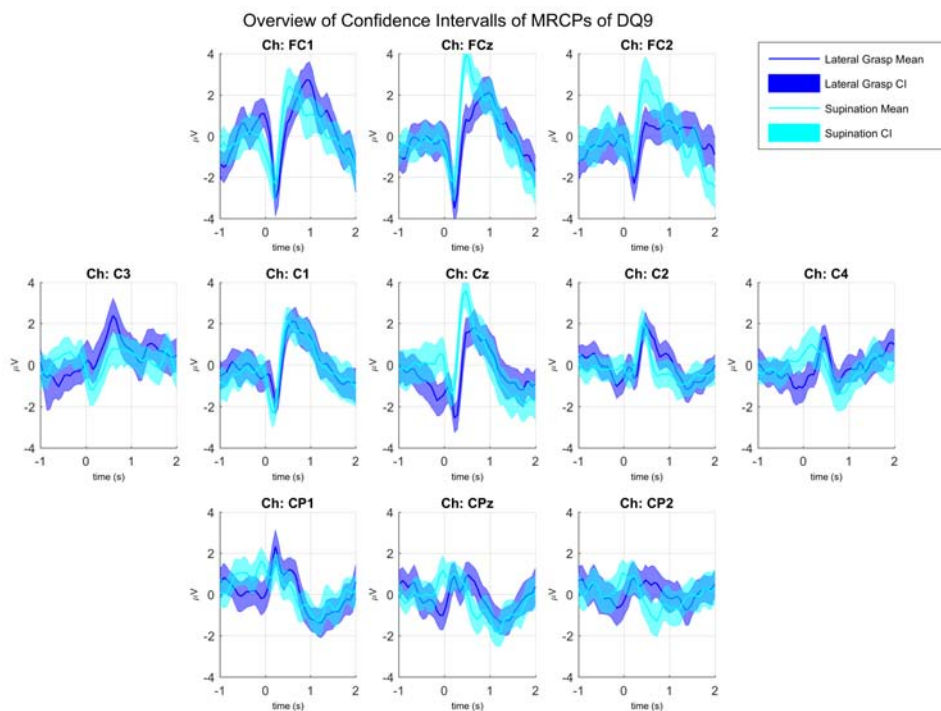

Figure 6.10: Overview of the MRCPs of Subject DA4 palmar grasp and supination, epoched around the movement onset over the central electrodes: FCz, C1, Cz and C2. The continuous lines show the grand average while the shaded areas present the mean confidence intervals.
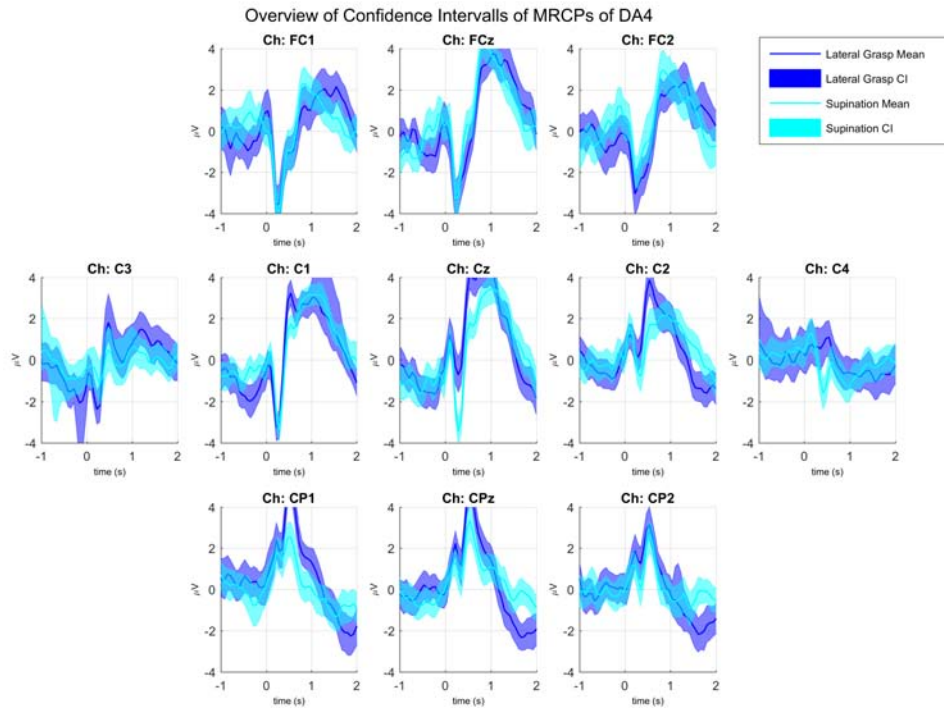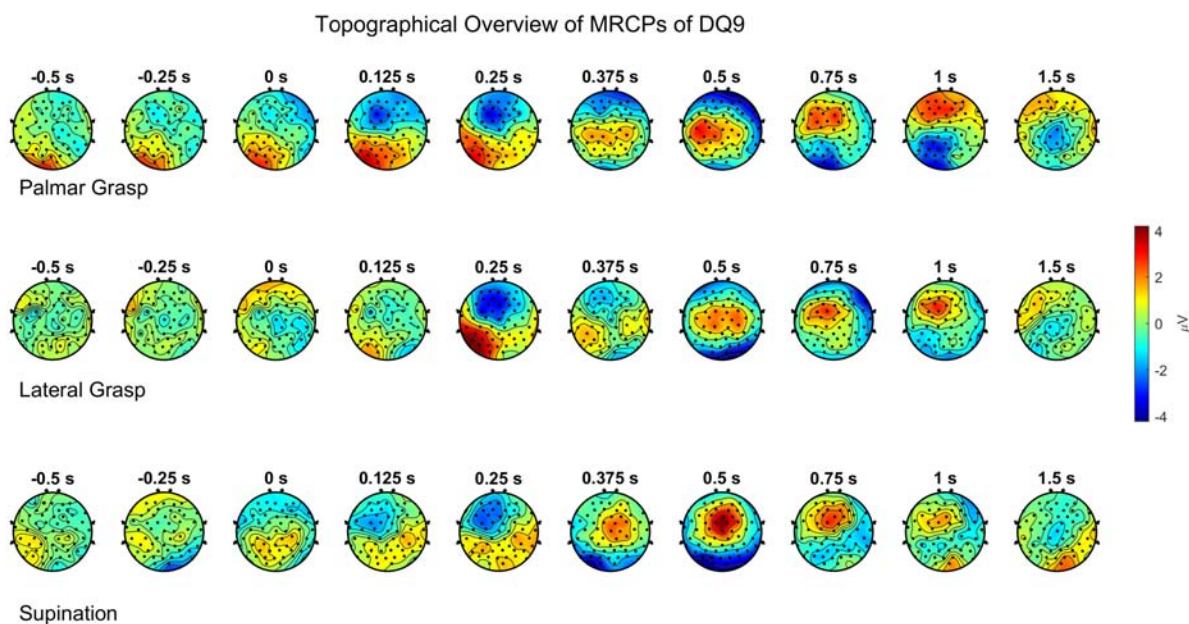
Figure 6.11: Overview of the MRCPs of Subject DA4 lateral grasp and supination, epoched around the movement onset over the central electrodes: FCz, C1, Cz and C2. The continuous lines show the grand average while the shaded areas present the mean confidence intervals.
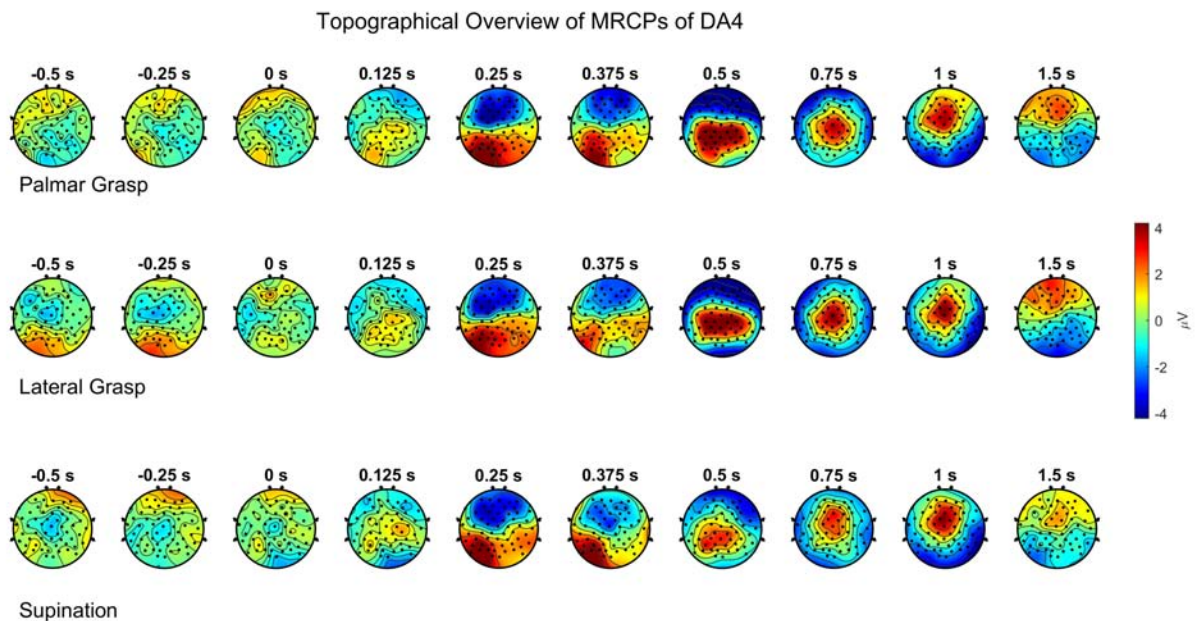
Figure 6.12: Topographical overview the MRCPs of Subject DA4 of palmar close, lateral close and supination classes. Time points are distributed from -0.5 to 1.5 s around the movement onset, with a focus on the MRCP.
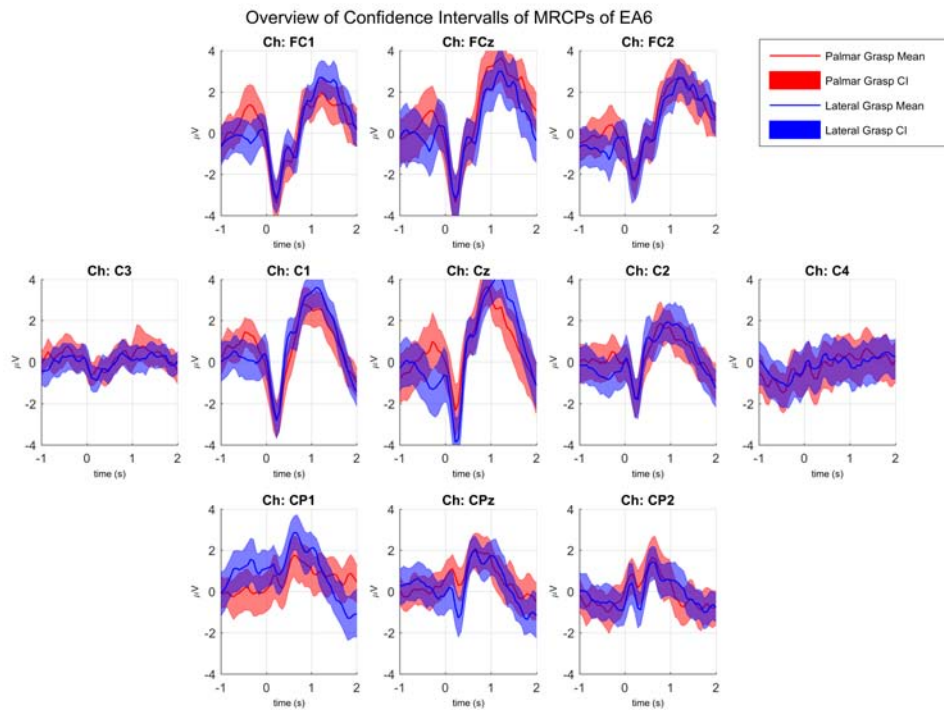
Figure 6.13: Overview of the MRCPs of Subject DJ7 of palmar and lateral grasp, epoched around the movement onset over the central electrodes: FCz, C1, Cz and C2. The continuous lines show the grand average while the shaded areas present the mean confidence intervals.
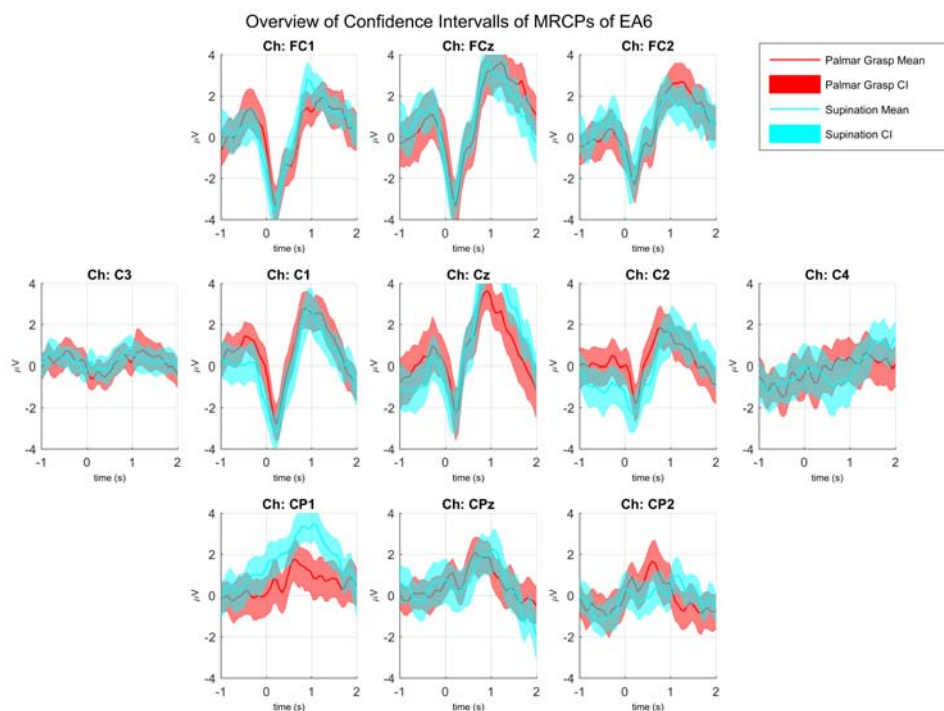

Figure 6.14: Overview of the MRCPs of Subject DJ7 palmar grasp and supination, epoched around the movement onset over the central electrodes: FCz, C1, Cz and C2. The continuous lines show the grand average while the shaded areas present the mean confidence intervals.
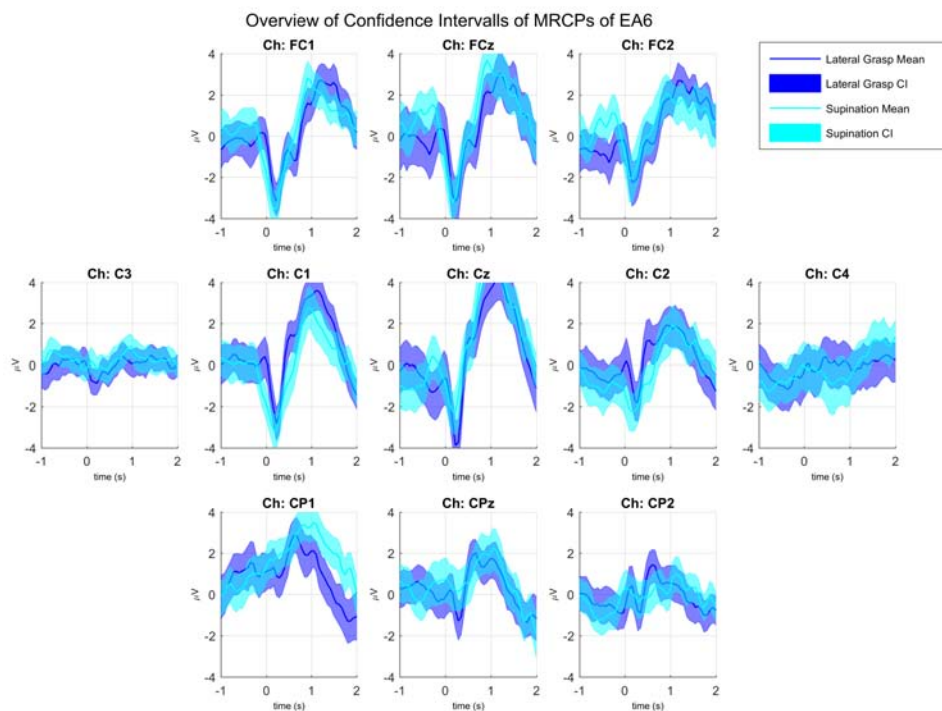
Figure 6.15: Overview of the MRCPs of Subject DJ7 lateral grasp and supination, epoched around the movement onset over the central electrodes: FCz, C1, Cz and C2. The continuous lines show the grand average while the shaded areas present the mean confidence intervals.
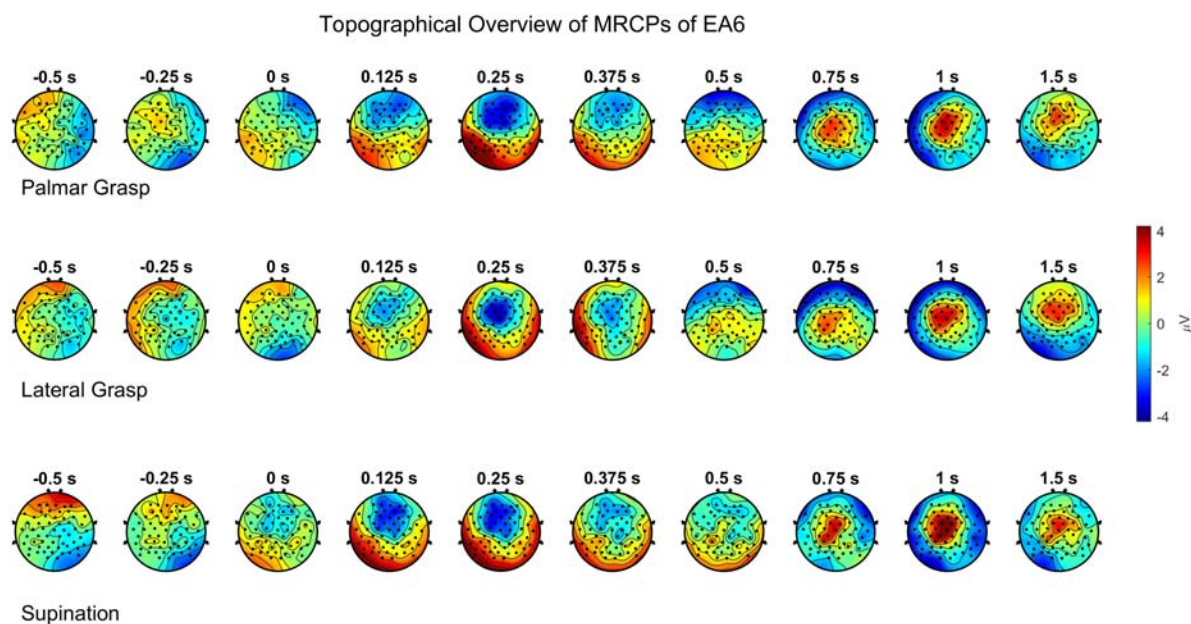

Figure 6.16: Topographical overview the MRCPs of Subject DJ7 of palmar close, lateral close and supination classes. Time points are distributed from -0.5 to 1.5 s around the movement onset, with a focus on the MRCP.
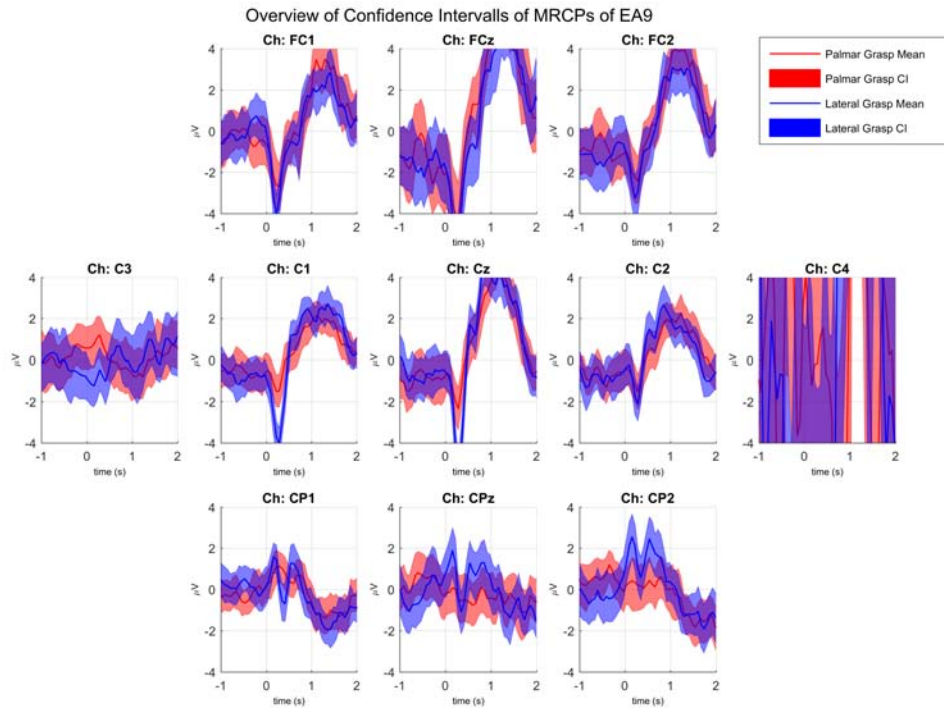
Figure 6.17: Overview of the MRCPs of Subject DQ9 of palmar and lateral grasp, epoched around the movement onset over the central electrodes: FCz, C1, Cz and C2. The continuous lines show the grand average while the shaded areas present the mean confidence intervals.

Figure 6.18: Overview of the MRCPs of Subject DQ9 palmar grasp and supination, epoched around the movement onset over the central electrodes: FCz, C1, Cz and C2. The continuous lines show the grand average while the shaded areas present the mean confidence intervals.
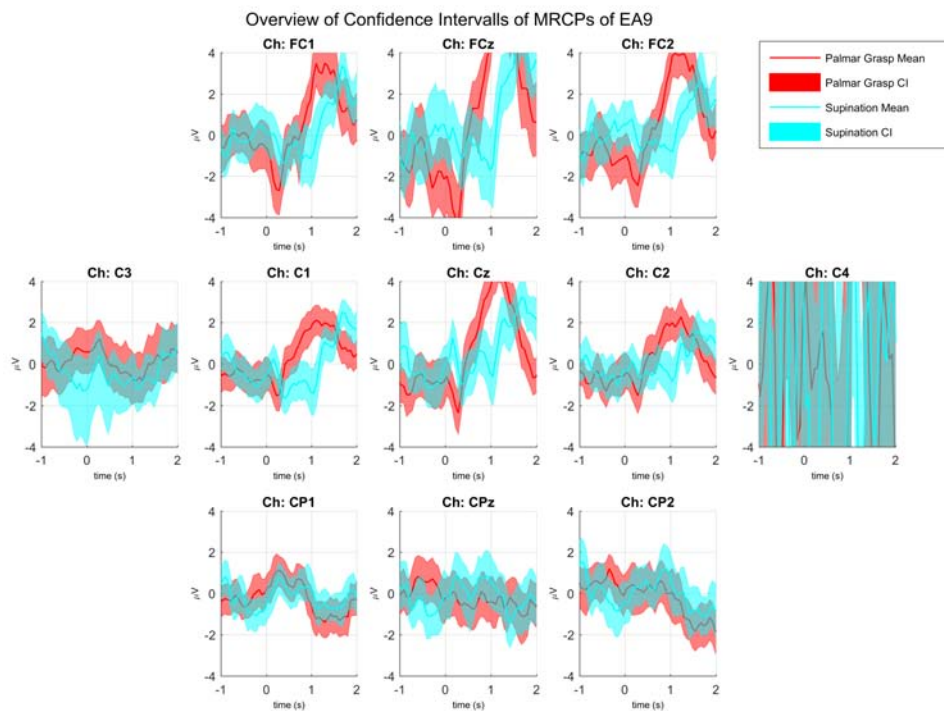
Figure 6.19: Overview of the MRCPs of Subject DQ9 lateral grasp and supination, epoched around the movement onset over the central electrodes: FCz, C1, Cz and C2. The continuous lines show the grand average while the shaded areas present the mean confidence intervals.

Figure 6.20: Topographical overview the MRCPs of Subject DQ9 of palmar close, lateral close and supination classes. Time points are distributed from -0.5 to 1.5 s around the movement onset, with a focus on the MRCP.

Figure 6.21: Overview of the MRCPs of Subject EA6 of palmar and lateral grasp, epoched around the movement onset over the central electrodes: FCz, C1, Cz and C2. The continuous lines show the grand average while the shaded areas present the mean confidence intervals.
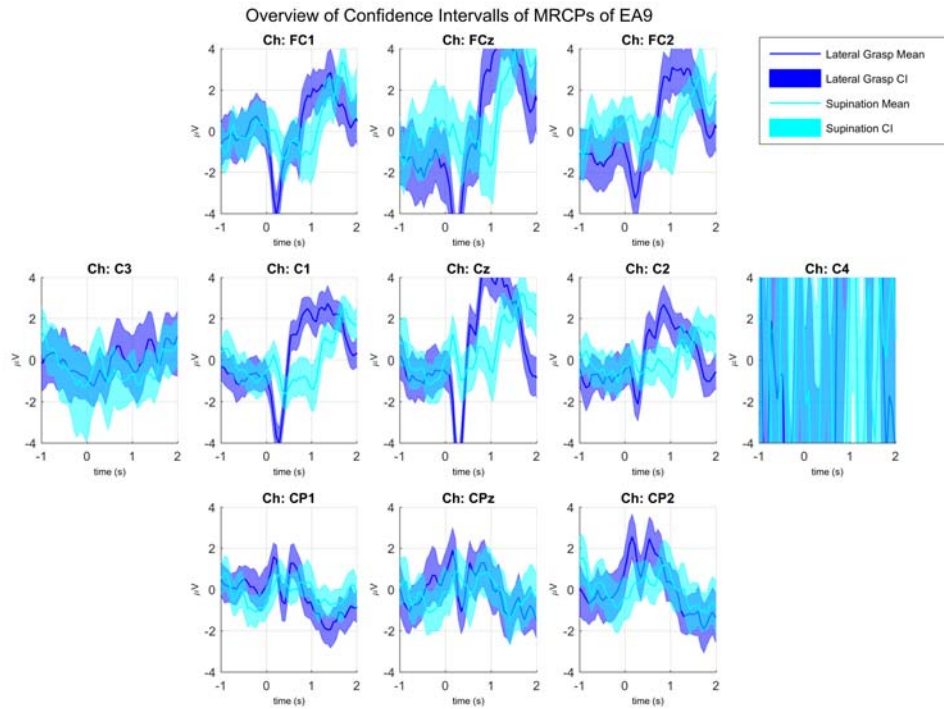

Figure 6.22: Overview of the MRCPs of Subject EA6 palmar grasp and supination, epoched around the movement onset over the central electrodes: FCz, C1, Cz and C2. The continuous lines show the grand average while the shaded areas present the mean confidence intervals.
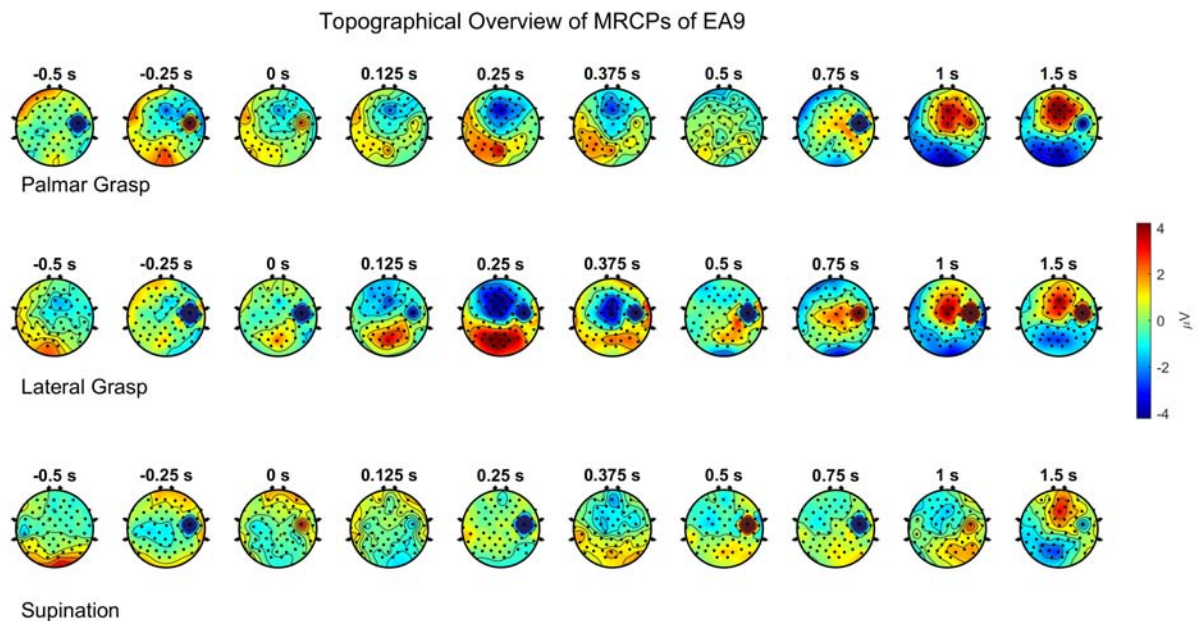
Figure 6.23: *Overview of the MRCPs of Subject EA6 lateral grasp and supination, epoched around the movement onset over the central electrodes: FCz, C1, Cz and C2. The continuous lines show the grand average while the shaded areas present the mean confidence intervals.*

Figure 6.24: *Topographical overview the MRCPs of Subject EA6 of palmar close, lateral close and supination classes. Time points are distributed from -0.5 to 1.5 s around the movement onset, with a focus on the MRCP.*
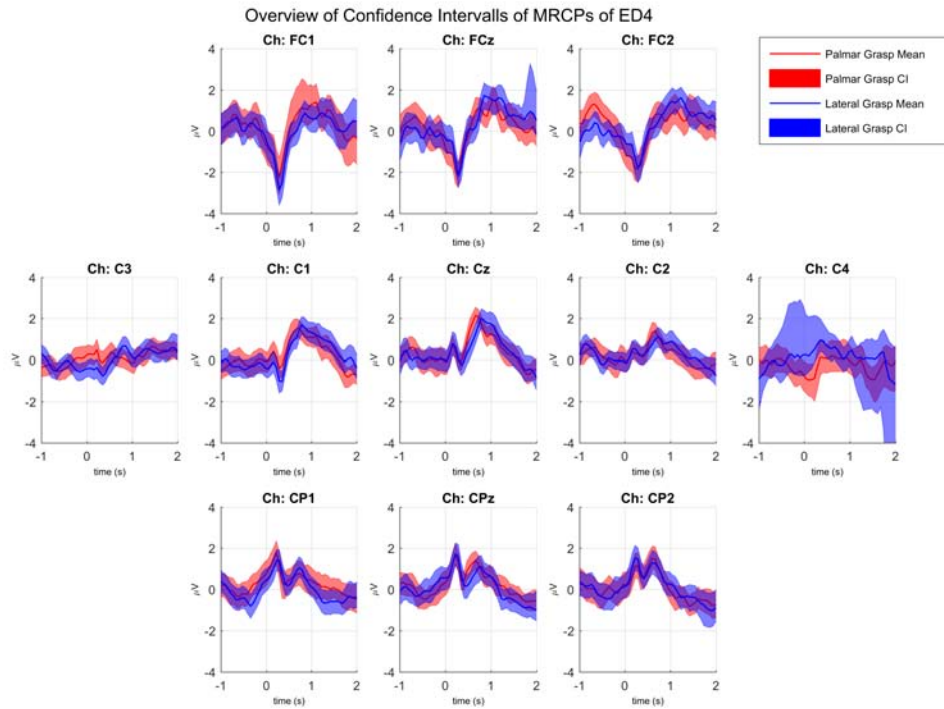
Figure 6.25: Overview of the MRCPs of Subject EA9 of palmar and lateral grasp, epoched around the movement onset over the central electrodes: FCz, C1, Cz and C2. The continuous lines show the grand average while the shaded areas present the mean confidence intervals.
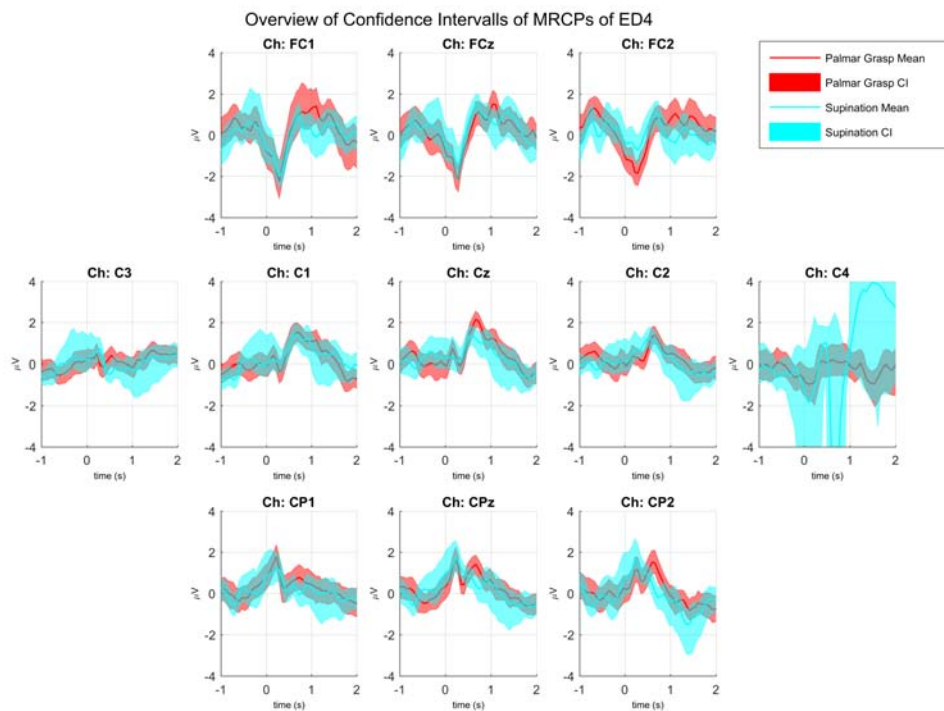

Figure 6.26: Overview of the MRCPs of Subject EA9 palmar grasp and supination, epoched around the movement onset over the central electrodes: FCz, C1, Cz and C2. The continuous lines show the grand average while the shaded areas present the mean confidence intervals.
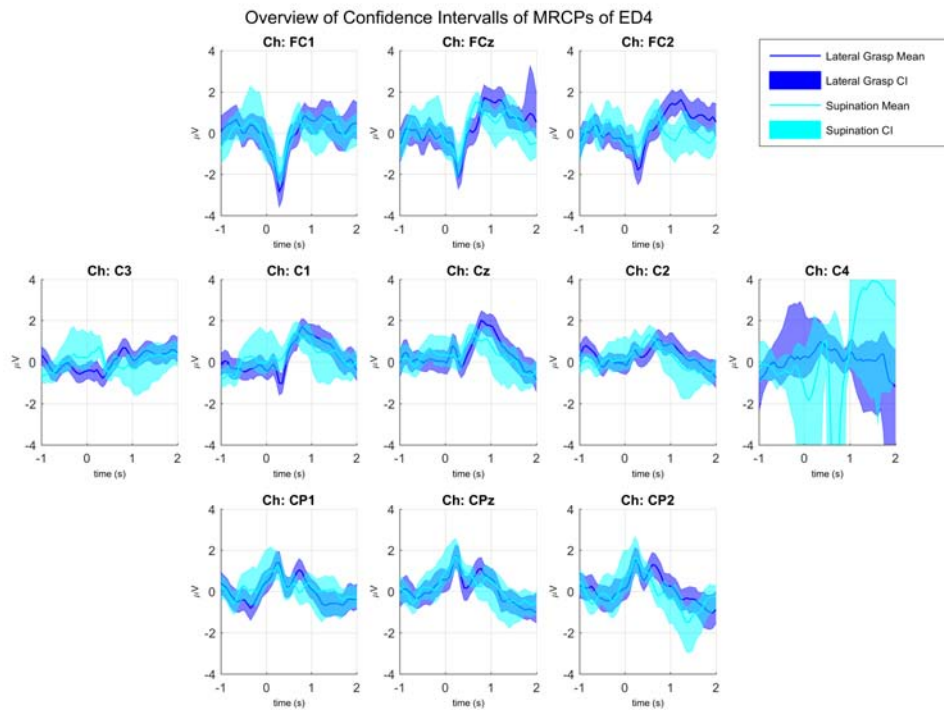
Figure 6.27: *Overview of the MRCPs of Subject EA9 lateral grasp and supination, epoched around the movement onset over the central electrodes: FCz, C1, Cz and C2. The continuous lines show the grand average while the shaded areas present the mean confidence intervals.*
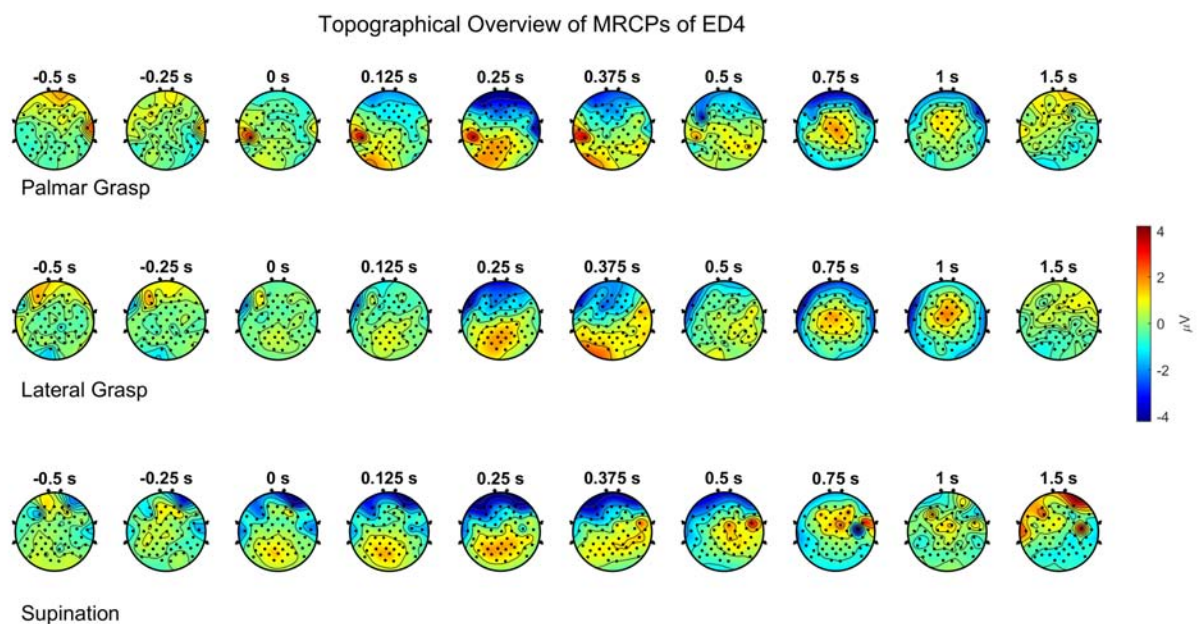

Figure 6.28: *Topographical overview the MRCPs of Subject EA9 of palmar close, lateral close and supination classes. Time points are distributed from -0.5 to 1.5 s around the movement onset, with a focus on the MRCP.*
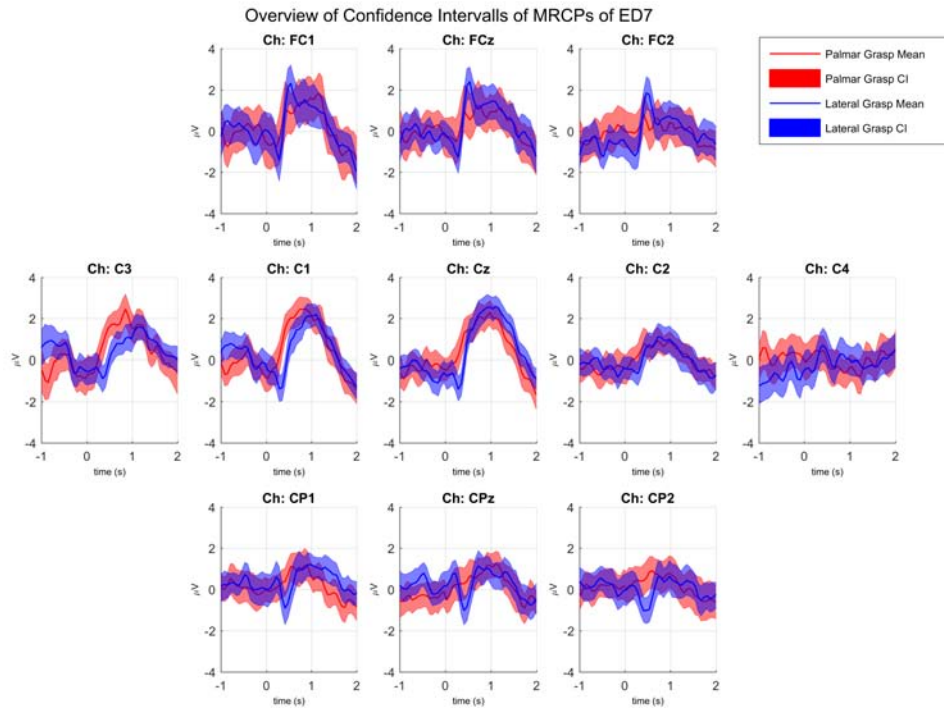
Figure 6.29: *Overview of the MRCPs of Subject ED4 of palmar and lateral grasp, epoched around the movement onset over the central electrodes: FCz, C1, Cz and C2. The continuous lines show the grand average while the shaded areas present the mean confidence intervals.*

Figure 6.30: *Overview of the MRCPs of Subject ED4 palmar grasp and supination, epoched around the movement onset over the central electrodes: FCz, C1, Cz and C2. The continuous lines show the grand average while the shaded areas present the mean confidence intervals.*
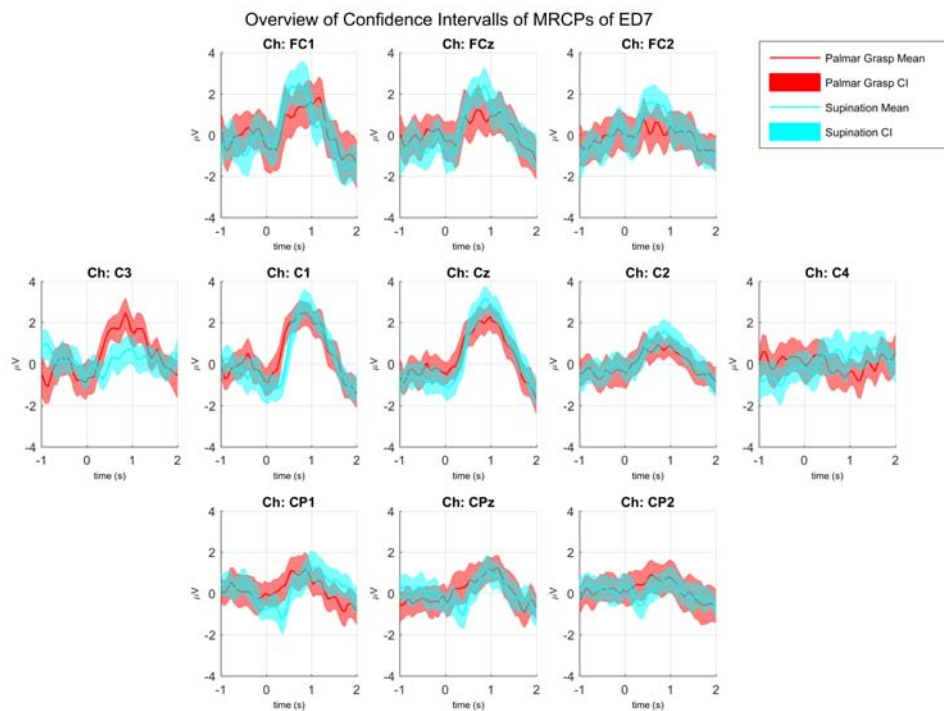
Overview of Confidence Intervalls of MRCPs of ED4

Figure 6.31: Overview of the MRCPs of Subject ED4 lateral grasp and supination, epoched around the movement onset over the central electrodes: FCz, C1, Cz and C2. The continuous lines show the grand average while the shaded areas present the mean confidence intervals.
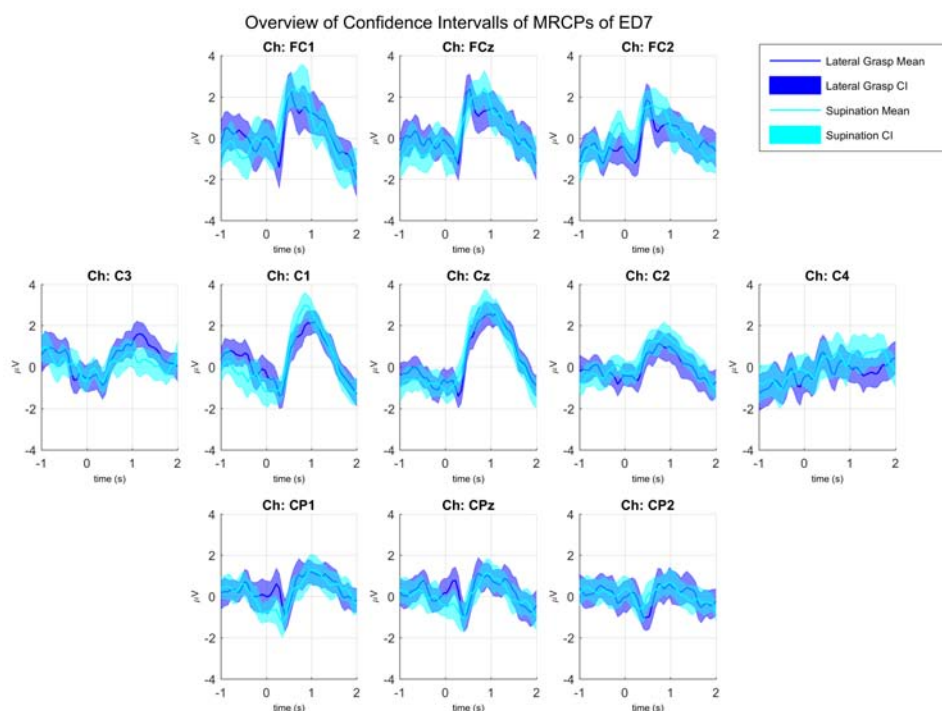
Topographical Overview of MRCPs of ED4

Figure 6.32: Topographical overview the MRCPs of Subject ED4 of palmar close, lateral close and supination classes. Time points are distributed from -0.5 to 1.5 s around the movement onset, with a focus on the MRCP.

Figure 6.33: *Overview of the MRCPs of Subject ED7 of palmar and lateral grasp, epoched around the movement onset over the central electrodes: FCz, C1, Cz and C2. The continuous lines show the grand average while the shaded areas present the mean confidence intervals.*
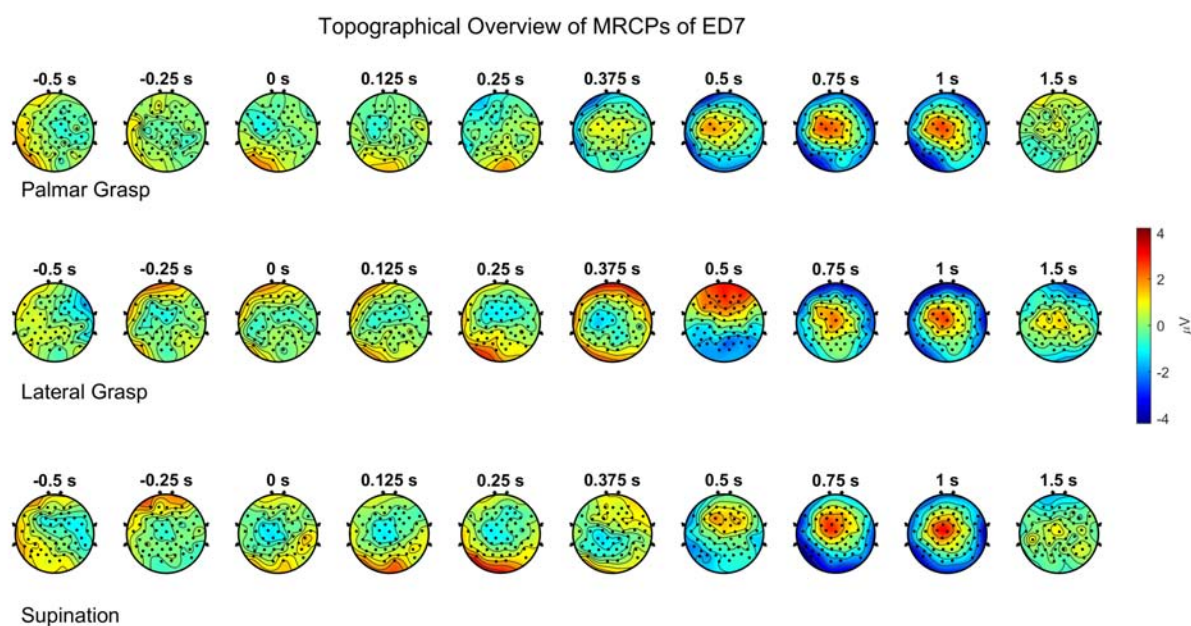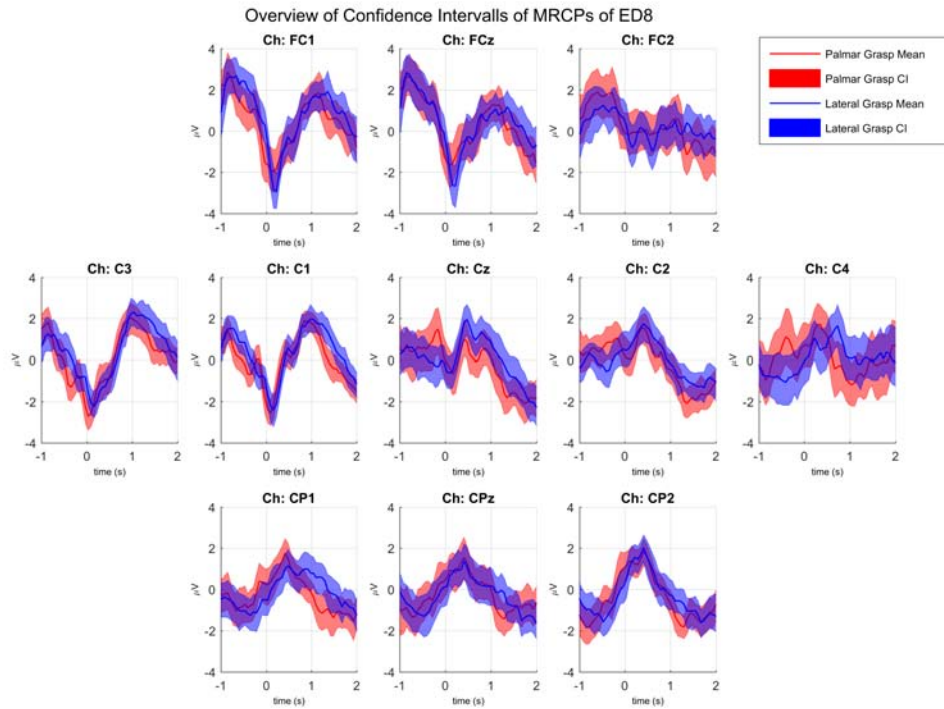

Figure 6.34: *Overview of the MRCPs of Subject ED7 palmar grasp and supination, epoched around the movement onset over the central electrodes: FCz, C1, Cz and C2. The continuous lines show the grand average while the shaded areas present the mean confidence intervals.*

Figure 6.35: Overview of the MRCPs of Subject ED7 lateral grasp and supination, epoched around the movement onset over the central electrodes: FCz, C1, Cz and C2. The continuous lines show the grand average while the shaded areas present the mean confidence intervals.

Figure 6.36: Topographical overview the MRCPs of Subject ED7 of palmar close, lateral close and supination classes. Time points are distributed from -0.5 to 1.5 s around the movement onset, with a focus on the MRCP.

Figure 6.37: Overview of the MRCPs of Subject ED8 of palmar and lateral grasp, epoched around the movement onset over the central electrodes: FCz, C1, Cz and C2. The continuous lines show the grand average while the shaded areas present the mean confidence intervals.
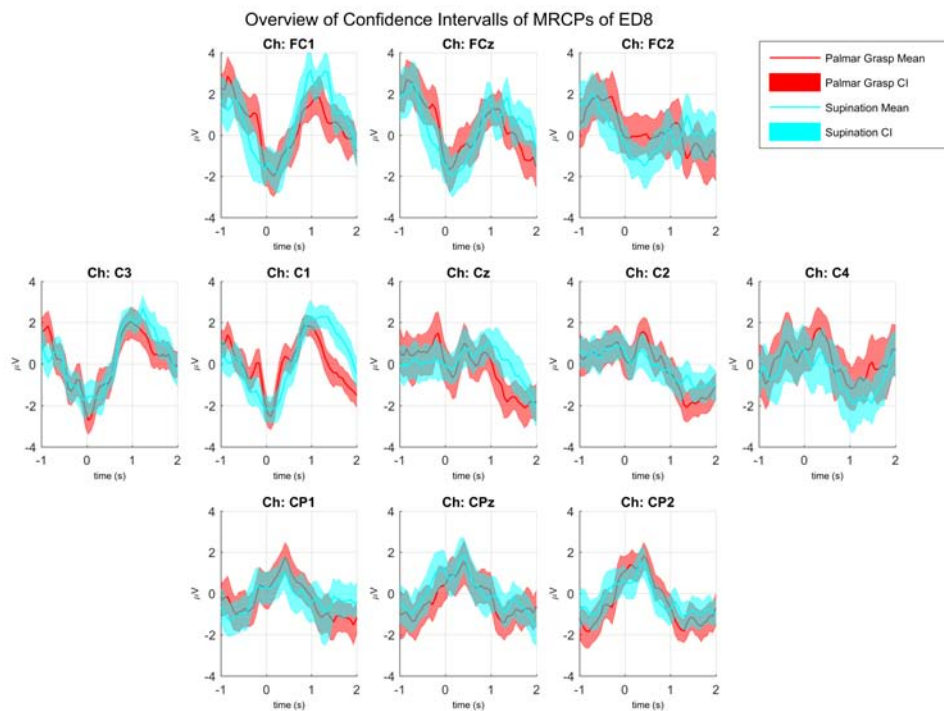

Figure 6.38: Overview of the MRCPs of Subject ED8 palmar grasp and supination, epoched around the movement onset over the central electrodes: FCz, C1, Cz and C2. The continuous lines show the grand average while the shaded areas present the mean confidence intervals.
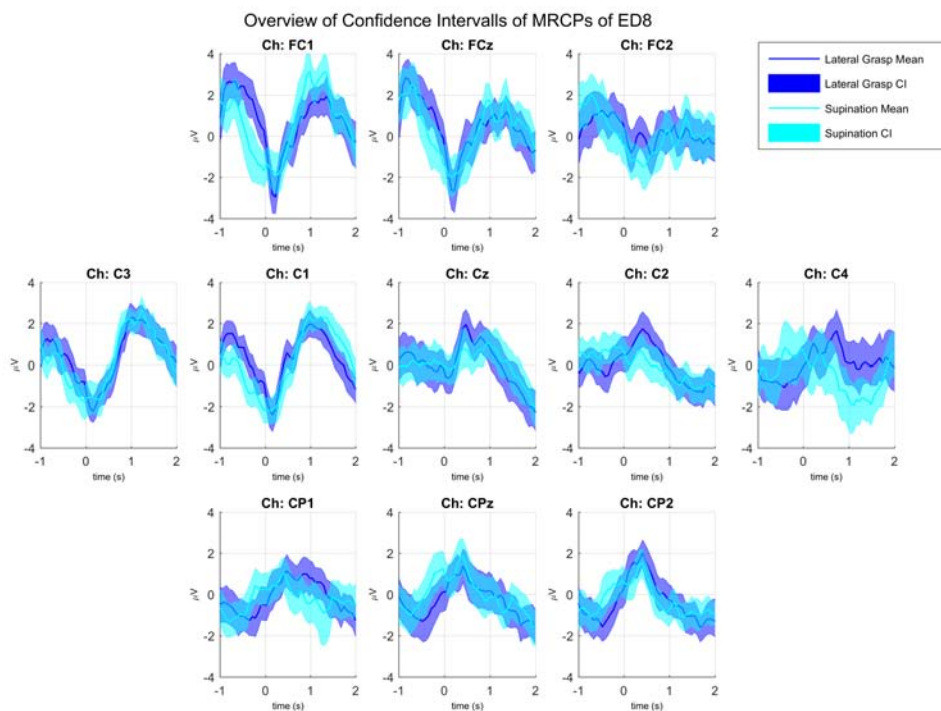
Figure 6.39: Overview of the MRCPs of Subject ED8 lateral grasp and supination, epoched around the movement onset over the central electrodes: FCz, C1, Cz and C2. The continuous lines show the grand average while the shaded areas present the mean confidence intervals.
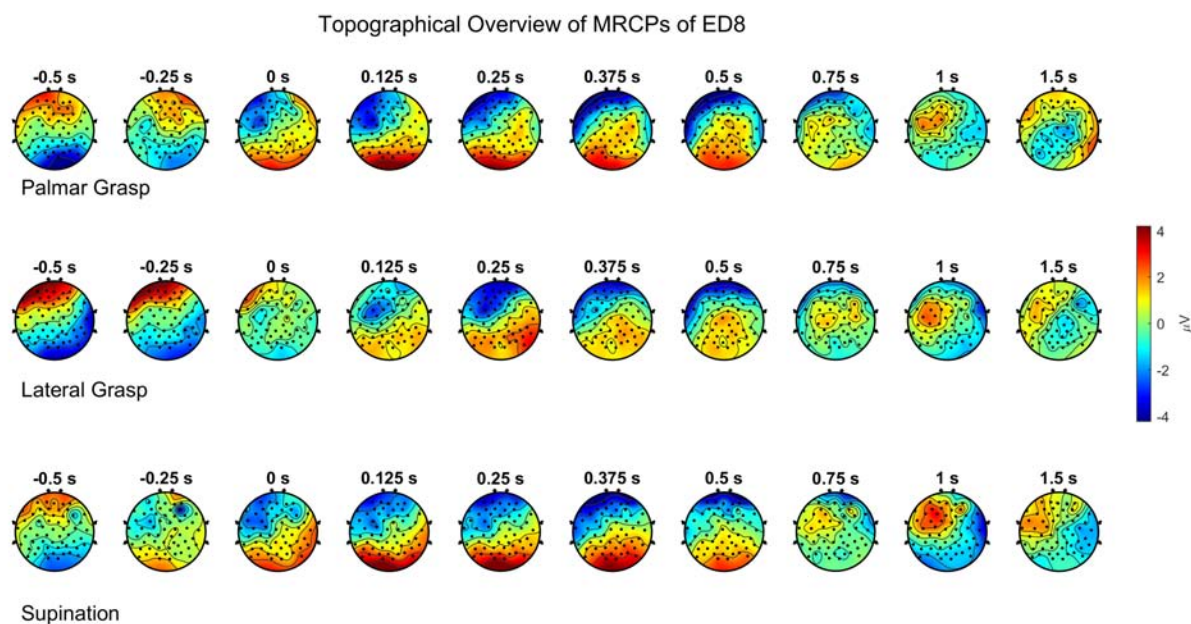

Figure 6.40: Topographical overview the MRCPs of Subject ED8 of palmar close, lateral close and supination classes. Time points are distributed from -0.5 to 1.5 s around the movement onset, with a focus on the MRCP.